CHALMERS

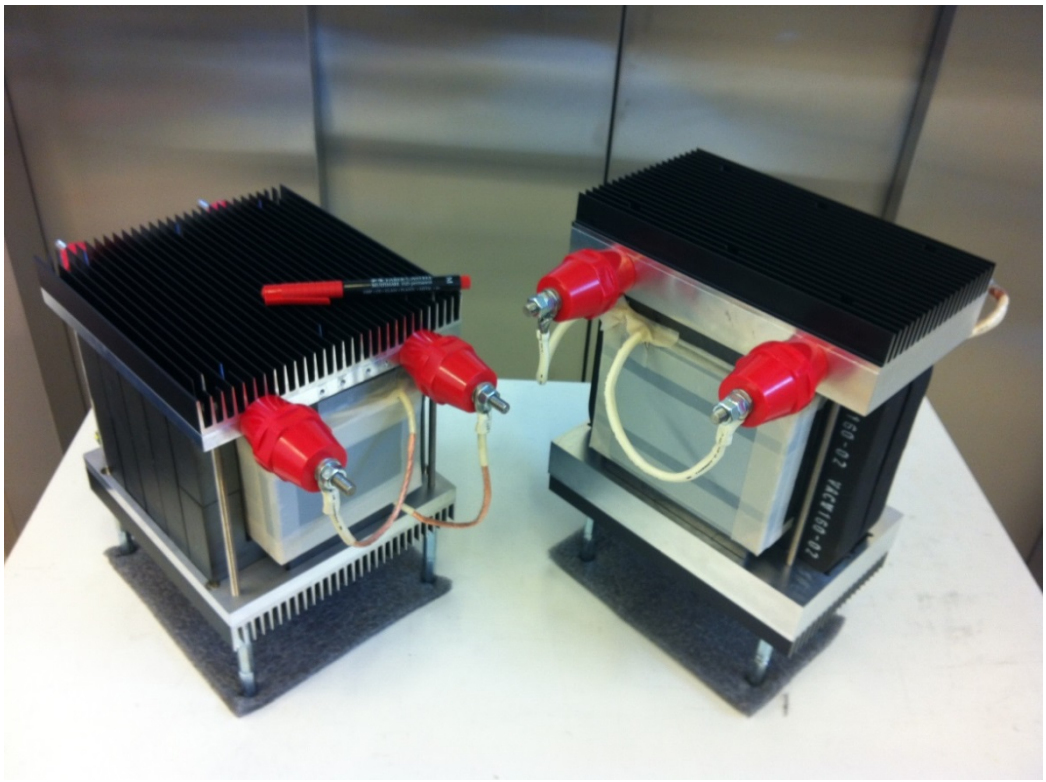

Constructional Design, Manufacturing and Evaluation of High Power Density Medium Frequency Transformer Prototypes

Master of Science Thesis

MOHAMMAD KHAREZY

Department of Energy and Environment
Division of Electric Power Engineering
CHALMERS UNIVERSITY OF TECHNOLOGY
Gothenburg, Sweden 2014

CHALMERS


SP
Science Partner


CHALMERS

Constructional Design, Manufacturing and Evaluation of High Power Density Medium Frequency Transformer Prototypes

MOHAMMAD KHAREZY

Department of Energy and Environment
Division of Electric Power Engineering
CHALMERS UNIVERSITY OF TECHNOLOGY
Gothenburg, Sweden 2014

Constructional Design, Manufacturing and Evaluation of
High Power Density Medium Frequency Transformer Prototypes
MOHAMMAD KHAREZY

Department of Energy and Environment
Division of Electric Power Engineering
Chalmers University of Technology
SE-412 96 Gothenburg
Sweden
Telephone +46 (0)31–772 1000

Cover:
Manufactured High Power Medium Frequency Transformer Prototypes

Chalmers Library, Report Service
Gothenburg, Sweden 2014

Constructional Design, Manufacturing and Evaluation of
High Power Density Medium Frequency Transformer Prototypes
MOHAMMAD KHAREZY
Department of Energy and Environment
Division of Electric Power Engineering
Chalmers University of Technology

Abstract

- The aim of this project is to manufacture and test two 60 kW, 1.2/3.6 kV, 6 kHz 46/28 µH prototype transformers.
- Based on the prepared high power medium frequency transformers' design data, the constructional design of two prototype transformers is performed. During the constructional design, determination of the type, shape and volume of the suitable magnetic, thermally conductive and dielectric materials available in the market was done. The materials were bought and processed, and two prototype transformers were manufactured. The important technical data regarding the insulation characteristics of insulation materials was examined at nominal wave shape and frequency considered for the transformer application and the insulation coordination of the transformers was updated accordingly. At the same time, to prepare for the design validation tests, evaluation of the available high voltage, high current and medium frequency square wave shape supplies and the voltage and current measuring equipment was performed. The transformers were subjected to a set of design validation tests and the results were recorded, analysed and compared with the calculated values.
- Key Words: Solid state transformer, Medium frequency Power transformer, DC-DC converter, DC grid collection, Transformer testing and design validation

Index Terms:
HV, High Voltage
LV, Low Voltage
PT, Voltage measurement Transformer
CT, Current measurement Transformer
LCP, Liquid Crystalline Polymer
HPMF, High Power Medium Frequency
DAB, Dual Active Bridge
ZVS Zero Voltage Switching
PWM, Pulse Width Modulator

Acknowledgements

This work has been carried out at the SP Technical Research Institute of Sweden and the Department of Energy and Environment at Chalmers University of Technology. The financial support was given by SP Wise measurements for smart grids platform.

First, I express my sincere thanks to Amin Bahmani, Jan Johansson and Valter Tarasso without their help the initiation and realization of this project would be impossible. While conducting this project, I had the warm and unconditional support of Amin Bahmani, Torbjörn Thiringer and Johan Söderbom. I thank them wholeheartedly. I need also to thank all my colleagues in SP whose warm technical help was invaluable; among them, Henrik Petersen and Mikael Björnram stand out in my memory. Special thanks go to Vacuumschmelze and Lars Kvarnsjö for providing the Nanocrystalline cores for free and Energimyndigheten for sponsoring the rest of the materials needed in the thesis work.

Eventually, my heartfelt gratitude goes to my family for all their support and love.

Mohammad Kharezy
Gothenburg, Sweden, 2014

Contents

1 Introduction

1.1 Background

Using high power density medium frequency transformers in DC/DC converters results in a considerable reduction in weight and volume of the transformer's magnetic part and consequently on the cost of the converter [1].

DC/DC converters are used for DC collection, transportation and distribution systems which have a huge potential in the future wind farms. They give a potential for reduced technical complexity and accordingly reduced cost in the future distribution systems (see Figure 1-1).

Renewable energy production using offshore wind farms and integration of it into existing power grids is significantly increasing. The latter can, for locations far out in the sea, be made cheaper by avoiding using conventional low frequency AC collection systems [2].

However, in order to make this development possible, a key component is missing, the dc transformer (smart transformer). To be more specific it is not a "dc transformer"; it is a dc/dc converter with a high power medium frequency (HPMF) transformer as the key component, as it is demonstrated in Figure 1-2. The rated power of such components can be from a few kVA to 1 MVA [2].

It is a well-known fact that, increasing the operation frequency reduces the magnetic device volume, this is something already put into practice in the low-power applications due to the availability of fast and efficient semiconductor devices. Nowadays, this is also becoming a reality in high power applications [3-7].

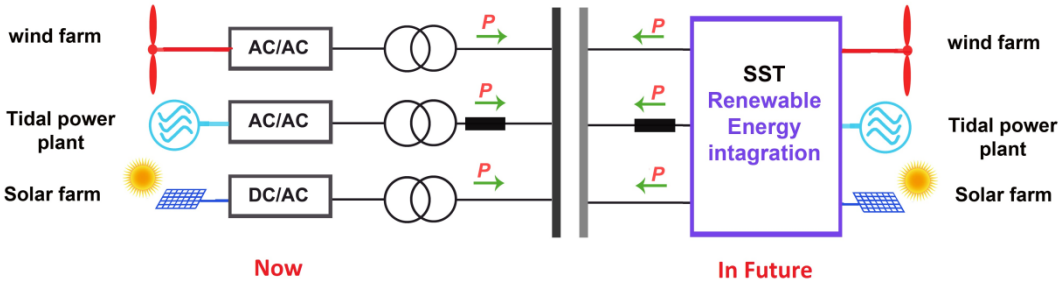

***Figure 1-1*: Potential application of SST in the future distribution systems [8].**

Despite the advantages and additional functionalities introduced by these new conversion systems, the main motivation for their application lays today in the possibility for volume, material and weight reductions in the restricted areas, such as ships, traction solutions and wind power. There is an obvious interest in developing such systems, clearly demonstrated by the effort made by several industrial companies, mainly related to the traction applications, which have proven the technical feasibility and advantages of the medium-frequency conversion systems. There are also similar initiatives in the wind power field, related to the offshore applications where spatial and weight restrictions are the driving factors [1].

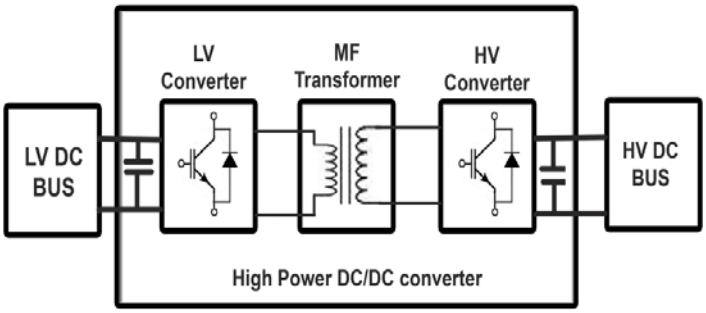

***Figure 1-2*: DC-DC converter interfacing two DC grids with different voltage levels**.

1.2 Previous work

Many research activities devoted to overcome the challenges regarding design and manufacturing of the medium frequency high power transformers which is mostly because of additional losses in the core and windings and originates from a high switching frequency [1].

At sinusoidal excitation, the core losses can easily be calculated using the supplied core datasheets [9]. However, considering the nonlinear magnetic characteristics of the core materials and non-sinusoidal waveforms, it is a challenge to estimate the losses of a so called a DC-DC high power high frequency transformer. Determination of losses is vital for designing a proper transformer cooling system [2]. The main elements of the losses are the core losses and the winding losses.

At high frequencies, the losses in the copper conductors will drastically rise because of the skin effect in the conductors and the proximity effect to the adjacent conductors. Having access to a set of precise formulas, the calculation of winding losses can be performed with an acceptable accuracy [9]. References [10] and [11] propose formulas to accurately calculate the AC resistance of the conductors under high frequency switching conditions. The formulas can be used for the windings of any combination arrangements of the number of the layers and turns [11].

Because of complexity of the supplying voltage and current wave shapes, it is difficult to estimate the core losses of so called DC-DC high power high frequency transformer without actual measurements on the prototype samples. This is true, especially considering nonlinear magnetic characteristics of the core materials [1]. References [2] and [9] present an overview of the selection procedures of the shell type and the loss calculations for transformers that will be implemented for high frequency non-sinusoidal wave shape applications. A shell type transformer is the best selection in the case of this application [2, 9].

1.3 Purpose

According to the highlights presented in previous section, to overcome the complexity of the core loss evaluation of an HPMF transformer, it is vital to manufacture a prototype transformer to be used for conducting the proper measurements and evaluation of the methods and theories applied for the designing of the transformer.

The main purpose of this master thesis is to construct and evaluate two high power medium frequency prototype transformers and verify the design. The transformers are designed for the Division of electric power engineering for studies on the losses and behaviour of these kinds of transformers.

Having the prototypes and using the available supplying equipment and measuring instrument, a set of preliminary measurements will be done to verify the design methodology of the transformers.

1.4 Contribution

Among the others, the results of this work are presented in a paper titled “Design Methodology and Optimization of a Medium Frequency Transformer for High Power DC-DC Applications” which has been accepted for presentation at the *“30th Annual IEEE Applied Power Electronics Conference (APEC) & Exposition”* to be held in Charlotte, North Carolina in March, 2015.

2 The transformer design

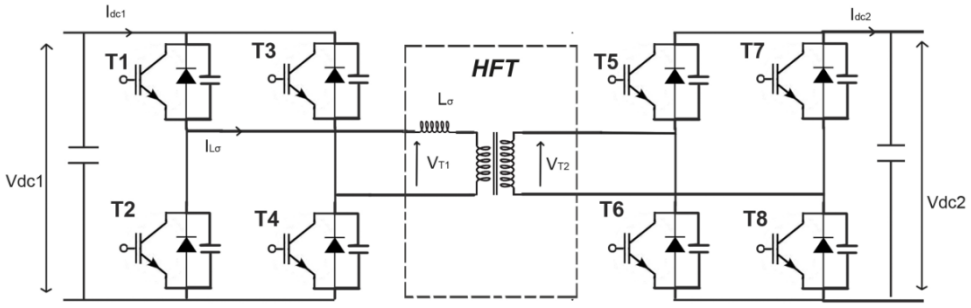

***Figure 2-1*: A transformer which serves as an inductance, in addition to its natural duty of voltage adoption and isolation between the DAB converter bridges [12].**

2.1 Calculations of dimensions based on defined leakage inductance and required insulation withstand voltage

A dual active bridge (DAB) converter for high power applications can benefit from a transformer leakage inductance (L_σ) to transfer the power between the input and output bridges and this will result in higher power density (see Figure 2-1). By controlling the switching on the two sides, the square wave voltage from the primary and the secondary converters will be adjusted to have a defined phase shift relative to each other. Such a transformer serves as an inductance, in addition to its natural duty of voltage adoption between the primary and secondary bridges. In the other words, the design of the transformer should fulfil the criteria of having a determined leakage inductance in addition to keeping the specified insolation, efficiency and the thermal requirements [12].

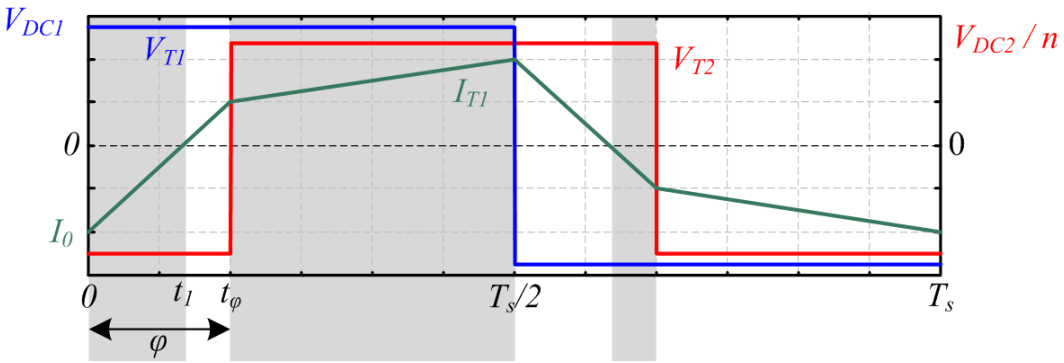

***Figure 2-2*: Expected voltage and current wave shapes and switching cycles of the transformer used in a DAB converter [1].**

Figure 2-2 shows the voltage and current wave forms applied to the HPMF transformer in a DAB converter. It is notable that, unlike a conventional low frequency transformer, the wave shapes are not sinusoidal for this case.

The core loss is highly dependent to the duty cycle and the rise time of the wave shapes [9]. The lowest loss is achieved at the zero voltage switching (ZVS) which occurs at the minimum phase shift, φ_{min} between the primary and secondary bridges. Therefore, in case of this type of transformer, the leakage inductance and its related phase shift is under consideration and the transformer leakage inductance, L_σ corresponds to the value calculated from (2.1) [12].

$$L_\sigma = V_{DC1} V_{DC2} \varphi_{min} (\pi - \varphi_{min}) / (2 P_{out} \pi^2 f n) \tag{2.1}$$

where
P_{out} is the output power of the DAB converter
V_{DC1} is the DC voltage of the LV side of the DAB converter
V_{DC2} is the DC voltage of the HV side of the DAB converter
n is the turns ratio of the transformer
f is switching frequency

An optimization flowchart is proposed which takes the rated power, the input and output voltages and their ratio, the frequency and the defined leakage inductance as input requirements and based on these, defines the fixed parameters like the core material, distances between the windings and between them and the ground in addition to the insulation materials properties. To optimize the design regarding the efficiency, size and the heat dissipation, a set of free parameters are chosen based on a set of iterative calculations. These include the core cross section, number of the turns per layer and number of layers, the thickness of rectangular wires and finally the maximum allowed current density [1]. The most important parameters to be decided about are the number of turns of the primary winding and the distance between the primary and the secondary windings [2].

Figure 2-3 demonstrates a typical 2D schematic of all the defined transformer dimensions.

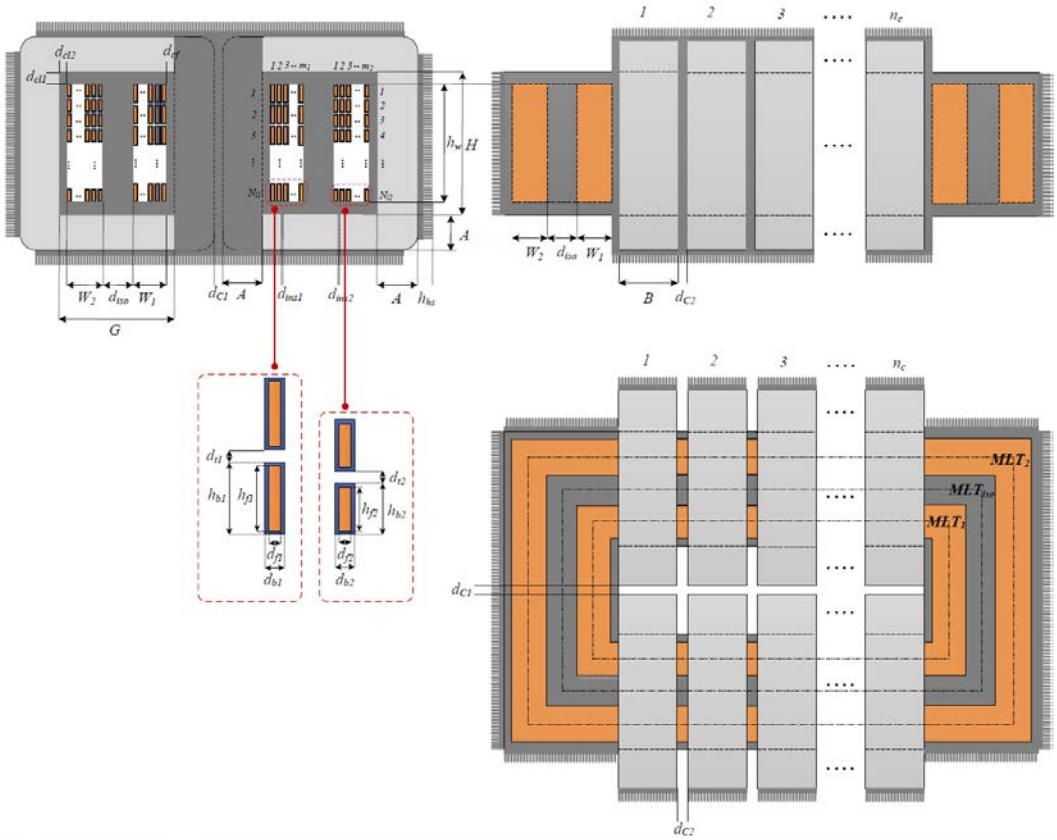

***Figure 2-3*: Illustration of the dimensional parameters of the design [1].**

The following formulas are used for calculation of the geometrical and isolation distances in the transformers [1].

$$A_c = V_{rms1}/(k_f k_c N_1 B_m f) \tag{2.2}$$

and

$$A_c = 2n_c AB$$

where
A_c is the cross section area of the core
n_c is the number of stacks of the core (Each stack includes 4 pieces of the U shaped core pieces.)
A is the length of the frontal side of the core
B is the length of the lateral side of the core
V_{rms1} is the RMS of the primary voltage
N_1 is the number of turns of the primary winding
B_m is 80% of the saturation level of the selected magnetic core (0.52T for Ferrite & 1.2T for Nano)
k_c is the filing factor of the core (the ratio of effective cross section of the core to its physical cross section: 1 for Ferrite cores and 0.75 for Nano cores)

$$k_f = 2\sqrt{2D - \tfrac{8}{3}R}/(D - R) \tag{2.3}$$

where
D is the duty cycle (0.5 for phase shift modulation in the DAB converter)
R is the relative rise time of the rectangular wave form (0 for phase shift modulation in the DAB converter)

$$d_{cf} = V_{DC1}/(k_{saf} E_{ins}) \tag{2.4}$$

where
d_{cf} is the clearance of the inner winding to the core
K_{saf} is the safety factor (30%)
E_{ins} is the dielectric strength of the isolating material (29 kV/mm for CoolPoly-D5108)

$$d_{cl1,2} = V_{DC2}/(k_{saf} E_{ins}) \tag{2.5}$$

where
$d_{cl1,2}$ is the horizontal or vertical clearance of the outer winding to the core

$$d_{iso-min} = V_{iso}/(k_{saf} E_{ins}) \tag{2.6}$$

where
$d_{iso\text{-}min}$ is the minimum allowed isolation distance between the windings (which should also fulfil the requirement regarding the desired leakage inductance)
V_{iso} is the isolation level between primary and secondary bridges (60 kV)

$$J_{max} = I_{T1}/[(h_{b1} - 2d_{ins1})d_{f1}] \tag{2.7}$$

where
J_{max} is the maximum allowable RMS value of the current density in the conductor
I_{T1} is the LV side current
h_{b1} is the height of the insulated LV wire
d_{ins1} is the insulation thickness of the LV winding
d_{f1} is the width (thickness) of the wire conductor

$$J_{max} = I_{T1}/[n(h_{b2} - 2d_{ins2})d_{f2}] \tag{2.8}$$

where
J_{max} is the maximum allowable RMS value of the current density in the conductor
I_{T2} is the HV side current
h_{b2} is the height of the insulated HV wire
d_{ins2} is the insulation thickness of the HV winding
d_{f2} is the width (thickness) of the HV wire conductor

$$I_{T1}(rms) = [\frac{nV_{DC1}+V_{DC2}}{nL_\sigma}]\sqrt{(4t_1^2 t_\varphi + T_s t_1^2 + 4t_\varphi^2 t_1 - T_s t_1 t_\varphi + T_s t_\varphi^2)/(3T_s)} \quad (2.9)$$

where
T_s, t_1 and t_φ are demonstrated in Figure 2-2.
I_{T1} is the LV side current and has an inverse relation with the targeted leakage inductance. It is also a function of phase shift. (At φ_{min}, there is a zero voltage switching in the DAB converter.)

$$h_w = (N_{l1} + 1)h_{b1} + N_{l1}d_{t1} \quad (2.10)$$

where
h_w is the winding height
N_{l1} is number of turns per layer of LV winding
d_{t1} is vertical distance between the wires

$$W_1 = m_1(d_{f1} + 2d_{ins1})(m_1 - 1)d_{ins1} \quad (2.11)$$

where
W_1 is the total thickness of the LV winding
m_1 is the number of layers of the LV winding

$$H = h_w + 2d_{cl1} \quad (2.12)$$

where
H is the core window height

N_{l2} and W_2 can be calculated similarly. The core window width, G and maximum dimension of the transformer are calculated having the d_{iso} which is the permitted isolation distance between the windings which also fulfils the requirement regarding the desired leakage inductance. The calculation of d_{iso} is presented in details in Reference [1].

2.2 The designed transformer

In this project the following information is used as the input for designing two 60 kW, 1.2/3.6 kV, 6 kHz 46/28 µH prototype transformers.

According to explained method, considering Coolpoly–D5108 as main insulation material and Ferrite and Nanocrystalline as the core materials, the dimensional parameters displayed in Figure 2-3 were calculated during the design process. The calculated results used for starting the manufacturing process are presented in the Table 2-1 [1].

***Table 2-1*: Optimized parameters for the prototype transformers [1].**

Ferrite		Nano	
Parameters/Dimensions	Values	Parameters/Dimensions	Values
n_c	5	n_c	2
A	28 mm	A	36 mm
B	30.3 mm -> 30 mm	B	27.4 mm -> 31 mm
G	25.9 mm -> 34 mm	G	31 mm -> 40 mm
h_w	85.5 mm	h_w	117.6 mm
H	87.5 mm -> 96 mm	H	119.6 mm -> 120 mm
d_{iso}	9.2 mm	d_{iso}	19.2 mm
N1/N2	21 / 63	N1/N2	20 / 60
n_{s1}/ n_{s2}	540 / 180	n_{s1}/ n_{s2}	540 / 180
$m_1 \times N_{l1}$	3 × 7	$m_1 \times N_{l1}$	2 × 10
$m_2 \times N_{l2}$	2 × 22 + 1 × 19	$m_2 \times N_{l2}$	2 × 30
$d_{b1} \times h_{b1}$	2.4 mm × 10.6 mm	$d_{b1} \times h_{b1}$	2.4 mm × 10.6 mm
$d_{b2} \times h_{b2}$	2.4 mm × 3.6 mm	$d_{b2} \times h_{b2}$	2.4 mm × 3.6 mm
d_{c1} , d_{c2}	3 mm , 3 mm	d_{c1} , d_{c2}	3 mm , 3 mm
d_{cf}	1 mm	d_{cf}	1 mm
d_{cl1} , d_{cl2}	1 mm , 1 mm	d_{cl1} , d_{cl2}	1 mm , 1 mm
MLT_1	483 mm	MLT_1	293 mm
MLT_2	615 mm	MLT_2	486 mm
d_{t1} , d_{t2}	0.1 mm , 0.1mm	d_{t1} , d_{t2}	0.1 mm , 0.1mm

Interlayer distances min 0.1 *mm*, max 0.4 *mm* (*HV*)
One insulation on three litz wires for the *LV* windings
$W_1+W_2+d_{iso}+d_{cf}+d_{cl}$ <= 34 *mm* for Ferrite
$W_1+W_2+d_{iso}+d_{cf}+d_{cl}$ <= 40 *mm* for Nano
d_{cf} or d_{cl} can be between 1 and 2 *mm*

In the Table 2-1:
n_c is the number of stacks of the core
A is the length of the frontal side of the core
B is the length of the lateral side of the core
G is the width of the core window
h_w is the height of the winding
H is the height of the core window
d_{iso} is the isolation distance between two windings
$N_{1,2}$ is number of the turns
$n_{s1,2}$ is number of the strands
$m_{1,2}$ is number of the winding layers
$N_{l1,2}$ is number of the turns per layer
$d_{b1,2}$ is the width of the litz wire
$h_{b1,2}$ is the height of the insulated litz wire
$d_{c1,2}$ is the distance between the cores
d_{cf} is the clearance of the inner winding to the core
$d_{cl1,2}$ is the clearance of the outer winding to the core
$MLT_{1,2}$ is the mean length of the winding turns
$D_{ins1,2}$ is the horizontal distance between the wires

Based on the above mentioned dimension data of two transformers, the calculation of the resistance of the winding and magnetising inductance of the cores are performed and presented here. Later in the Table 5-1, the calculated results are compared with the measured results.

2.3 Calculation of resistance of the windings

The winding resistance is calculated from the formula

$$R = \rho \frac{l}{A} = \rho(MLT * N)/(\pi r^2 n_s) \tag{2.13}$$

where
R is the resistance of the winding
ρ is the resistivity of the copper wire
MLT is the mean length of the winding turns
N is the number of the turns of the measurement side
r is the radius of the each wire strand
n_s is the number of the strands

The calculated magnetising inductances for both transformers are presented in Table 2-2 and these are compared with the measured results in Table 5-1.

***Table 2-2*: Calculated winding resistances.**

	Ferrite		**Nano**	
	HV	LV	HV	LV
ρ (Ω/m)	1.68×10^{-8}	1.68×10^{-8}	1.68×10^{-8}	1.68×10^{-8}
MLT (m)	0.615	0.475	0.510	0.295
N	54	18	48	16
r (m)	0.1×10^{-3}	0.1×10^{-3}	0.1×10^{-3}	0.1×10^{-3}
n_s	181	543	181	543
R (mΩ)	**98.1**	**8.4**	**72.3**	**4.6**

2.4 Calculation of magnetisation inductance

For the calculation of the magnetising inductances, the initial permeability should be extracted from the cores technical data sheets. Table 2-3 and Table 2-4 present the initial permeability values given by the producers of Ferrite and Nanocrystalline cores respectively.

***Table 2-3*: The technical data of the used Ferrite core material [13].**

N87

Material properties

Preferred application			Power transformers
Material			N87
Base material			MnZn
	Symbol	Unit	
Initial permeability (T = 25 °C)	μ_i		2200 ±25%
Flux density (H = 1200 A/m, f = 10 kHz)	B_S (25 °C) B_S (100 °C)	mT mT	490 390
Coercive field strength (f = 10 kHz)	H_c (25 °C) H_c (100 °C)	A/m	21 13
Optimum frequency range		kHz	25 … 500
Hysteresis material constant	η_B	10^{-6}/mT	<1.0
Curie temperature	T_C	°C	>210
Mean value of α_F at 25 … 55 °C		10^{-6}/K	4
Density (typical values)		kg/m³	4850
Relative core losses (typical values)	P_V		
25 kHz, 200 mT, 100 °C		kW/m³	57
100 kHz, 200 mT, 100 °C		kW/m³	375
300 kHz, 100 mT, 100 °C		kW/m³	390
500 kHz, 50 mT, 100 °C		kW/m³	215
Resistivity	ρ	Ωm	10
Core shapes			RM, P, PM, ETD, EFD, E, ER, EP, EQ, ELP, U, Toroid

***Table 2-4*: The technical data of Nanocrystalline Vitroperm 500 core material [14].**

Property	Nanocrystalline cores	Permalloy cores	Si-steel cores
Saturation induction (T)	1.25	0.76	2.03
Initial permeability (at 0.8 mA/cm)	40,000 ~ 80,000	> 80,000	1,000
Maximum permeability	> 250,000	> 200,000	40,000
Density (g/cm^3)	7.2	8.85	7.65
Curie temperature (°C)	570	400	740
Thickness (mm)	0.025 ~ 0.035	0.1	0.3
Stacking factor	≥ 0.75	0.9	0.95

The magnetising inductance can be calculated from (2.15).

$$L_m = {\mu_0 A_c N^2}\Big/{(\frac{l_c}{\mu_i} + l_g)} \tag{2.14}$$

where
L_m is the magnetising inductance of the transformer
$l_c = 2H + 2G + 4A$ is the length of the core
l_g is the inevitable air gap length
$A_c = 2n_c.A.B$ is the cross section area of the core
$\mu_0 = 4\pi \times 10^{-7}$ is the absolute permeability
μ_i is the initial permeability of the core
$N = N_1$ is the number of the turns of measurement side
n_c is the number of the core stacks

The calculated values of magnetising inductances for both transformers are presented in Table 2-5 and are compared with the measured results in Table 5-1.

***Table 2-5*: The calculated magnetising inductances for the transformers.**

	Ferrite	**Nano**
μ_i	2200±25%	40000
n_c	5	2
A (mm)	28	36
B (mm)	30	30
H (mm)	92	120
G (mm)	38	39
N_1	18	16
l_g (mm) *(assumption)*	0.4	0.1
L_m (mH)	**6.0**	**12.5**

Figure 2-4 shows a schematic 3D picture of the transformer that is expected to be manufactured during this project [1].

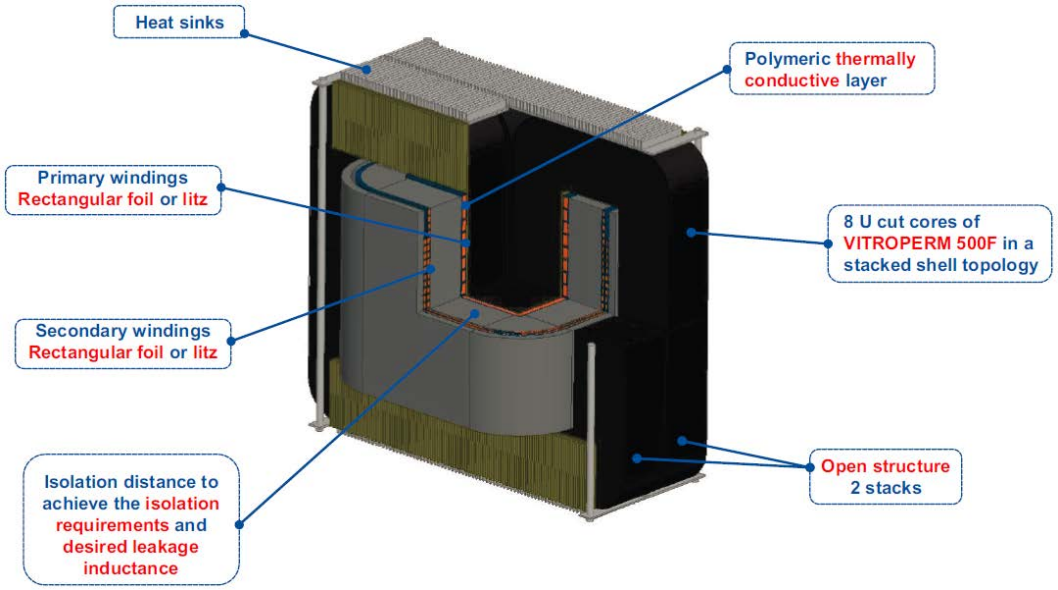

***Figure 2-4*: A schematic of the designed transformer to be manufactured during the project [1].**

3 Ferrite transformer

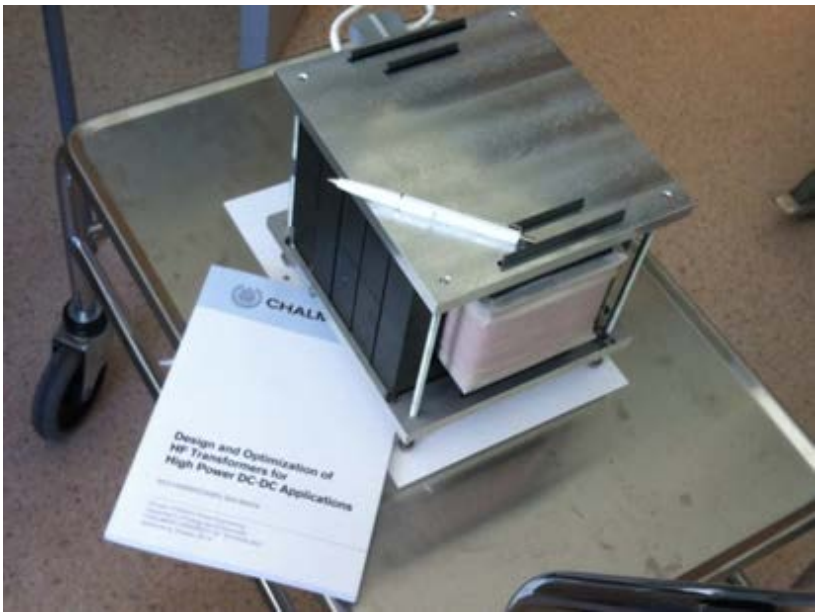

***Title photo*: The Ferrite transformer without heatsinks.**

3.1 Dimensioning the transformer

After having the preliminary design parameters as demonstrated in Chapter 2, the following parameters were considered to finalize the design dimensions of the prototype:

- the dimension of the core based on what is available in the market
- the dimension of the litz copper conductors based on what is available in the market
- The insulation characteristics of the material considered for production of the bobbins, insulation of winding layers and outer insulation of the conductors

3.1.1 Core material and dimension

The transformer under consideration consists of four U cores combined in a way that configure a three column core, in which the middle leg is wound (see Figure 3-1) [2].

***Figure 3-1*: One Ferrite core stack (left) compared with one Nanocrystalline core stack (right).**

For selection of the magnetic material to be used for the medium frequency high power transformer, four parameters shall be considered among the others: lower loss, higher saturation flux density, higher relative permeability and higher operation temperature. Higher power and loss density ask for higher endurance of the core material to the elevated temperature rating. Amorphous material has a higher saturation flux density but the losses in a transformer of the same rating with the Nanocrystalline core is much lower. Amorphous and Nanocrystalline are among the low loss and high saturation level ferromagnetic materials. Nanocrystalline and Ferrite are favoured to be used for manufacturing a medium frequency high power transformer. Ferrite has lower saturation level and this, results in a larger core cross section compared to a Nanocrystalline core used in a transformer with similar electrical ratings [9].

Table 3-1 presents the magnetic characteristics of three different magnetic materials [1].

***Table 3-1*: Sample magnetic characteristics of the different magnetic materials [1].**

Type	Material	Manufacturer brand	B_{sat} (T)	Specific losses (kW/kg) at 0.1T & 100kHz	Operating Temperature (°C)
Silicon Steel	10JNHF600	JFE	1.87	0.24	150
Ferrite	3C93	Ferroxcube	0.52	0.009	140
NanoCrys.	Vitroperm500F	VAC	1.2	0.01	120

Although Vitroperm 500F is the best available Nanocrystalline core material that has been used for production of similar transformers during previous research activities [1], a medium frequency Ferrite core material was used for the production of the first prototype. The advantages of using the Ferrite cores includes the lower price, better accessibility of the material in the market and possibility of studying pros and cons of using Ferrite in comparison with a Nanocrystalline core material. The selected core with the highest dimension available is [15]:

- U core N87, B67345B1X87
- Core combination U-U: Material = N87; AL value =5700 nH; μe =1900
- Manufacturer: EPCOS

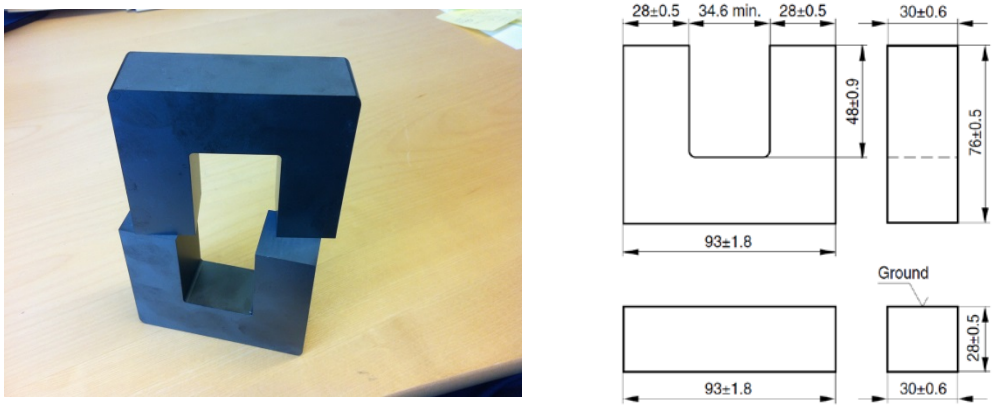

a **b**

***Figure 3-2*: The used Ferrite core appearance and the dimension [15].**

According to the transformer design, the parameter n_c introduces the number of stacks of the core. Each stack includes 4 pieces of the U shaped core pieces, with a UU configuration according to Figure 3-1. In the case of the Ferrite core, the window size will be 34.6×96 mm^2 and this is in agreement with the design parameters of a core window height H (87.5-96 mm) and width G (25.9-34 mm).

Some accessible suppliers in Sweden for this material are introduced in Appendix A.

3.1.2 Conductors type and dimensions

Because of the high skin effect at high frequencies it is not economical to use normal wires to produce the windings. Copper foils are suitable alternatives for higher frequencies but they need a great care during the production and termination. With the introduction of litz wires (bunch of individually insulated conductors), higher flexibility in the production and lower losses can be gained.

A high-frequency litz wire consists of a group of enamelled strands (see Figure 3-3). The enamel insulation of the conductor is modified polyurethane. At higher frequencies, increasing the number of strands together with the reduction of the strand's diameters, counteract the increase in conductor impedance. The alternating current causes eddy currents in the conductor which acts against the flow of current. At higher frequencies, the effect of these eddy currents increases and an AC resistance which is dependent on frequency is added to the DC resistance. The eddy current loss in the middle of the conductor is at its minimum value and increases moving toward the out of the conductor. This causes that the current to flow more close to the surface of the conductors instead of in the centre of it (the skin effect). The skin depth is a representation of the thickness of the conductor which is carrying the current. Because of the proximity effect, the fields of the adjacent conductors increase the eddy losses. The cross-sectional area of the single conductor is reduced to minimize these losses. Several conductors in parallel are used to carry the nominal current of the whole wire. To compensate the effects of the fields on the individual strands, the conductors are twisted together so that, throughout the length of the wire, the position of one conductor changes regularly between the centre and the outside of the bunch. Because of the high capacitance effect of the conductor, litz wires can be used only up to 2 MHz. A typical diameter of each conductor as a function of frequency is 0.4 mm for 50 Hz – 1 kHz, 0.25 mm for 1 kHz – 10 kHz or 0.032 mm for 1.5 MHz – 2.8 MHz [16].

With an effective reduction of skin effect, litz wires have the best performance in high frequency circuits. Commercial production of several types and dimensions of the wire gives a good flexibility for getting the highest benefit in this project. Having a rectangular cross section, the rectangular litz wire is estimated to be one of the best candidates as the high and low voltage conductors of his project. The rectangular cross section helps for higher density and more mechanical strength of the winding. The available constructions from one of the leading litz wires manufacturers are presented in pages 127-165 of the Reference [16].

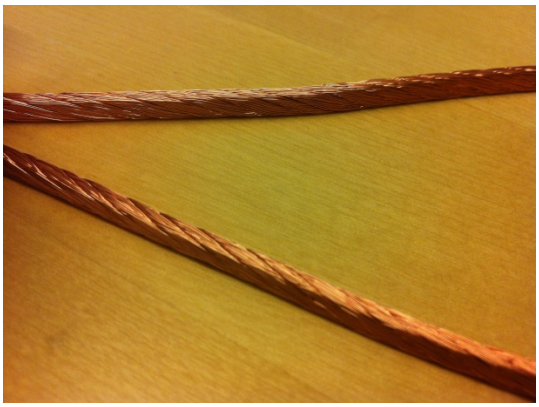

***Figure 3-3*: A rectangular litz wire.**

The wires considered for the prototype were:

- LV: 541 strands of 0.2 mm conductors, 7.0×4.0 mm^2 as total dimension
- HV: 181 strands of 0.2 mm conductors, 3.8×2.5 mm^2 as total dimension

The 541strands wire was not delivered and instead, a combination of three parallel 181 strands wire was used. According to the design, more than 60-80 meters of LV type (541 strands) and 120-130 meters of HV type (181 strands) were needed.

Some litz wire suppliers accessible in Sweden are introduced in Appendix A.

Table 3-2 was prepared and used to compare the price and the minimum delivery volume of the litz wires from the different manufacturers.

***Table 3-2*: Comparison table for selection of the best supplier of the litz wires.**

Manufacturer	Type designation	strand diameter (mm)	Fill factor of strands	Length	Price	price	Min. Delivery	Price
		mm	$1/cm^2$	m/kg	SEK/kg	SEK/m		SEK
Dahrentråd	Round copper wire	0.2	2012-2251	3247	500	0.153988	100 g	500
Dahrentråd	119 strands	0.2	-	27.28571	59500	2180.628		
NewE.	(17×7/36) ($3.9\times0.81mm^2$)	0.127	3767.014878	66.22517	5761.649	87.0009	305 m	26535.28
NewE.	(17×7/33) ($5.5\times1.1mm^2$)	0.18	1966.942149	33.0033	2422.334	73.39672	305 m	22386
Vonroll	(541/-) ($7.0\times4.0mm^2$)	0.2	1932.142857				100 kg	
Vonroll	(181/-) ($3.8\times2.5mm^2$)	0.2	1905.263158				50 kg	

The wire that was possible to purchase was a 3.80×2.50 mm^2 rectangular copper HF-litz wire, having 180 strands of 0.2 mm with the product name of Polysol 155 with the properties presented in Table 3-3 from Elektrisola Germany.

***Table 3-3*:.The supplied litz wire properties [18].**

Product name	Polysol155
Properties	Very good solder-ability and high thermal properties
Breakdown voltage (at 20 °C, 35% humidity)	180 V/µm
Solder-ability for grade 1 wires	0.7s / 370 °C & 0.5s / 390 °C

According to the technical data the wires have the breakdown voltage of 180 V/µm and based on the information received from the producer, having a wall thickness of 73 µm, the wires can withstand 2.5-3 kV to ground which means the breakdown voltage of maximum 6 kV between the wires (or turns in the case of a winding). However as it is explained in section 5.6, the breakdown voltage is much lower at the practical 6 kHz tests.

3.2 Other elements of the prototype

After determining the material and dimensions of the core and winding materials, the decision was made regarding insulation and cooling material, the parts used for fixing the coils and those for clamping the cores and also regarding holding the whole structure. Considerations for leading out and termination of the high voltage conductors were also made.

3.2.1 Insulation and cooling material

In a normal oil type power transformer, the oil has two main roles:

- to increase insulation level between the energized electrodes (and accordingly reduce the size of transformer) and
- to assist in the removal of produced heat from the heated up elements.

In this project, the transformer is a dry type transformer. For normal dry type power transformers a special mixture hardened with epoxy resin is used as insulation material which has enough thermal conduction to conduct the produced heat inside the windings to the cooling air. The other parameters to be considered are:

- the volumetric mass density of the material which helps with the reduction of the total weight of the transformer and
- the mechanical properties of the material at the transformer normal operation temperature which serves as a fixture for the core and coil assembly.

According to the explanations given under chapter 2, to fulfil the electromagnetic and electrical criteria, the windings should have a defined distance from each other and this distance should withstand the defined high voltage level. On the other hand, the insulation material should help for

conducting out the produced heat inside the windings out to the heat sinks on the outer surfaces of the transformer. A HPMF transformer having lower volume and higher loss density needs much higher thermal conductivity compared with a normal low frequency transformer [2]. These requirements call for a material with high insulation and high thermal conductivity. Searching the available materials in the market led to acquaintance with a new type of polymer, Coolpoly-D5506. The material has 10 W/mK as thermal conductivity and 46 kV/mm as insulation withstand voltage.

The purchasable main insulation and cooling material for this project was Coolpoly-D5108, a thermally conductive liquid crystalline polymer (see Figure 3-4) [19].

a **b**

***Figure 3-4*: The CoolPoly thermally conductive electrically isolative polymer granules (a) and produced sheets (b).**

Several parameters led to selection of this material for this purpose:

- Very high thermal conductivity (10 W/mK)
- Very high insulation withstand voltage (29 kV/mm)
- Very high temperature of deflection suitable for manufacturing the bobbins (>240 ºC)

The CoolPoly-D5108 supplier is introduced in Appendix A.

A set of insulating adhesive materials were selected to be used in the proper applications as will be described later in the report (see Figure 3-5).

a **b** **c**

***Figure 3-5*: The 3M tape (a), Electrolube paste (b), 3M epoxy (c).**

The tape (Figure 3-5a) considered as insulation between layers and as insulation between the winding and the grounded electrodes were selected as follows [20]:

- Tape 3M 8943
- Thermally conductive, 200MMX10M
- Thermal conductivity, 0.9 W/mK
- External length, 10 m
- External width, 200 mm
- Thickness, 0.2 mm
- Breakdown voltage, 55 kV/mm or 11kV/0.2mm

During the insulation tests which have been performed and presented later in this report, the actual breakdown voltage was proved to be much less than the mentioned level where the frequency was 6 kHz and the test setup was similar to the transformer under consideration in this project.

An accessible supplier of the insulating tape in Sweden is introduced in Appendix A.

The paste material (Figure 3-5b) considered for filling the possible air packets between the windings or the core and the polymer heat sink was [21]:

- Thermal Paste HTSP50T
- Thermal conductivity, 2.5 W/mK
- Dielectric strength, 18 kV/mm
- Resistivity, 1015 Ω/cm
- Density, 2.10 g/cm³@ 20 °C
- Silicon oil, metal oxide powder based
- Operating temperature, -50...+200 °C

To facilitate the possibility of potential improvements or repairs on the transformers, application of this paste was postponed up to the time when the heat run test is going to be performed on the transformer.

An accessible supplier of the thermally conductive paste in Sweden is introduced in Appendix A.

The glue (Figure 3-5c) considered to keep the bobbins' parts strongly together was [22]:

- Epoxy adhesive DP760
- Non-sag, two-part room temperature curing adhesive
- High temperature resistance
- Work life (minutes), 45-60
- Time to handling strength (minutes), 360-480
- Full cure (days), 7

The epoxy adhesive DP760 supplier accessible in Sweden is introduced in Appendix A.

Two heat sink plates were installed on two upper and lower pressing aluminium plates (see Figure 3-6).

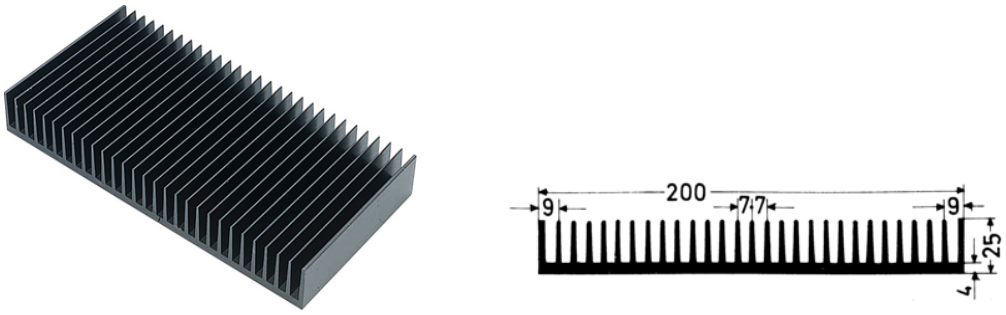

***Figure 3-6*: Heat sinks to be installed on the aluminium pressing plates [23].**

For the Ferrite transformer the suitable width was 200 mm and best selection was the one which helped for more mechanical strength along the longer direction of the pressing plate.

Although the width of the Nano transformer pressing bars were 142 mm, the same concept was applied and the bought heat sink for the Ferrite transformer was used for this transformer too.

The selected heat sink was the model, KS200, width: 200 mm, height: 25 mm and length: 1000 mm.
Two distributors are:

- Elfa (Model: KS200, width: 200 mm, Height: 25mm, Length: 1000 mm [23])
- RS components AB (Model: WA 217.0B, Width: 200 mm, Height: 25 mm, Length: 1000 mm [24])

To investigate more about the existing models, the following catalogues have useful information:

- Online catalogue Fischerelektronik [25]
- Online catalogue Austerlitz-electronic [26]

Some heat sinks suppliers accessible in Sweden are introduced in Appendix A.

To insulate the outgoing wires from adjacent grounded conducting surfaces a set of heat shrink tubing was used (see Figure 3-7).

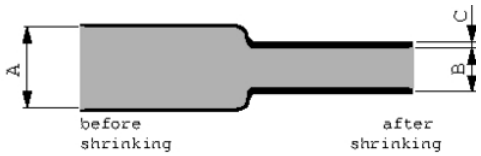

***Figure 3-7*: A heat shrink tube dimensions to be considered during a selection process [27].**

Three parameters were considered to select them among the others:

- High withstand voltage (here >30 kV/mm),
- High temperature withstand stability (here >175 ^{0}C),
- Proper dimension before and after shrinkage.

For LV side the following material was selected [27]:

- A, 12.7 mm
- B, 6.4 mm
- C, 0.3 mm
- Material, polyvinylidene fluoride (PVDF)
- Dielectric strength, ≥ 30 kV/mm
- Temperature range, -55 to +175 °C

For HV side the following material was selected [28]:

- A, 4.8 mm
- B, 2.4 mm
- C, 0.25 mm
- Material, polyvinylidene fluoride (PVDF)
- Dielectric strength, ≥ 30 kV/mm
- Temperature range, -55 to +175 °C

A heat shrink tubing supplier is introduced in Appendix A.

3.3 Production of the parts and the assembly

3.3.1 Moulding the polymer, producing the sheets, and manufacturing the coil bobbins

Safety cares were taken because of the strict safety precautions given in the MSDS-D5108 data sheet [29] and according to the information sticker on the 5 kg package received.

The required data for moulding was extracted from the product's processing guideline. The rear, centre and front zone temperatures in the moulding machine should be approximately 285, 310 and 320 °C consequently. The temperature of melt polymer is in the range of 310-330 °C and the mould should have a temperature of 135-180 °C.

For the produced sheet, the temperature of deflection is 276 °C at 0.45 MPa which means that the material is very hard at a low environment temperature. The tensile modulus is 23600 MPa which means that the material is very hard in its nature and the nominal strain at breaking point is 0.16 % which means that there is nearly a zero elongation possibility for the material.

A 280×210 mm^2 frame of 2 mm thick metal sheet was produced (see Figure 3-8b). This frame was used to keep the mould in itself under pressure and to form the polymer sheets.

The density of the material is 1.82 g/cc according to the data sheet, so to produce sheets for building bobbins for the two LV and HV windings having 2 mm of thickness and 280×210 mm^2, the amount of material needed to be moulded is approximately 250 g (see Figure 3-8c).

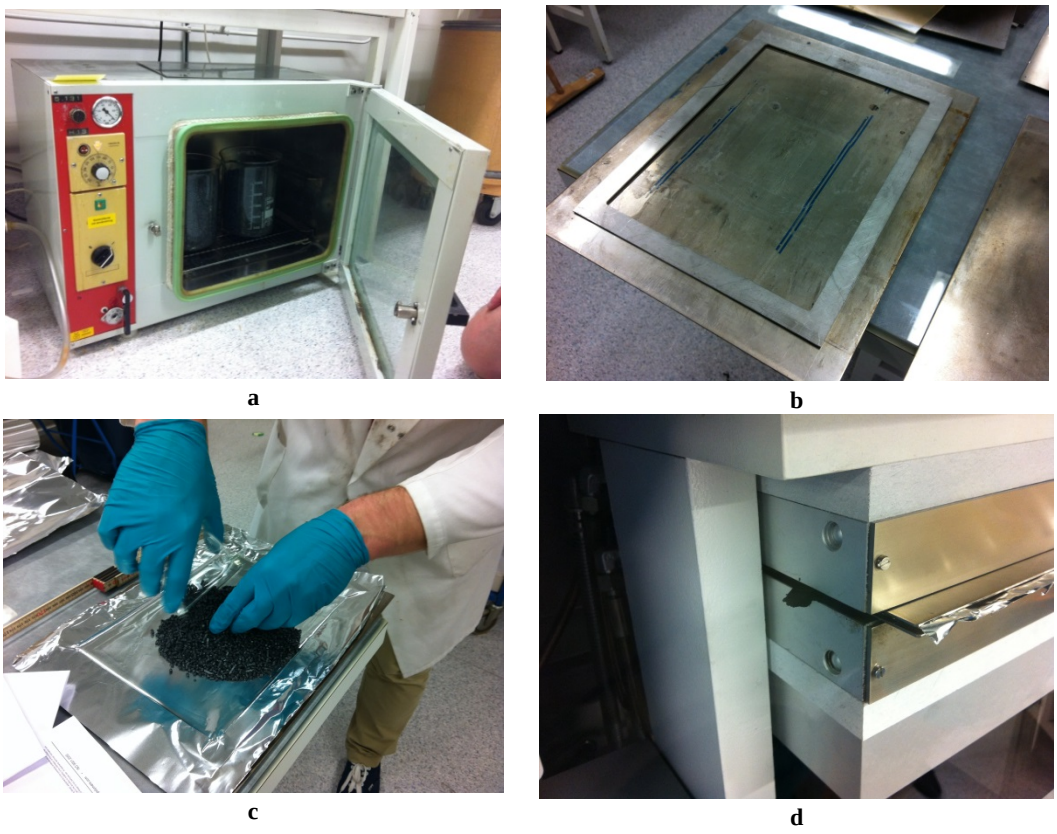

a **b** **c** **d**

***Figure 3-8*: The stages of production of the polymer sheets.**

To produce a 2 mm sheet, the granules are preheated for 5 minutes placed at 20mm distance between the upper and lower pressing jaws, after having 300 °C for the upper pressing jaw and 290 °C for the lower one. Then the pressing process was performed at 200 kN for 3minutes (see Figure 3-8d).

The whole process took 2-3 hours for each sheet considering the time required for heating up and cooling down the machine. If the granules are kept out of the sealed package for a long time, the material should be dried out at 120 °C for 4-6 hours in the heating chamber before starting the moulding process (see Figure 3-8a). According to the technical data, the injection moulding temperature is 310-330 °C which means that the selected 300 °C is suitable for a compression moulding process.

Using the prepared drawings presented in Appendix D, the produced sheets were then cut by a water jet cutting machine to have precise dimensions and 90 degrees edges. The cut parts are glued together using the high temperature epoxy glue (see Figure 3-9).

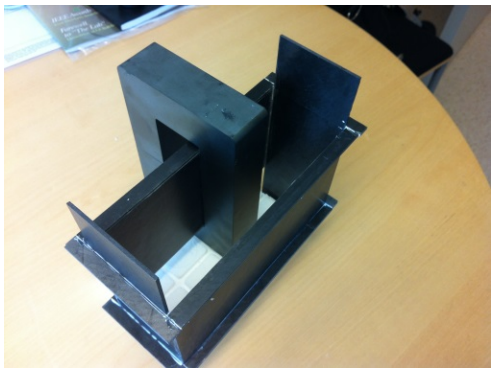

***Figure 3-9*: The glued polymer sheets.**

3.3.2 Winding the coils

As a rule of thumb, the length of the wire spent for each corner is equal to its thickness in the direction of the bending (here 4 mm). Therefore, having a bobbin of 165×70 mm^2 and bending thickness of approximately 4 mm and 4 bending edges, each conductor will have the length of 9324 mm.

For the LV winding, three 3.8×2.50 mm^2 litz conductors were placed on top of each other to form a 11.4×2.50 mm^2 conductor (see Figure 3-10a). The LV winding was coiled as 3 layers of 6 turns of conductors to have a total number of 18 turns. Based on the explained results of insulation coordination tests, one 0.2 mm layer of the thermally conductive tape was placed between every two winding layers.

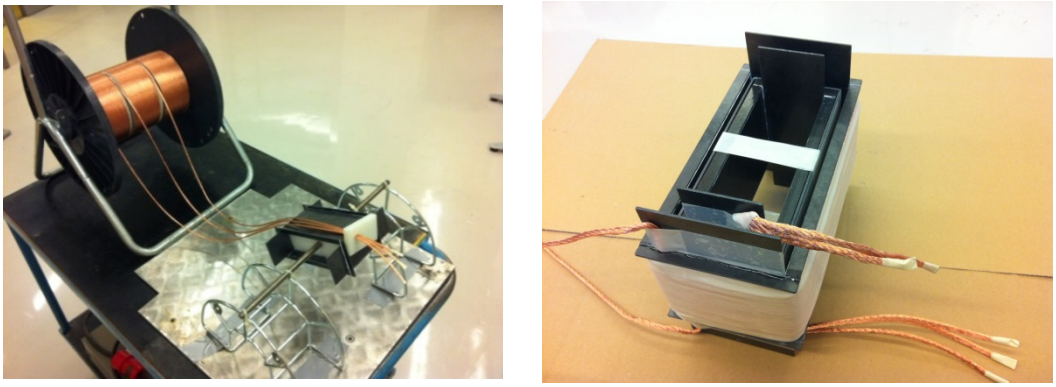

a **b**

***Figure 3-10*: Windings on the bobbins.**

The HV winding was coiled as 3 layers of 18 turns of 3.8×2.50 mm^2 litz conductor, having the total 54 number of turns. Based on the explained results of insulation coordination tests, presented in Section 5.6, two 0.2 mm layers of thermally conductive tape were placed between every two winding layers. The completed windings are demonstrated in Figure 3-10b.

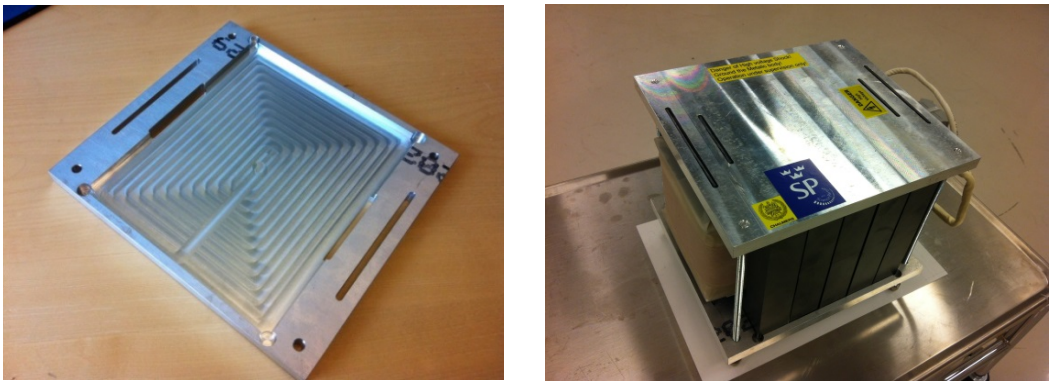

***Figure 3-11*: Pressing plates of the core and coil assembly.**

3.3.3 Pressing the core and coils assembly using the aluminium plates

The mechanical design of the transformer was performed targeting the usage of a minimum number of mechanical fixing parts. No additional material is used for keeping the distances and the coil and core assembly were fixed using only four nuts.

Two aluminium plates were designed according to the drawing presented in Appendix D and produced by a CNC cutting machine at SP's work shop. The plates, each 12 mm thick, were screwed together at the points 192 mm apart from each other (see Figure 3-11). This caused to experience bendings in the longitudinal direction of the two pressing rectangular plates. To improve and strengthen the pressing uniformity on the all core stacks, the direction of the heat sinks blades was considered to be in a direction which helps the pressing plates to have a better strength in the longitudinal direction. In this way the construction was improved after fixing the heat sinks to the plates.

3.3.4 Soldering the conductors and terminating the windings

Because of having a film insulated multi strand wire, care must be taken to remove the required amount of insulation of all the individual strands before applying a tin soldering process to the wire.

Figure 3-12 shows the setup used for this purpose and the result of the soldering work. More details regarding the soldering of litz wires can be found in Reference [29].

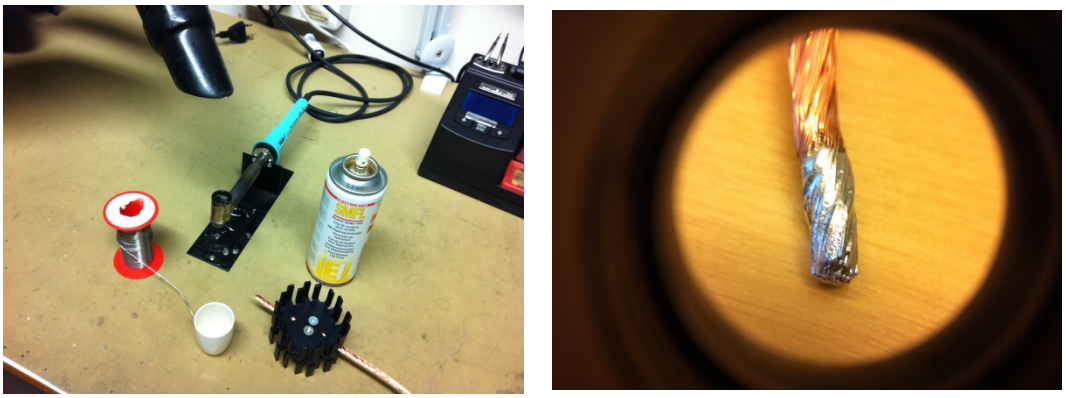

***Figure 3-12*: Soldering the litz wires.**

3.4 Extraction of the actual parameters for the transformer

During the construction of the transformer and having access to the real data from purchased materials and manufactured components and typical dimensions, the design parameter values were finalised. The final updated data is presented in Table 3-4.

***Table 3-4*: The mechanical design values updated with the construction of the Ferrite transformer [1].**

Parameters/Dimensions	*Values*
n_c	5
A	28 mm
B	30 mm
G	34 mm
h_w	88 mm
H	92 mm
d_{iso}	9.6 mm
N1/N2	18 / 54
n_{s1} / n_{s2}	540 / 180
$m_1 \times N_{l1}$	3 × 6
$m_2 \times N_{l2}$	3 × 18
$d_{b1} \times h_{b1}$	2.5 mm × 11.4 mm
$d_{b2} \times h_{b2}$	2.5 mm × 3.8 mm
d_{c1} , d_{c2}	2 mm , 2 mm
d_{cf}	2 mm
d_{cl1} , d_{cl2}	2 mm , 2 mm
MLT_1	475 mm
MLT_2	615 mm
d_{ins1} , d_{ins2}	0.2 mm , 0.4 mm

4 Nanocrystalline transformer

***Title photo*: The Nanocrystalline transformer without heatsinks.**

4.1 The cores

The second transformer design is based on Vacuumschmelze Vitroperm® 500 Nanocrystalline as the core material [31].

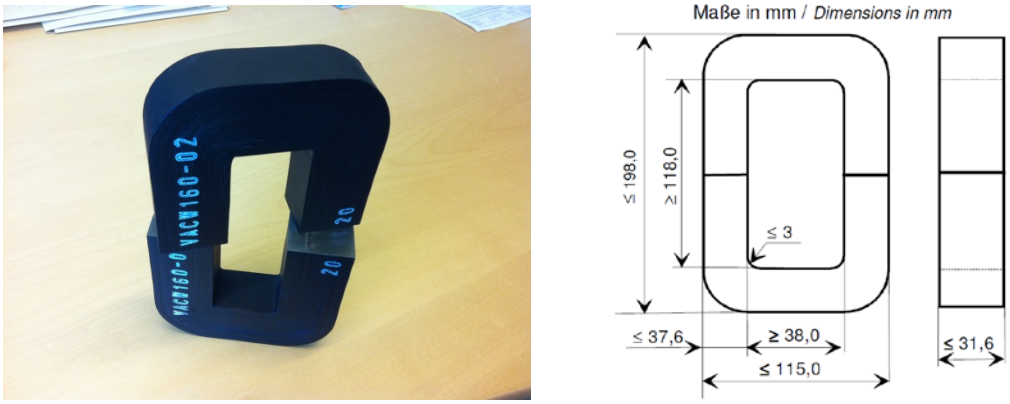

***Figure 4-1*: Delivered core and its drawing [32].**

The delivered cores have the cross section of 35.6×29.6 mm^2 instead of 37.6×31.6 mm^2 which was given in the technical data (see Figure 4-1). Therefore, the design of the transformer was done based on the actual measurements rather than the dimensional data presented in the datasheets.

4.2 The bobbins

To manufacture the bobbins, the polymer sheets were produced based on the similar concepts as presented in Chapter 3. The total weight of the polymer material used for two prototypes was 4.7 kg.

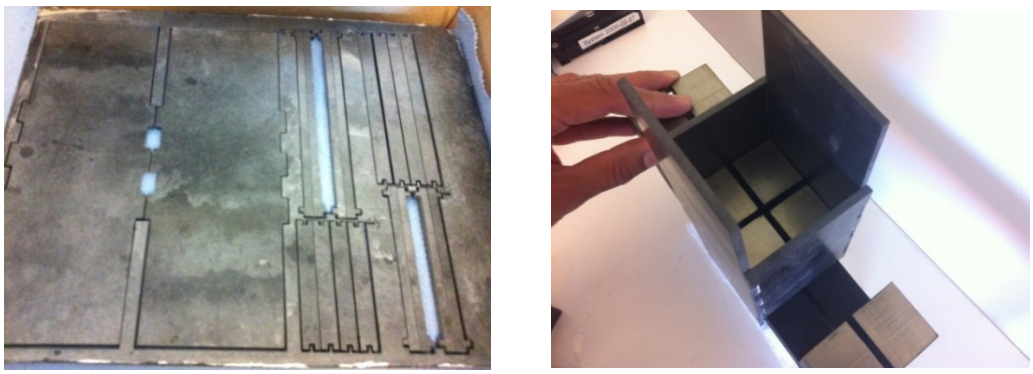

Figure 4-2: Corrugated 4 mm polymer sheets and the produced bobbin.

Based on the experience gained during the manufacturing of the first Ferrite sample, as an improvement, a thickness of 4 mm was considered for the sheets. In addition, to improve the fitting of the pieces together, the edges of the plates were cut along a square wave pattern. This gives the possibility for an easier assembly process, a better thermal conductivity between the sheets and a higher mechanical strength to the bobbins (see Figure 4-2).

The drawings were made using the free LibreCad 2007 software which can directly be used as input file for the water jet cutting machine. The requirement for the drawings was to have 5mm clearance on the sides and 0.8 mm between the cut parts. The drawings for the Nano transformer are presented in Appendix D.

To produce the 4mm sheets, the granules are preheated for 6 minutes placed in the minimum distance between the upper and lower pressing jaws, after having 300 ^{0}C for the upper and the lower pressing jaws. The pressing process was performed at 200 kN for 5 minutes.

The cut parts are glued together using the introduced high temperature epoxy glue.

4.3 The windings

Three 3.8×2.50 mm^2 litz conductors were placed on top of each other to form a 11.4×2.50 mm^2 conductor. The LV winding is coiled as 2 layers of 8 turns of conductors to have a total number of 16 turns. Based on the explained results of the insulation coordination tests, two 0.2mm layers of thermally conductive tape were placed between the two winding layers.

The HV winding was coiled as 2 layers of 24 turns of 3.8×2.50 mm^2 litz conductor, having the total 48 number of turns. Based on the explained results of the insulation coordination tests, three 0.2mm layers of the thermally conductive tape is placed between every two winding layers.

All the cavities besides the windings were filled with the cooling polymer pieces. This increases the heat transfer capacity of the winding medium and decreases the vibration of the conductor. Lower vibration gives a longer life to the insulation, decreases the noise and gives more short circuit withstand capability to the winding (see Figure 4-3a).

The windings were covered by the frames of cooling polymer. Using the plates both under and over the copper windings helps to keep the conductors exactly in the required distance from each other. In this way the dimensional requirements are fulfilled and consequently, the electrical parameters of the transformer become near to the targeted design values. In addition, this helps for improvement of the heat conduction from all the surfaces of the windings and also to reduce the sound and vibration of the windings which is produced by the high current they carry. In addition, this increases the electrical insulation to the nearby conducting surfaces (see Figure 4-3b).

a **b**

***Figure 4-3*: Winding on the bobbins: the filling polymer piece (a) and the winding cover (b).**

4.4 The pressing assembly

According to the drawing presented in Appendix D, two aluminium plates were designed and cut by a CNC cutting machine at SP. The plates were selected to have a 30 mm thickness instead of the 12 mm for the previous design. This was done to improve the undesirable bending condition of the plates and for a better fixation of the curved core edges.

4.5 The conductors high voltage terminations

The transformer terminations were designed considering the three parameters of the mechanical strength, the voltage and the rated current.

To standardize the high voltage terminations, a set of standard supporting insulators were used; a 1000 V insulator for LV and a 3000 V for HV (see Figure 4-4a) [33]. Some accessible suppliers of supporting insulators in the region are introduced in Appendix A.

Considering the cross section of the cables and diameter of the screwing bolt, two types of cable shoes were selected (see Figure 4-4b). The cable ends are soldered in the soldering bath, then they are pressed in the cable shoe and final soldering was performed.

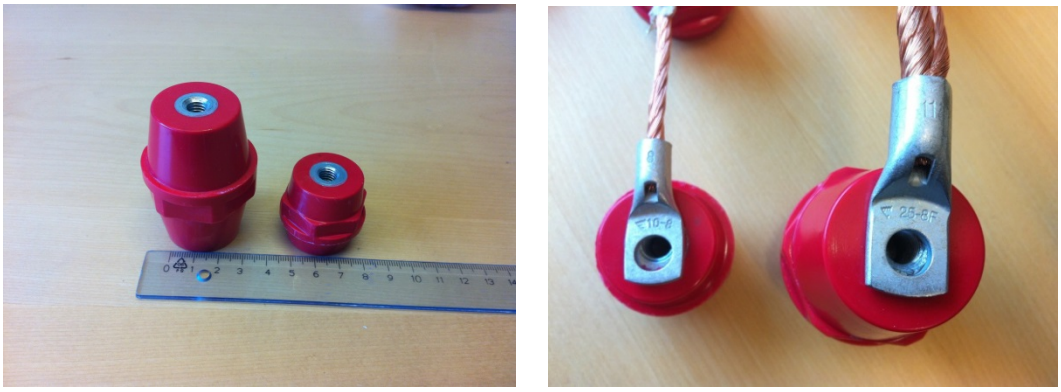

a **b**

***Figure 4-4*: The high and low voltage side terminals and the cable shoes.**

4.6 Extraction of the actual parameters for the transformer

During the construction of the transformer and having access to the real data from purchased materials and manufactured components and typical dimensions, the design parameter values were finalised. The final updated data is presented in Table 4-1.

***Table 4-1*: The mechanical design values updated with the construction of the Nano transformer [1].**

Parameters/Dimensions	*Values*
n_c	2
A	36 mm
B	30 mm
G	39
h_w	112 mm
H	120 mm
d_{iso}	21.5 mm
N1/N2	16 / 48
n_{s1} / n_{s2}	540 / 180
$m_1 \times N_{l1}$	2 × 8
$m_2 \times N_{l2}$	2 × 24
$d_{b1} \times h_{b1}$	2.5 mm × 11.4 mm
$d_{b2} \times h_{b2}$	2.5 mm × 3.8 mm
d_{c1} , d_{c2}	4 mm , 4 mm
d_{cf}	4 mm
d_{cl1} , d_{cl2}	4 mm , 2 mm
MLT_1	295 mm
MLT_2	510 mm
d_{ins1} , d_{ins2}	0.3 mm , 0.6 mm

5 Test and analysis

The main purpose of the testing is to validate the design parameters. However, additional tests relevant to the low frequency power transformers are defined to help to discover the differences and additional considerations for designing the next prototypes.

5.1 Standard tests for low frequency power transformers

After more than hundred years of production of power transformers, the methods of type and routine tests that should be performed on these types of high voltage equipment are well established and the details are internationally accepted. Although the methods are not directly applicable for the transformer that is under consideration in this project, listing the related tests will help as a guide for applicable tests and selectable methods for this special case. Considering the whole commercial productions of new types of medium frequency power transformers, it is clear that technical standards will be developed and released in this regard in future.

A list of standardized tests on dry type medium sized power transformers is presented in Appendix B [40].

5.2 Test equipment

The list of test equipment which is used during the project is presented in Appendix C for future reference and in case it is needed for possible repetition of the tests. A benefit of having the list is much shorter time to search for the proper equipment during a future work.

5.3 Preliminary tests on a downscaled transformer

As it is explained in Section 2.1, unlike a conventional low frequency transformer, the voltage and current wave forms applied to the HPMF transformer in a DAB converter are not sinusoidal. Therefore, to investigate the possibility of feeding a transformer with a high current, high voltage, and medium frequency source before delivery of the ordered materials, a 1:3 transformer was manufactured using an existing round Ferrite core and pieces of existing litz wires. The transformer was short circuited and supplied with a square wave produced by a signal generator and amplified by an audio power amplifier which was loaded by a set of high power 4 Ω resistors. A scope meter was used to register the supply side voltage and current wave shapes. The current was measured using a high precision current shunt (see Figure 5-1).

a

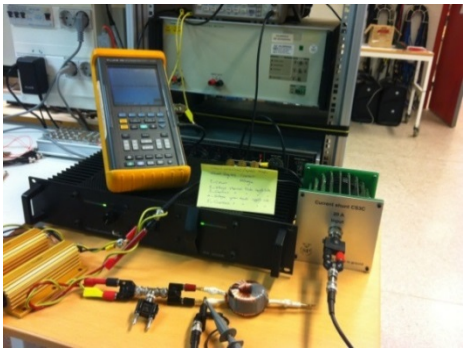

b

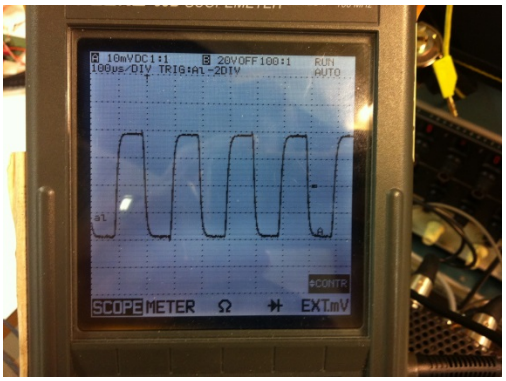

c

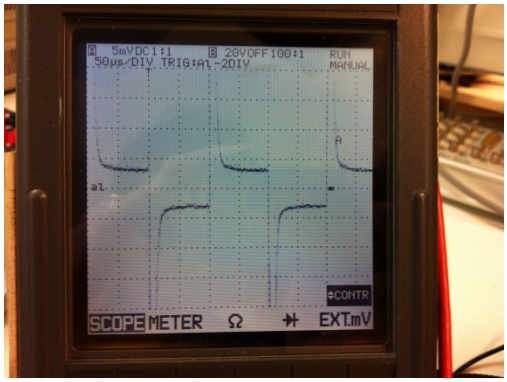

d

***Figure 5-1*: Investigations on a typical short-circuited Ferrite transformer supplied with a 5 kHz square wave voltage; The 1:3 Ferrite transformer (a), the circuit (b), the voltage wave shape (c) and the current wave shape (d).**

5.4 Resistance and inductance measurements

5.4.1 DC resistance measurement

DC resistance of HV and LV sides of the transformer were measured using a Fluke 8508A multimeter and the results are presented in Table 5-1 (see Figure 5-2).

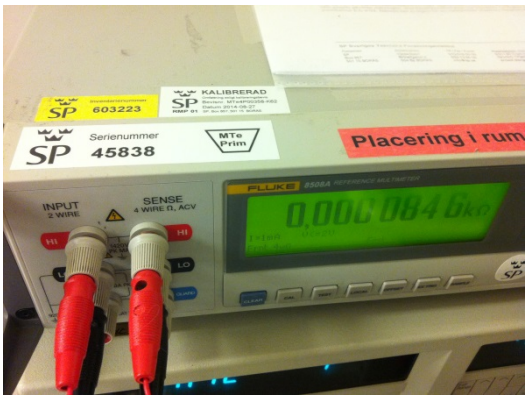

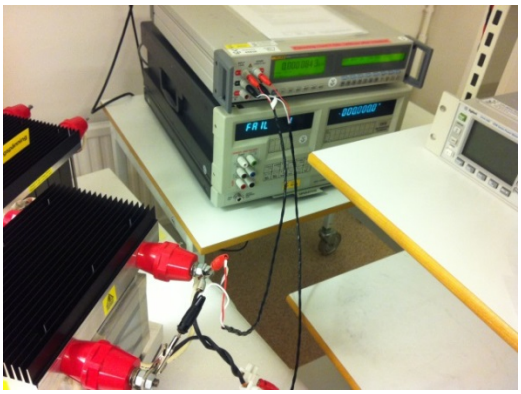

***Figure 5-2*: LV Resistance measurement using a reference multimeter and the 4 wire method.**

HV/LV resistance measurements were repeated using the volt-ampere method at 2 A (current measurement using SP's 0.4 Ω shunt) and the results were the same.

5.4.2 Inductance measurement

The leakage and magnetising inductance values were measured using a precision LCR meter. Measurements were made at 6 kHz from the LV side of the transformers. The results are presented in Table 5-1.

a **b**

***Figure 5-3*: A precision LCR meter (a) and a network analyser coupled with a test fixture (b).**

***Table 5-1*: Results of the inductance and resistance measurements.**

		Ferrite transformer				Nanocrystalline transformer			
		HV		LV		HV		LV	
		Meas.	Cal.	Meas.	Cal.	Meas.	Cal.	Meas.	Cal.
Secondary, open circuit	Ls (mH)	-	-	6.5	6.0	-	-	12.0	12.5
	Rdc (mΩ)	109.8	98.1	10.2	8.4	85.6	72.3	7.9	4.6
Secondary, short circuit	Ls (µH)	-		39.3	46	-		29.2	28

The inductance measured at the open circuit condition is the magnetising inductance of the transformer. An accurate measurement can be done after the demagnetising process. The core can become magnetised after a DC resistance measurement or even during the production process at the production stage. The other deviation source for the measured inductance can be any possible air gap in any of the core stacks which is inevitable. The presented values are calculated with the assumption of an air gap distance over the magnetic circuit.

For the DC resistance measurements, the deviations from the calculated values are in the range of 11-42 %. The deviations can originate from using a very low current for the measurements compared with the high rated current of the windings. During the future work, the resistances can be measured on windings without the cores and at a higher current level. Disassembling the cores eliminates the effect of the core magnetisation current on the resistance measurement. The terminating cable shoes can be re-soldered in case of a high deviation from the calculated values.

The inductance measured at the short circuit condition is the leakage inductance of the transformer. There is an acceptable agreement between the measured and the calculated values.

Because of importance of the leakage inductance value, the single frequency measurements which had been performed using a LCR meter were repeated using an Agilent network analyser coupled with a HP16047C test fixture. The leakage inductance measurement has been performed over the range of 1-10 kHz for both the transformers. The instruments used for inductance measurements are presented in Figure 5-3 and the results are presented in Figure 5-4.

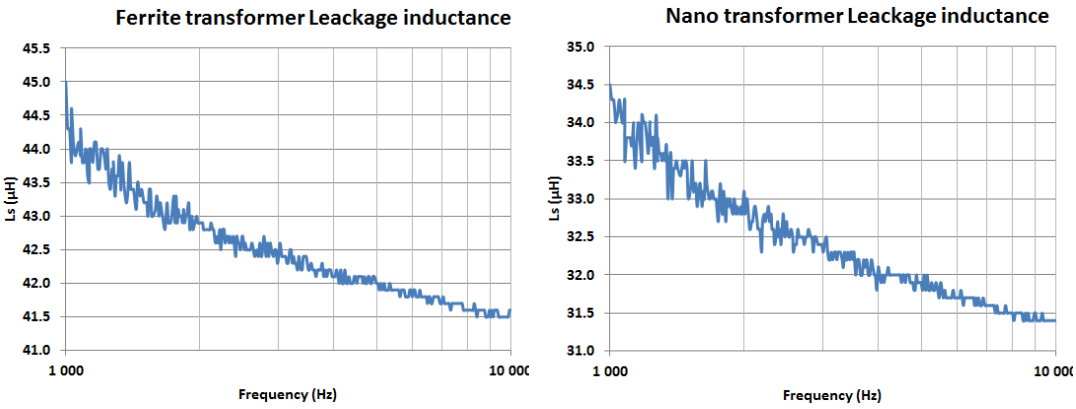

***Figure 5-4*: The leakage inductance at one to ten kHz frequency sweep using a network analyser.**

5.5 Ratio measurement

Transformer voltage ratio was controlled by applying 6 kHz low voltage to the primary side of the transformers and measuring the secondary side voltage. The results were equal to the specification and no inter-turn short circuit observed.

Any turn to turn short circuit inside any of the windings can cause a circulating current to pass in the winding. This circulating current opposes the flux in the core and causes the voltage on the secondary side to be much less than the expected value calculated from the ratio of the numbers of the turns.

5.6 Insulation coordination tests

Due to the normal application purpose of the insulation materials, the presented data in the insulation material data sheets are normally achieved doing DC or 50Hz insulation tests. As the insulation of the conductors and the isolative coverage of the winding layers and its corners by a layer of insulation are very important for insulation coordination of the transformer, using the actual voltage wave shape and the frequency, a set of simulated insulation tests were performed.

Considering proper safety factors, the number of insulation layers between the winding layers and between the windings and grounded electrodes were examined. The evaluated thickness of required insulating tapes was entered in the construction schemes.

5.6.1 Insulation tests at 50 Hz using a 5 kV insulation tester

According the information achieved from the producer, the litz wires used, having a wall thickness of 73 µm, can withstand 2.5-3 kV to ground. In addition, according the product data sheet, the thermally conductive tape used, having a thickness of 0.2 mm, can withstand 11 kV if it is tested between two high-voltage electrodes of a standard shape. To check the actual limits for the transformer construction geometry, two test specimen were set. In the Figure 5-5, the prepared test objects (a&b), the high voltage supply (c) and the peak voltmeter (d) used is shown.

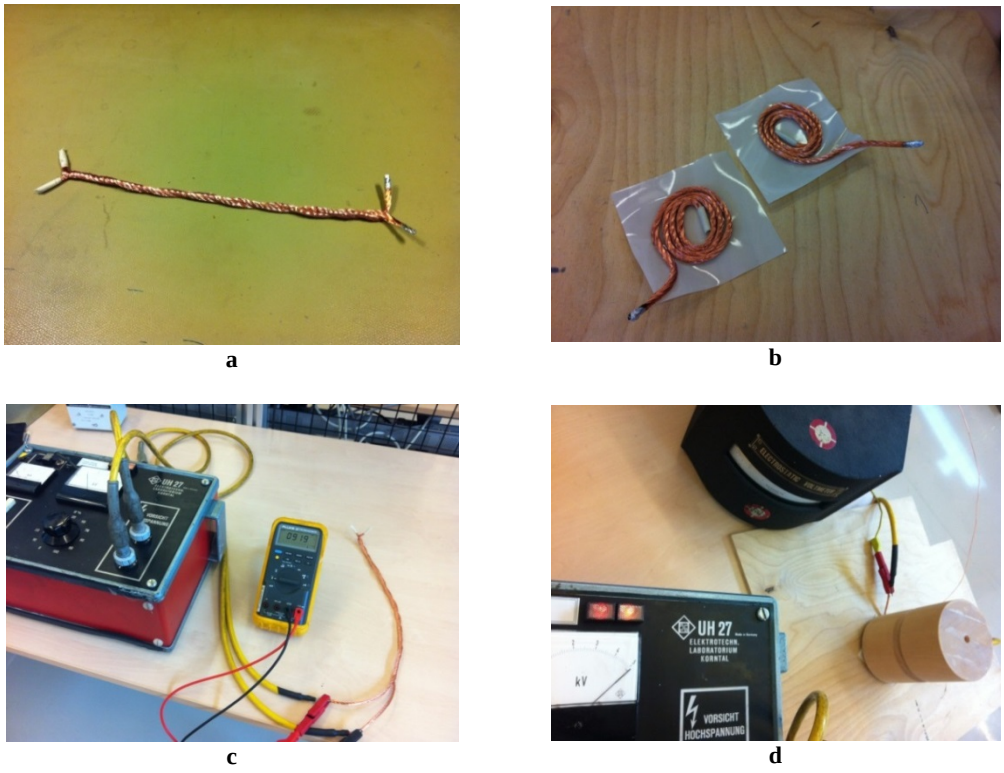

***Figure 5-5*: 50 Hz insulation tests; The wire to wire object (a), the wire-insulation-wire object (b), the 5kV HV supply (c)and a pressing log and the peak voltmeter (d).**

The withstand tests presented in Table 5-2 showed that the bare lacked wire's withstand voltage is <900 V and the bare lacked wires insulated by a layer of insulating tape withstand voltage is >5 kV. The test results dictates placing a layer of insulating tape even for the LV side of the transformer where the voltage between the two adjacent wires can reach up to 800 V.

***Table 5-2*: The test setup and the breakdown voltages at 50Hz test.**

	Test setup	**Failure voltage RMS (kV)**
wire-one layer insulation-wire	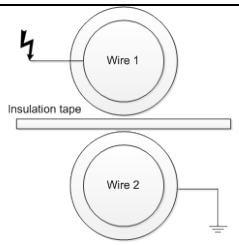	>5 (No failure accrued)
wire-wire	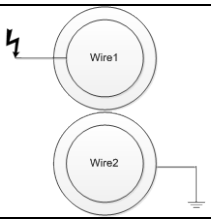	0.9

The tests performed on the Ferrite transformer after these insulation tests showed that the insulation level may decrease applying a high frequency voltage. For different insulation materials used in the project, a study was required to investigate the relation of insulation strength and the power frequency. A 6 kHz sinusoidal PWM amplifier was used to do the high frequency tests on one of the prototype transformers and later also on the different insulation systems used in the project.

5.6.2 Insulation test at 6 kHz on the Ferrite transformer

To evaluate the suitability of a 6 kHz sinusoidal PWM source for the insulation tests of the produced transformers, a test setup was arranged according to Figure 5-6.

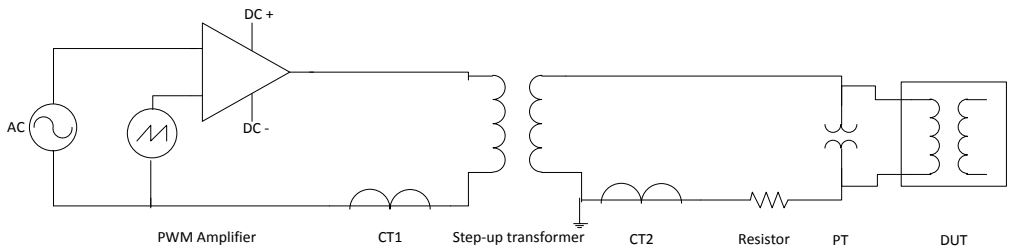

***Figure 5-6*: The circuit for insulation test on the prototype transformer.**

At the first stage a 6 kHz 1200 V sinusoidal voltage was successfully applied to the HV side of the Ferrite transformer. At the second stage the supply side was changed to the LV side to supply the transformer with its nominal voltage.

The following equipment, instrument and settings are used for the testing (see Figure 5-7):

- Signal generator (output voltage: 2.2 V_{p-p}, 6 kHz)
- PWM amplifier (gain setting: 50)
- DC supply (setting: 250V)
- CT2: 50 A/5 V, Pearson wide band current monitor (measured transformer input current: 100 mA)
- CT1: 400A/4V, Pearson wide band current monitor to measure the step-up transformer primary side current (measured value: 23 A)
- Step-up transformer: 600 V/3 kV, 333 A/(9.1A@22kV)
- PT: 3 kV/100 V, MWB standard voltage transformer
- Resistor: 33 Ω, 9 A
- HP34401A multimeters for measurement of currents and voltages

a **b**

c **d**

e **f**

g **h**

***Figure 5-7*: The circuit elements to supply 1200V to the Ferrite transformer from HV side; The test object (a), the voltage transformer (b), the signal generator and multimeters (c), the PWM and DC source (d), the step up transformer (e), the resistance (f), the 400 A Pearson current transformer (g) and finally the 50 A Pearson current transformer (h).**

The test was not successful. Investigation presented in next section shows that according to the wave shape presented in Figure 5-12, the applied voltage has had much high frequency content and it reached 3-4 times of the measured RMS voltage. As a result, this source was not a suitable source to be used for testing of the transformer.

5.6.3 Insulation tests at 6 kHz using a PMW amplifier

Figure 5-8 , Figure 5-9, Figure 5-10 and Figure 5-11 demonstrate the test setup used for insulation tests at a sinusoidal 6 kHz voltage.

a

b

***Figure 5-8*: A 35A fuse (a) is used in the primary side of step-up transformer (b) to protect the test equipment.**

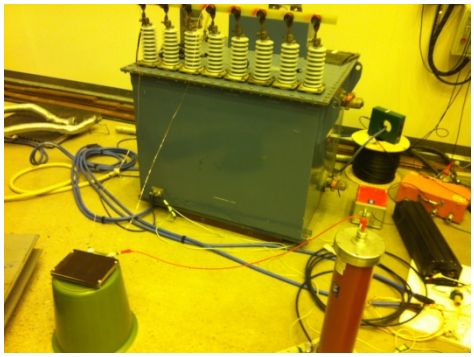

a

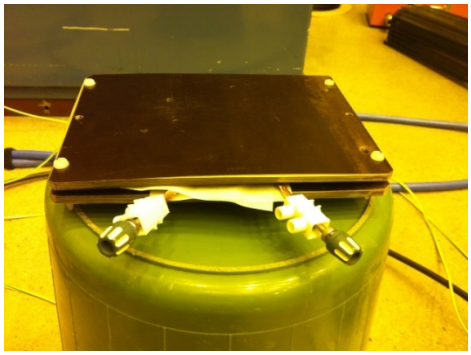

b

***Figure 5-9*: Test circuit arrangement overview (a) and the pressing bakalite plates over two under test electrodes (b).**

a

b

***Figure 5-10*: Two test object arrangements, wire to grounded plate (a) and wire to wire with an insulating tape layer in between (b).**

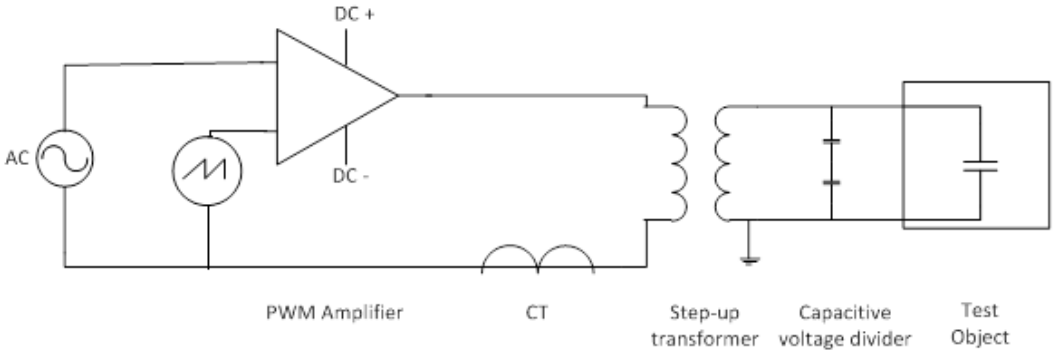

***Figure 5-11*: The circuit for insulation test on different conductor-tape combinations.**

The applied voltage wave shape was recorded using a Tektronix oscilloscope. The output voltage of the PWM amplifier was 150 V over the test object and 150×600/9900=9 V at the output of the PWM (see Figure 5-12). It was observed that the noise level remained the same with increased voltage level.

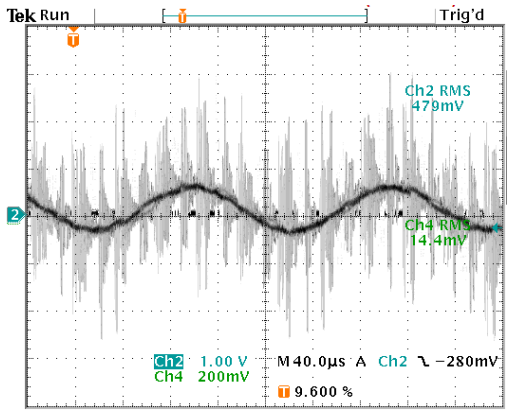

***Figure 5-12*: The output wave shape of the PWM amplifier.**

The withstand tests recorded using a modular data acquisition system named DEWE-50-USB2-8 (see Figure 5-13a). The voltage measurement was done using a compressed gas capacitor in series combination with an AC divider low voltage arm as a 6700V:1V capacitive voltage divider instead of the pre-mentioned standard voltage transformer (see Figure 5-13b). The reason was to protect the very expensive lab equipment from experiencing a failure during the withstand tests and to investigate the possibility of using a capacitive voltage divider for measurement of the 6 kHz voltage. A pre-calibration of the voltage measurement system is performed using the standard voltage transformer at a low voltage level.

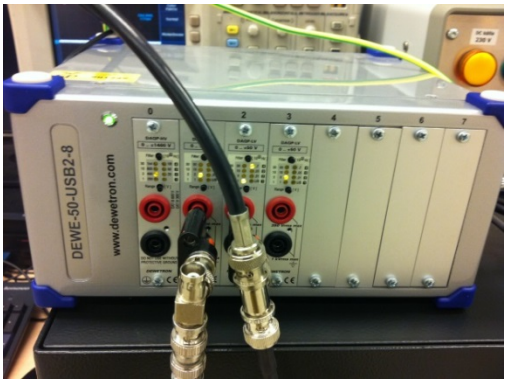

a

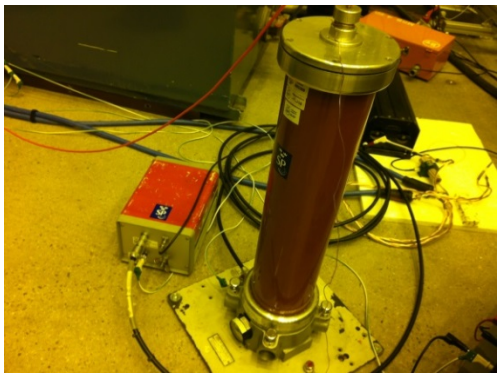

b

***Figure 5-13*: The DEWE recorder (a) and the capacitive voltage dividing system (b).**

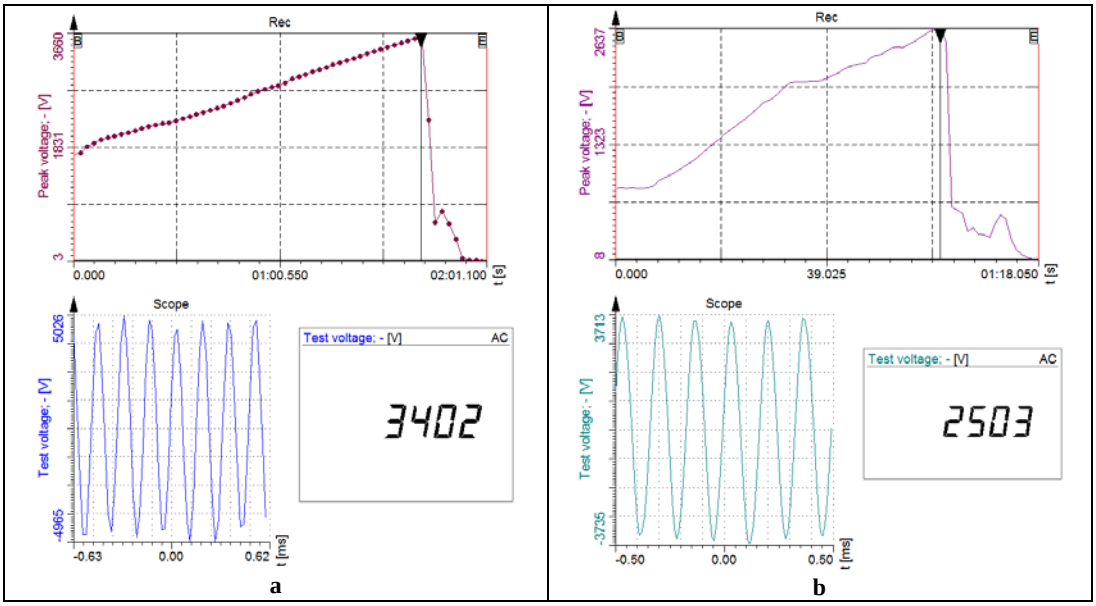

***Figure 5-14*: Samples of recorded breakdown voltage and current values during the 6 kHz sinusoidal insulation tests: wire-insulation-wire (a) and wire-insulation- grounded plate (b).**

The step-up transformer primary current, the RMS and the peak value of the applied voltage and the wave shape were recorded during the withstand tests (see Figure 5-14).

The schematic diagram of the test specimen and the results of the tests are presented in Table 5-3.

***Table 5-3*: Summery of the results of the 6kHz withstand tests.**

6 kHz voltage applied between		Test setup	Failure voltage RMS (V)
wire-one layer insulation-wire		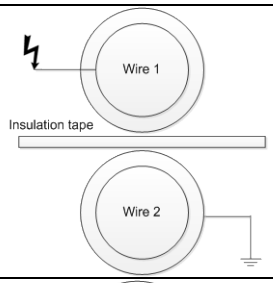	**3400**
wire-grounded plate		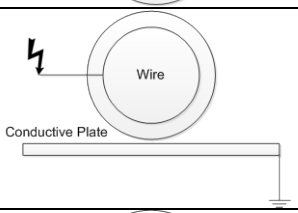	**210**
wire-grounded plate	repeat	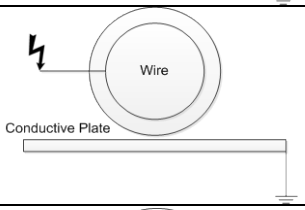	**220**
wire-one layer insulation-grounded plate		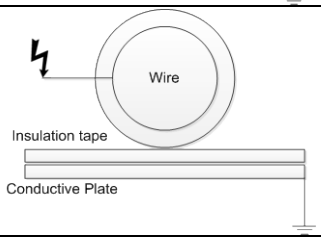	**2500**

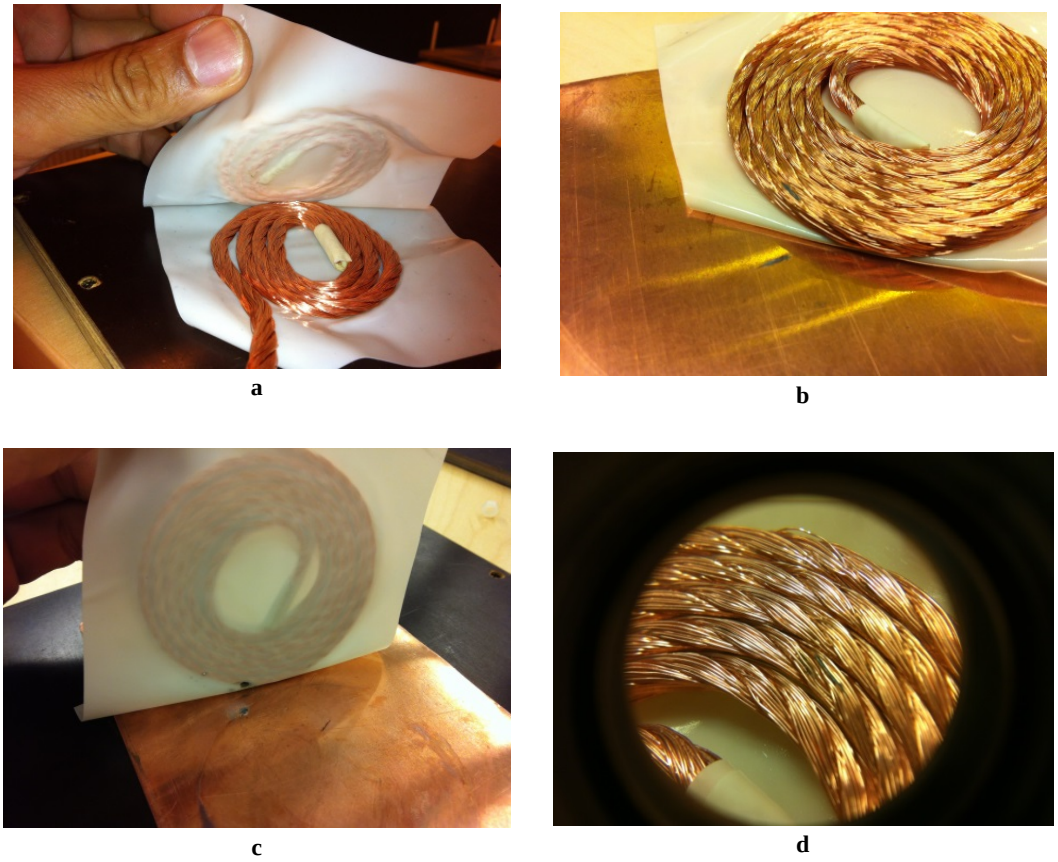

***Figure 5-15*: Breakdown points; the wire-tape-wire composition (a), the wire-plate composition (b), and the wire-tape-plate composition (c) and the effect of discharge on the wire's lack.**

Figure 5-15 presents photos from the traces of electrical discharges on the wires and insulations.

5.6.4 Insulation coordination based on the test results

The Ferrite transformer has three layers for each winding for both high voltage and low voltage sides and the Nano transformer has two. The voltage distribution along the transformers windings are according to Figure 5-16.

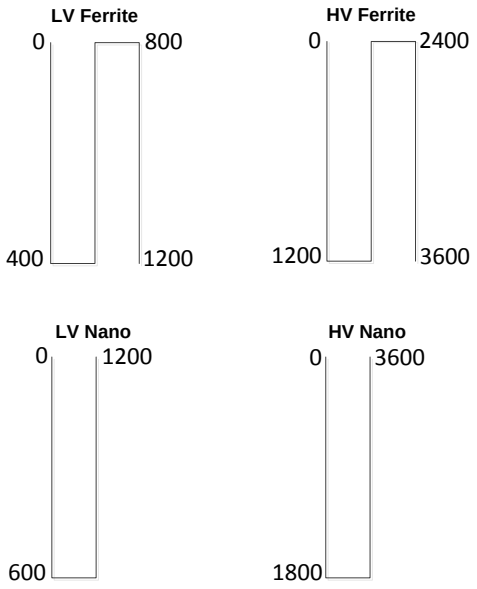

***Figure 5-16*: The schematics of the voltage distribution along the windings.**

According to the test data presented in Table 5-3, considering 210V as minimum withstand voltage between two bare wires and 2500 V as minimum withstand voltage between the wire, insulated with one layer of tape to a grounded plate, Table 5-4 can be used as the transformers insulation coordination schemes. The required number of insulation layers to be applied between the winding layers to fulfil the targeted safety factors is presented in the table.

***Table 5-4*: The transformers insulation coordination scheme based on the results of the 6 kHz insulation tests.**

	Winding	**LV**	**HV**
Ferrite	Nominal voltage	1200	3600
	Number of turns	18	54
	Number of layers	3	3
	Maximum voltage between adjacent turns	66.7 V	66.7 V
	Maximum voltage between adjacent layers	800 V	2400 V
	Required additional insulation between wires	No (Safety factor 3)	No (Safety factor 3)
	Required additional insulation between layers	1 layer (Safety factor 3) ***(1 layer was applied.)***	1 layer (No Safety factor) ***(2 Layers were applied.)***
Nano	**Winding**	**LV**	**HV**
	Nominal voltage	1200	3600
	Number of turns	16	48
	Number of layers	2	2
	Maximum voltage between adjacent turns	75 V	75 V
	Maximum voltage between adjacent layers	1200 V	3600 V
	Required additional insulation between wires	No (Safety factor 3)	No (Safety factor 3)
	Required additional insulation between layers	1 layer (Safety factor 2) ***(1.5 layers were applied.)***	2 layers (Safety factor 1.5) ***(3 layers were applied.)***

Although the Ferrite transformer that was tested using the PWM amplifier seemed to be failed, after disassembly of the transformer, no sign of breakdown was found inside the transformer. It was decided to remanufacture the Ferrite transformer and produce the Nano transformer based on the insulation test results performed using the 6 kHz PWM amplifier. After production of the transformers, four no-load tests were performed on the transformers using the existing voltage supplies. First a 6 kHz square shaped voltage was applied to the Ferrite transformer and the voltages of the primary and secondary sides together with the primary side current were recorded. Then the test was repeated applying a sinusoidal voltage and finally the same tests were repeated for the Nano transformer. The details are presented in the following section.

5.7 No-load tests

For the complete evaluation of the losses for the manufactured transformer, they should be supplied with nominal current and nominal voltage. It is not possible to simulate the real transformer working condition without having a real load. In order to determine the main elements of losses in the transformer it should be subjected to full voltage and full current. This can be performed in two separate stages, at the no-load condition when the primary winding is supplied with the nominal voltage and the secondary is open and at short circuit condition when the primary winding is supplied with the nominal current and the secondary is short circuited.

Because of a very low phase angle between voltage and current, every small phase shift error in measured voltage or current introduces a notable error to the indicated power. An accurate measurement of losses under short circuit condition needs a high precision power analyser. The high voltage and the high current should be divided to reach a suitable scale to be fed into a power analyser. The wave shapes should not be neither deformed nor shifted over time in a precise loss measurement process. A high frequency voltage divider and a current shunt is required which should be calibrated and have a defined scale factor and phase displacement error values. Reference [33] presents examples of core loss measurement systems on the typical magnetic core materials magnetized with a symmetrical/asymmetrical rectangular voltage. The voltage at the open secondary coil together with the current at the primary coil is measured and (5.1) is used for determination of the core losses [34].

$$P_i = \frac{1}{w_e * T} \frac{N_1}{N_2} \int_0^T v_L * i_L d_t \tag{5.1}$$

where
w_e is the mass of the core
T is the period
N_1 is the number of the turns of the primary winding
N_2 is the number of the turns of the secondary winding
v_L is the inevitable air gap length
i_L is the inevitable air gap length

The same formula can be used for calculation of the losses based on the voltage and current measurement data which is presented in the following section.

5.7.1 No load test using a signal generator and a power amplifier

To create and apply the nominal voltage, the transformer shall be left open at the secondary side. In this way a high voltage low current source will be strong enough to supply the created losses in the transformer. For a 50 Hz transformer it is easy to use a step-up transformer supplied with a variable voltage source directly connected to the mains voltage. However, a high frequency and a non-sinusoidal wave shape for this project calls for a signal generator and a power amplifier. In this case the available instrument is a Fluke 5205A Precision power amplifier which has a maximum of 1000 V at 200 mA at its output (see Figure 5-17a) [35].

a **b**

***Figure 5-17*: Fluke 5205A power amplifier (a) and Yokogawa WT3000 power analyser (b).**

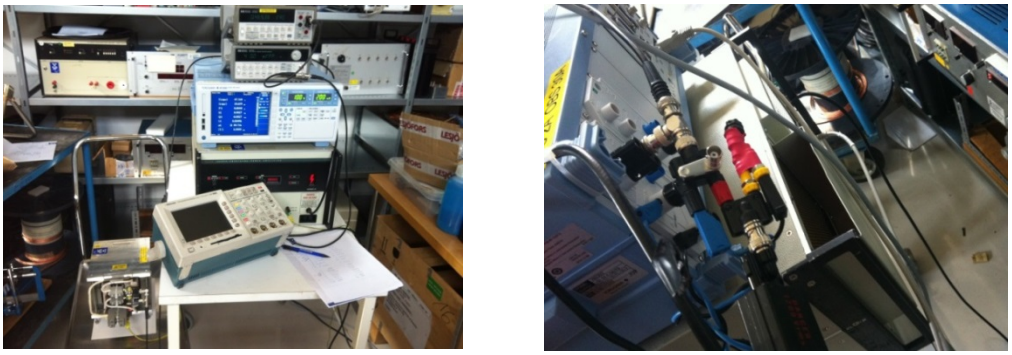

a b

***Figure 5-18*: Test circuit (a) and the 2 A fast fuse in series with LV side in a red fuse holder (b).**

The voltage, current and the power parameters are registered using an existing Yokogawa, WT3000, precision power analyser which is shown in Figure 5-17b. A Tektronix oscilloscope was used to control the wave shapes (see Figure 5-18a). A 2 A fast fuse was installed in series with the supply side in a fuse holder shown in Figure 5-18b. The maximum applicable voltages available from the amplifier for two types of wave shapes were registered. The results are presented in Table 5-5. The wave shapes of the applied voltages are presented in Figure 5-19.

***Table 5-5*: Maximum available supply voltage and measured parameters using the power amplifier.**

	Sinusoidal wave		Square wave	
Parameter	Supplied from HV side	Supplied from LV side	Supplied from HV side	Supplied from LV side
Urms1 (V)	88.2	84.6	47.3	10.1
Irms1 (mA)	96.6	126.7	19.7	91.5
P1 (w)	0.02	0.39	0.005	0.009
S1 (VA)	8.5	10.7	0.93	0.92
Q1(var)	8.5	10.7	-0.93	-0.92
λ1	0.003	0.04	0.005	0.0096
Φ1	89.8	87.9	89.7	89.4
fU1(kHz)	6.0	6.0	6.0	6.0

At the next step, using a Fluke 5700 calibrator, at 6 kHz, 100 and 200 V sinusoidal voltages were applied to the transformers LV sides respectively and 0.132 and 0.238 A were recorded. It was the maximum applicable voltage using this voltage source. The nominal current of Fluke 5700 is 10 mA at 6 kHz. It seems that the calibrator has no protection in the case of inductive loading. Normally these kinds of calibrators are made for supplying a highly resistive or capacitive load of the voltage meters. Controlling the measured current using a wide band resistive shunt showed the same current as it was read by the multimeter.

***Figure 5-19*: Sinusoidal and square waves at the maximum applicable voltage by Fluke 5205.**

5.7.2 No-load test using a PWM

After application of the additional insulation layers between the windings and adding 1-3 layers of insulation tape on the open corners, between the windings and grounded metallic parts, the no-load tests at 6 kHz were continued using a PWM source designed and manufactured based on a common SP-Chalmers master thesis work [36]. The primary and secondary voltages and the supply side current were recoded using a 4 channel, 25 MHz, 200 MS/s PicoScope oscilloscope, two Lecroy AP032 differential voltage probes and a Pico TA018, AC/DC 60/20 A current clamp (see Figure 5-20).

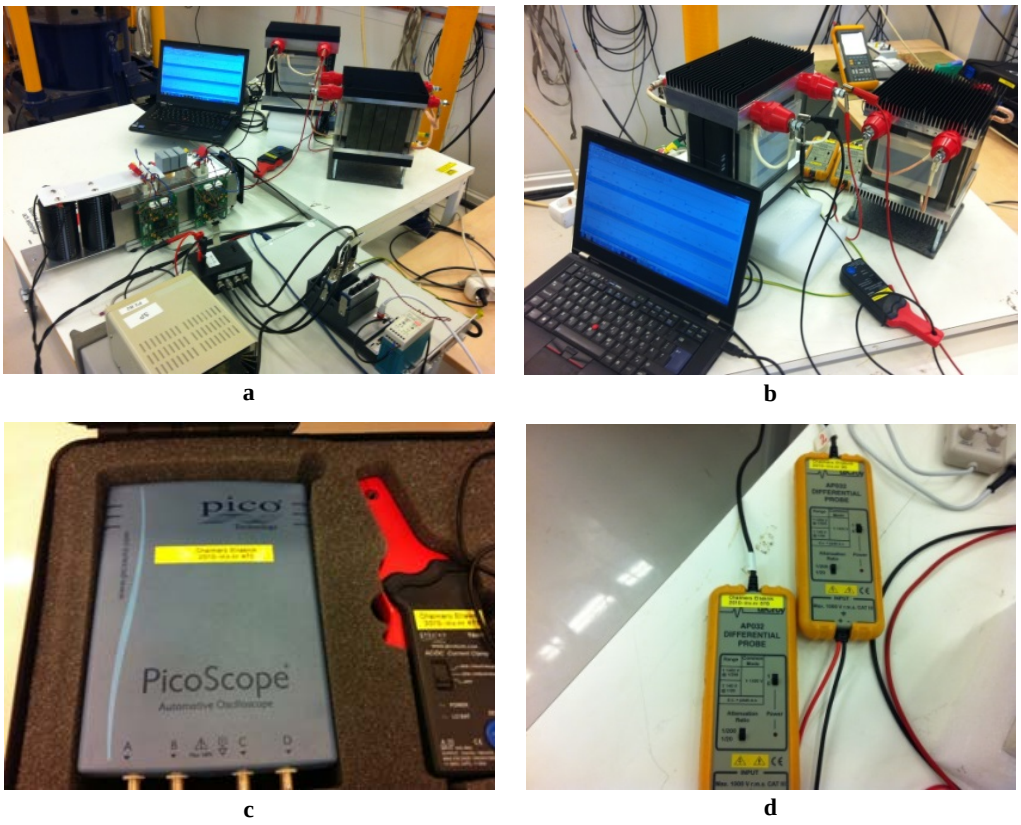

a b c d

***Figure 5-20*: The 6 kHz square wave source (a), test and measurement circuit (b) and the measurement equipment used (c&d).**

A rectangular 180 V voltage supplied to the primary side of the Nano transformer, and then the primary current and secondary voltage were recorded using a Pico clamp probe and a Lecroy differential voltage probe connected to a four channel Picoscope. It should be noted that the output of the PWM cannot be grounded at one of the output terminals. Therefore, it is not possible to use a conventional voltage probe to measure the voltage. In addition, the HPMF transformer application which requires having the high pulsed DC voltage on both terminals of each winding dictates a non-grounded supply and measurement circuit.

To investigate the amplitude of the spikes on the voltage at the output of the PWM supplier (the primary side of the transformer) and at the secondary side of the transformer a set of recordings at the 6 kHz were done which are presented in Figure 5-21.

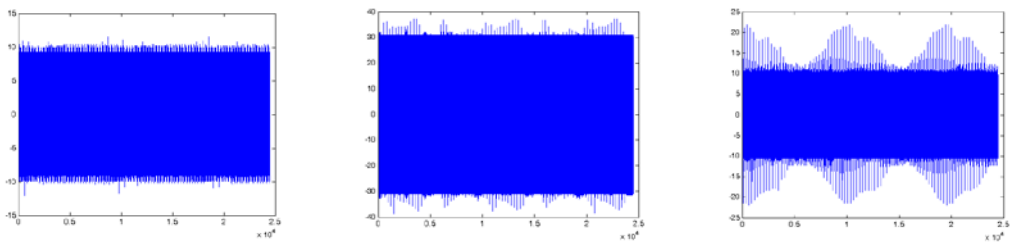

a b c

***Figure 5-21*: The source voltage without connection to the load (a), the source voltage with connection to the HV side of the transformer (b) and the voltage measured at the LV side (c).**

Figure 5-21c demonstrates the measured high frequency spikes which are >100% higher than the fundamental voltage level at the secondary side of the transformer and in the range of 25% at the primary side of the transformer. To have a true squared shape voltage signal, some improvements were done on the supply circuit elements.

5.7.3 The final no-load tests with 300 V, 6 kHz rectangular wave

Some possible improvements on the supplying system were performed. A set of capacitors which were connected to the DC link using connecting wires, were disconnected and soldered on the low inductance busses and the gate resistors of the converter were increased.

No-load tests were performed with the maximum available rectangular voltage on both transformers. Voltages from 50 V to 300 V were applied to the HV side of the transformers in steps of 50 volts. The results are summarized using the Matlab software and presented in the Figure 5-22 and Figure 5-23.

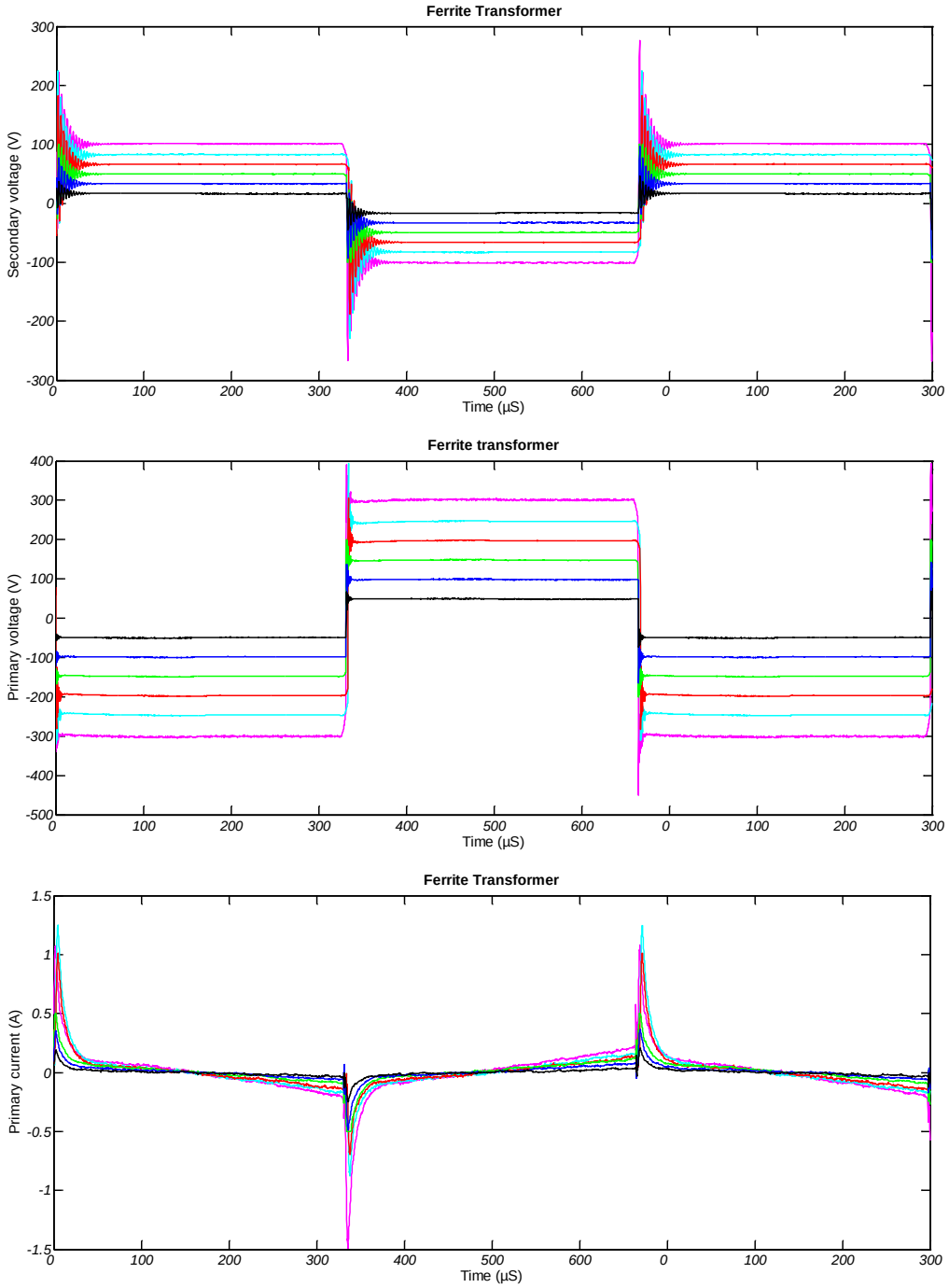

***Figure 5-22*: Voltage and current wave shapes of the Ferrite transformer.**

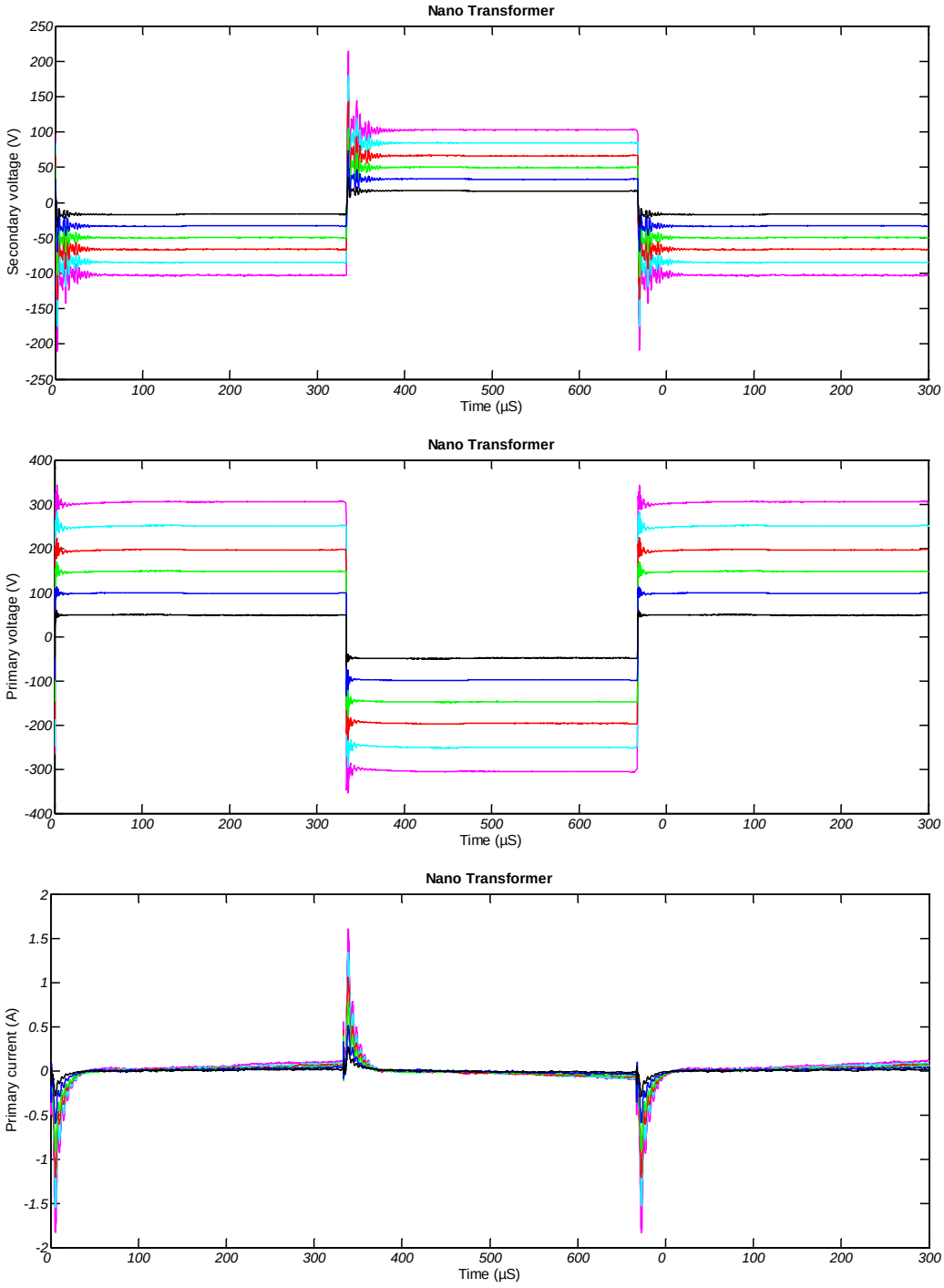

Figure 5-23: **Voltage and current wave shapes of the Nano transformer.**

Figure 5-24 and Figure 5-25 present the results recorded on the Picoscope dashboard's display. It is notable that the high frequency spikes cannot be observed directly on the display. In addition, the RMS values of the primary and secondary voltages and the supplied current can be read from the display.

***Figure 5-24*: Picoscope's on screen recordings for the Ferrite transformer; 100 V at secondary, 300 V at primary and 204 mA supplied current.**

***Figure 5-25*: Picoscope's on screen recordings for the Nano transformer; 100 V at secondary, 300 V at primary and 196 mA supplied current.**

5.7.4 The final no-load tests with 300 V, 6 kHz sinusoidal wave

In addition, the transformers were supplied by a Fluke 5500 A Calibrator and the no-load tests were performed with the maximum available sinusoidal voltage which was 300 V (see Figure 5-26). The results were recorded as Matlab files. The displayed voltages and the current are presented in Figure 5-27 and in Figure 5-28.

***Figure 5-26*: No-load test circuit (a) on transformers at 6 kHz with sinusoidal voltage performed using a Fluke 5500 calibrator as a voltage source (b).**

***Figure 5-27:* Picoscope's on screen recordings for the Ferrite transformer; 100V sinusoidal at secondary, 300V at primary and 150 mA supplied current.**

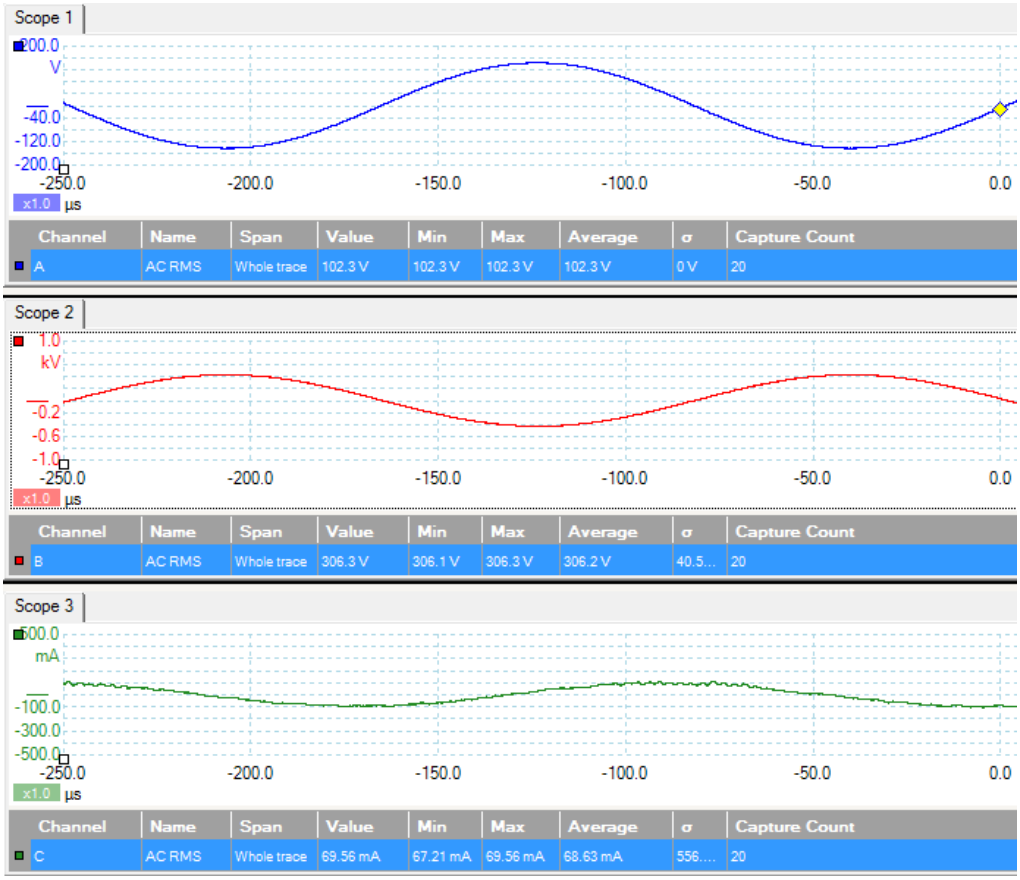

***Figure 5-28*: Picoscope's on screen recordings for the Nano transformer; 100V sinusoidal at secondary, 300V at primary and 70 mA supplied current.**

5.8 Evaluation of the load loss testing facilities

To create and inject the nominal current, the test object shall be short circuited on the secondary side. In this way a low voltage, high current source will be strong enough to supply the consumed losses in the transformer. For a 50 Hz transformer, it is not hard to use a step-down transformer supplied with a variable voltage supply connected to the mains voltage as a source. Having high frequency and a non-sinusoidal wave shape for this project, calls for a signal generator and a current amplifier. In this case the available instrument was a Clarke-Hess, 8100, Trans-conductance amplifier which can supply 100 A at 100 kHz and at a maximum output voltage of 7 volt (see Figure 5-29) [37].

The maximum voltage and current available at 6 kHz to supply the HV side of the LV short circuited transformer, was 5.7 V & 0.43 A. The maximum voltage and current available at 6 kHz to supply the LV side of the HV short circuited transformer, was 6.4 V & 4.3 A. The maximum applicable voltage and current at minimum frequency (900 Hz) to the transformer at the maximum input voltage of the amplifier and maximum output voltage of the amplifier was 6.2 V & 28.4 A. As a result, this system cannot be used for the winding loss measurements on the transformers.

***Figure 5-29*: The load loss test on transformers using a Clarke-Hess, 8100, Trans-conductance amplifier.**

5.9 Evaluation of the temperature measurement facilities

Because of the presence of high voltage, a general propose temperature sensor is not suitable for direct measurement of temperature on high frequency and high voltage coil or winding. Nowadays, optical fibre sensors are used for direct winding hotspot temperature measurements of high voltage transformers. The price of theses temperature measuring systems can be high and out of this project's financial scope. The simplest instrument available on the Swedish market is LumaSense, LUXTRON 812, a single channel industrial temperature monitor which is shown in Figure 5-30 [38].

***Figure 5-30*: LumaSense, LUXTRON 812, single channel industrial temperature monitor [38].**

Several sensors can be installed and fixed on the targeted points during the manufacturing process of the transformers. In this way, a real validation of calculated temperatures is possible. Using the introduced system, only two online measurements at a time is possible and the terminations can be switched every time it is necessary. Some accessible system suppliers in Sweden are introduced in Appendix A.

The other possibility comes with this consideration that the high temperature only exists during a heat run test which is performed by short circuiting the transformer and applying a very low voltage to it. During the heat run test, the total losses of the transformer under test (which is nearly equal to the sum of the core and windings losses) is fed into the transformer.

In this case, it is possible to use normal PT1000 sensors to measure the temperature of the targeted points. A set of conducting pipes can be installed inside the transformer body, filled with thermally conductive paste to be used for penetration of the sensors during a thermal test and pulling them out during a high voltage test.

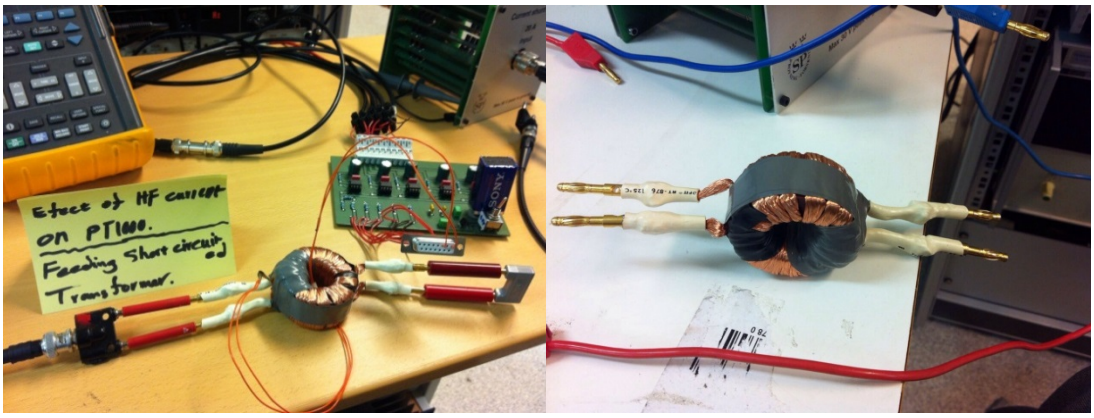

***Figure 5-31*: Investigation of the effect of high frequency high current on a PT1000 temperature sensor.**

To investigate the effect of the high frequency electromagnetic field on the temperature measuring system a test setup was prepared using a prototype 18:3 HF transformer supplied with approximately 10 A, at 5 kHz (see Figure 5-31). The effect was not considerable and the measured temperature was stable inside the accuracy range of 0.1 ºC.

6 Conclusion and discussion

6.1 Results from present work

The constructional design of two prototype 60 kW, 1.2/3.6 kV, 6 kHz 46/28 µH shell type transformers was performed.

The required technical data and the quantity of the materials including Ferrite EPCOS N87 and Nanocrystalline Vacuumschmelze Vitroperm cores, Elektrisola's Polysol155 Litz wire and Coolpoly-D5108, thermally conductive liquid crystalline polymer were determined and the alternatives of the suppliers were introduced and the materials were purchased.

The insulation characteristics of the supplied insulation materials were examined performing typical tests and the insulation coordination of the transformer was strengthened accordingly. It was observed that the breakdown voltage at 6 kHz square wave voltage is much lower than the breakdown voltage at 50 Hz sinusoidal wave shape.

The proper machinery and qualified suppliers of services for production of different parts were identified, and the constructional design drawings were prepared. Having access to SP's polymer sheet production machine, the bobbins were produced in the form of glued polymer sheets. The polymer sheets were cut by a water jet cutting machine. The pressing aluminium plates were produced by a CNC machine, owned by SP.

Two prototype transformers were manufactured and became ready for the design validation tests.

The evaluation of the available high voltage high current and medium frequency square wave shape supplies as well as the voltage and current measuring equipment were performed. A Fluke 5500 calibrator was used to apply a sinusoidal voltage with the maximum level of 300 V to the HV side of the transformers. In addition, an existing PWM amplifier was used to apply a 300V, 6 kHz voltage to the HV side of the transformers. The existing amplifier needs improvements for the eliminations of square wave's overshoots, to be qualified for application of the full 1200V to the LV side of the transformers. Regarding evaluation of available equipment for performing a load loss test, in contrary to what was thought, the application of the nominal current at low voltage is not possible using the existing Clarke-Hess, 8100, Trans-conductance amplifier. A Yokogawa, WT3000, precision power analyser together with the introduced SP's precision voltage and current dividers can be used for power loss measurements during no-load and load loss conditions. A temperature measurement system based on the fibre optic sensors can be used for measuring the hot spot temperatures of the transformers at the same time with the application of the high voltage.

Using a precision multitier, a precision LCR meter and a network analyser, the transformers were subjected to preliminary design validation tests and the results were recorded, analysed and compared with calculated values. The design parameters of the transformers were validated to be compatible with the practical results within the acceptable tolerances. The measured resistances, magnetising inductances and the leakage inductances are in a good compliance with the calculated values. The most important parameter is the leakage inductance which was measured as 39.3 and 29.2 µH compared with the calculated 46 and 28 µH for the Ferrite and the Nano transformers respectively.

6.2 Future work

The following tests and investigations are proposed to be done and the results to be used for development of the next prototype transformers:

- Investigations regarding the production of a desired square wave shape supply for conducting a full no-load test. (The source should be able to supply at least 1200 V square shaped voltage without spikes at the rise and fall events. The supply power should be more than the power needed to feed the losses of a transformer.)
- Loss measurements using square wave supply including measurement of the no-load losses in the core by applying the nominal voltage to the open circuit transformers and the load losses in the windings by applying the rated current to the short circuited transformers.
- Insulation tests on the simulated conditions on the different conductor-insulation combinations using a high frequency (much higher than 6 kHz which practically exists at the voltage rise time), high voltage source. It is specially proposed to repeat the performed tests until coming to a reliable breakdown voltage and to continue the insulation tests on the two and three layer combinations. The latter is for investigating if the breakdown voltage will be doubled when the number of insulation layers increases to a double layer.
- Insulation evaluation tests on the transformers including insulation resistance measurement, applied power frequency test, induced overvoltage tests and partial discharge measurements. Passing these tests is vital for the purpose of a long term practical application of the transformers.
- Heat run test including temperature measurements on various points of the transformers.
- Verification of the thermal model of the transformer.
- Making a dummy coil and doing measurements to check the true winding losses.

The following should be done as improvements for the reproduction of prototypes:

- The insulation tape layers between the windings and between the windings and the grounded electrodes should be decided in detail before preparing the constructional drawings. These insulation layers should be placed on the corners over the bobbins and covering the windings before starting the winding and after finishing it.
- Mechanical tests should be done on the produced polymer sheets. SP has the 300°C limit for the production of the sheets which is at the minimum range of the production temperature limit of the Coolpoly. It was not possible to investigate the effect of increasing the temperature on the mechanical strength of the plates.
- The 4 pressing bolts are used as supporting legs, they should be changed from M6 to M8.
- The conductors should be insulated using a tape insulator or a heat shrink insulator before leaving the winding and passing through the bobbin's hole. A suitable space between the winding and the upper polymer sheet should be considered for this.
- The 12 mm cooling and pressing aluminium plates of the Ferrite transformer should be changed to 30 mm thick plates for a more even distribution of the pressing forces on the five core stacks.
- The polymer insulation sheets of the Ferrite transformer should be changed from 2 mm to 4 mm thick sheets with corrugated edges for better mechanical coupling stability, higher thermal conductance and better dimensional positioning of the windings.
- Thin tubes should be installed inside the transformer body on proper positions for penetrating and conducting the PT1000 temperature sensors inside the transformer every time it is needed.
- In case of need for a sealing glue with the high thermal conductivity and relatively high voltage insulation level, the TCOR, a thermally conductive RTV (Oxime) can be used [39].
- The nuts and bolts screwed into the support terminating insulators should be changed from steal to copper to reduce contact resistance where the high current flows through the transformer.

7 References

[1] M. A. Bahmani, "Design and optimization of HF transformers for high power DC-DC applications," Thesis for the degree of licentiate of engineering, Chalmers university of technology, 2014

[2] Bahmani, M. A. and Agheb, E. and Thiringer, T. and Høidalen, H. K. and Serdyuk, Y.,"Core loss behavior in high frequency high power transformers—I: Effect of core topology," *Journal of Renewable and Sustainable Energy*, 4, 033112, 2012

[3] W. Shen, "Design of High-density Transformers for High-frequency High-power Converters," Doctoral thesis, Blacksburg, Virginia, July 2006

[4] L. Max, "Design and Control of a DC Collection Grid for a Wind Farm," Doctoral thesis, Chalmers, Göteborg, 2009

[5] C. Meyer, "Key Components for Future Offshore DC Grids," RWTH Aachen, Germany, July 2007

[6] Rylko, M.S.; Hartnett, K.J.; Hayes, J.G.; Egan, M.G., "Magnetic Material Selection for High Power High Frequency Inductors in DC-DC Converters," *Applied Power Electronics Conference and Exposition, 2009. APEC 2009. Twenty-Fourth Annual IEEE* , vol., no., pp.2043,2049, 15-19 Feb. 2009

[7] Heinemann, L., "An actively cooled high power, high frequency transformer with high insulation capability," *Applied Power Electronics Conference and Exposition, 2002. APEC 2002. Seventeenth Annual IEEE* , vol.1, no., pp.352,357 vol.1, 2002

[8] Xu She; Burgos, R.; Gangyao Wang; Fei Wang; Huang, AQ., "Review of solid state transformer in the distribution system: From components to field application," *Energy Conversion Congress and Exposition (ECCE), 2012 IEEE* , vol., no., pp.4077,4084, 15-20 Sept. 2012

[9] Agheb, E. and Bahmani, M. A. and Høidalen, H. K. and Thiringer, T., "Core loss behavior in high frequency high power transformers—II: Arbitrary excitation," *Journal of Renewable and Sustainable Energy*, 4, 033113, 2012

[10] Bahmani, M.A; Thiringer, T.; Ortega, H., "An Accurate Pseudoempirical Model of Winding Loss Calculation in HF Foil and Round Conductors in Switchmode Magnetics," *Power Electronics, IEEE Transactions on* , vol.29, no.8, pp.4231,4246, Aug. 2014

[11] Bahmani, M.A.; Thiringer, T., "A high accuracy regressive-derived winding loss calculation model for high frequency applications, "*Power Electronics and Drive Systems (PEDS), 2013 IEEE 10th International Conference on*, vol., no., pp.358,363, 22-25 April 2013

[12] Bahmani, M.A.; Thiringer, T., "Accurate Evaluation of Leakage Inductance in High Frequency Transformers Using an Improved Frequency-Dependent Expression," *Power Electronics, IEEE Transactions on* , vol.PP, no.99, pp.1,1

[13] *http://www.epcos.com/blob/528882/download/3/pdf-n87.pdf,* Accessed 2014-10-05

[14] *http://www.nanoamor.com/cat/catalog_amor.pdf,* Accessed 2014-10-05

[15] *http://www.epcos.com/inf/80/db/fer_13/u_93_152_30.pdf,* Accessed:2014-10-05

[16] *http://www.vonroll.com/media/files/downloads/brochures/Wire_US_20120516.pdf,* Accessed 2014-10-05

[17] *http://www.newenglandwire.com/newt-catalog.pdf,* Accessed 2014-10-05

[18] *http://www.elektrisola.com/enamelled-wire/enamelled-wire-types/iec/europe.html,* Accessed 2014-10-05

[19] *http://www.coolpolymers.com/files/ds/Datasheet_d5108.pdf,* Accessed 2014-10-05

[20] *http://www.farnell.com/datasheets/1318128.pdf,* Accessed 2014-10-05

[21] *https://www1.elfa.se/data1/wwwroot/assets/datasheets/HTSP_eng_tds.pdf,* Accessed 2014-10-05

[22]h*ttp://multimedia.3m.com/mws/mediawebserver?66666UuZjcFSLXTtl8&yNx&yEVuQEcuZgVs6EVs6E666666--*, Accessed 2014-10-05

[23] *https://www1.elfa.se/data1/wwwroot/assets/datasheets/ks200_ger_bro.pdf*, Accessed 2014-10-05

[24] *http://se.rs-online.com/web/p/heatsinks/4099931/*, Accessed 2014-10-05

[25] *http://www.fischerelektronik.de/web_fischer/blaetterbareKataloge/Heatsinks/#/72/*, Accessed 2014-10-05

[26]*http://www.austerlitz-electronic.info/Portals/0/PDF/Katalog/ae-Katalog12-web/ae-Katalog12-web/index.html*, Page 47, Accessed 2014-10-05

[27] *https://www.elfa.se/elfa3~se_sv/elfa/init.do?item=55-065-02&toc=19779*, Accessed 2014-10-05

[28] *https://www.elfa.se/elfa3~se_sv/elfa/init.do?item=55-064-99&toc=19779*, Accessed 2014-10-05

[29] *http://www.coolpolymers.com/Files/MSDS/MSDS_D5108.pdf*, Accessed 2014-10-05

[30]*http://www.newenglandwire.com/~/media/Files/Litz%20Wire%20Termination%20guide%204th%20Edition.pdf*, Accessed 2014-10-05

[31]*http://www.vacuumschmelze.com/fileadmin/Medienbiliothek_2010/Downloads/KB/Cut_Cores_flyer_2011.pdf*, Accessed 2014-10-05

[32]*http://www.vacuumschmelze.com/fileadmin/Medienbiliothek_2010/Produkte/Kerne_und_Bauelemente/Anwendungen/Kerne/Schnittbandkerne/W160.pdf*, Accessed 2014-10-05

[33] *http://www.metasistema.it/Catalogo2007Meta.pdf*, Accessed 2014-10-05

[34] Hatakeyama, T.; Onda, K., "Core Loss Estimation of Various Materials Magnetized With the Symmetrical/Asymmetrical Rectangular Voltage, "*Power Electronics, IEEE Transactions on*, vol.29, no.12, pp.6628,6635, Feb. 2014

[35] *http://www.testequipmentconnection.com/specs/FLUKE_5205A.PDF*, Accessed 2014-10-05

[36] A. Einarsson, A. Asgari vand "Construction of a low-ripple inverter with accurate phase control for calibration of measurement equipment, " Master of Science Thesis, Department of Energy and Environment, Chalmers University of Technology, Sweden, September 2014

[37] *http://www.clarke-hess.com/ta8100.pdf*, Accessed 2014-10-05

[38] *http://www.contika.dk/download/brochurer/impac/luxtron%20812.pdf*, Accessed 2014-10-05

[39] *http://www.electrolube.com/core/components/products/tds/044/TCOR.pdf*, Accessed 2014-10-05

[40] IEC 60076-1, Edition 2.1, Claus 10:Tests, 2000-04

Appendix A, Addresses and contact details

Addresses and contact specifications for the materials used for the project:

Ferrite cores:

- www.elfa.se/
- www.se.rs-online.com/

Nanocrystalline cores:

- Lars Kvarnsjö
  Vacuumschmelze Sales Office Denmark, Norway, Sweden
  Tel: +46 (0)8 7140835
  Mobile: +46 (0)70 2190835
  Email: lars.kvarnsjoe@vacuumschmelze.com

Insulating polymer :

- Kathleen Rush
  Cool Polymers
  Inside Sales/Customer Support
  51 Circuit Drive
  North Kingstown, RI 02852
  T: (401) 667-7830 / F: (401)667-7831
  kathleen.rush@coolpolymers.com

Litz wires:

Contact person	Mail address	Telephone	Representing Company	Holding Company	Limitation
Jerker Andersson	Jerker.andersson@lww.se	0512300345	Dahréntråd, Sweden	LiljedahlWinding Wire, Sweden	
Mikael olofsson	mikael.olofsson@bevi.se	049927197	Bevi AB, Sweden	Elektrisola, Germany	
Dominique Rey	Dominique.rey@vonroll.com	00416 17855370	Vonroll, Switzerland	Vonroll, Switserland	Min 50 kg
Lars Lundin	ll@moreelectronics.dk	0859086590	MoreElectronics, Sweden	NewEnglandWire, USA	Min 305 m

Insulating tape:

- http://se.farnell.com/

Thermally conductive paste:

- www.elfa.se/

Epoxy adhesive DP760:

- KA OLSSON & GEMS AB,
  Sallarängsgatan 3, 431 37 Mölndal
  Tel 031-74 64900

Aluminium heat sinks

- www.elfa.se/
- www.se.rs-online.com/

Heat shrink tubing:

- www.elfa.se/

Supporting insulators as HV terminals:

Supplier 1	Supplier 2
http://www.euroenergy.se/Catalogue Type: F-F	http://www.taljemat.se/document/isolator_db.pdf
LV:1000V Model: GM121	LV:1000V Artikel: DB34/P
HV:3000V Model: GM181	HV:3000V Artikel: DB65/P
Euro Energy Components AB Varlabergsvägen 25 434 39 Kungsbacka Tel: 0300-69 00 40	Tälje Mätinstrument AB Wedavägen 24A 152 42 SÖDERTÄLJE Tel: 08-550 312 12

Fiber optic temperature sensor:

- Pentronic, Per Bäckström,Tel. 070 543 02 84,
  http://pentronic.se/start/instrument/ir-pyrometrar.aspx
- BLInstruments, Agne Bogren, Tel 070516 39 95,
  http://www.blinstruments.se/index.html

Appendix B, List of standard tests

List of standardized tests on dry type medium sized power transformers [40]:

Routine tests:

- Measurement of winding resistance
- Measurement of voltage ratio and check of phase displacement
- Measurement of short-circuit impedance and load loss
- Measurement of no-load loss and current
- Dielectric routine tests (IEC 60076-3)

Type tests:

- Temperature-rise test
- Dielectric type tests (IEC 60076-3)

Special tests:

- Dielectric special tests (IEC 60076-3)
- Determination of capacitances windings-to-earth, and between windings
- Determination of transient voltage transfer characteristics
- Measurement of zero-sequence impedance(s) on three-phase transformers
- Short-circuit withstand test (IEC 60076-5)
- Determination of sound levels (IEC 60551)
- Measurement of the harmonics of the no-load current (10.6)
- Measurement of insulation resistance to earth of the windings
- Measurement of dissipation factor (tan δ) of the insulation system capacitances

Appendix C, List of equipment used

The list of test equipment which is used during the project:

- Fluke, 5205A, Precision power amplifier
- SP502130, Fluke 5500A Calibrator
- Lab Gruppen, SS 300B, Audio power amplifier
- SP BX31332, Yokogawa WT3000, Precision Power Analyser
- SP503045, HP 33120A, Function/Arbitrary Waveform Generator
- SP501155, HP 34401A, Multimeter
- SP603031, Tektronix TDS 3054B, 500MHz 5GS/s oscilloscope
- SP503042, Fluke 99B series II, 100MHz Scope-meter
- SP900414, Agilent E4980A, 20 Hz-2 MHz, Precision LCR Meter
- SP BX31914, Fluke 5700, High performance Multifunction calibrator
- SP503241, SP, 2A 0.4Ω, High precision current shunt
- SP5xxxx, SP, 20A 0.8Ω, High precision current shunt
- SP900408, Metrix AX 322, 30V 2.5A, DC power supply
- R&B, UH 27, 5kV 50Hz, High voltage insulation tester
- Sensitive research instrument corporation, ESH, Electrostatic voltmeter
- SP603237, Clarke-Hess, Model 8100, Trans-conductance amplifier
- SP900180, Pearson 301X, 400 A/4 V, Wide band current monitor
- Step-up transformer: 600 V/3 kV, 333 A/ (9.1A@22kV)
- SP900180, Pearson 3972, 50A/5V, Wide band current monitor
- SP501235, MWB, 3kV/100V, Standard voltage transformer
- SP901239, DEWE-50-USB2-8, Modular data acquisition system for USB
- SP603268, WSTS CP100, Compressed gas capacitor, 37pF
- SP602798, AC divider low voltage arm 0.25µF
- Chalmers Elteknik inv. Nr. 470, PicoScope, 4 channel, 25 MHz, 200 MS/s Oscilloscope
- Chalmers Elteknik inv. Nr. 578 & 90, Lecroy AP032 Differential probe
- Chalmers Elteknik inv. Nr. 471, Pico TA018, AC/DC Current clamp 60/20A
- SP603223, Fluke 8508A Reference multimeter
- SP902103, Agilent technologies, E5061B, 5 Hz to 3 GHz, ENA series Network analyser coupled with HP16047C HP test fixture

Appendix D, Drawings

Drawings:

- Drawings for production of Ferrite transformer HV and LV bobbins cooling polymers
- Drawings for production of Nano transformer HV and LV bobbins cooling polymers
- Drawings for production of Ferrite transformer Aluminum pressing plates
- Drawings for production of Nano transformer Aluminum pressing plates

Appendix E, Materials technical data

The list of attached technical data sheets of the materials used for the project:

- Polysol155 Enamelled Copper Litz wire
- Vitroperm 500 Nanocrystalline cut core
- U93, N87, Ferrite core
- CoolPoly D5108 Thermally conductive Polyphenylene Sulfide Polymer
- 3M 8943 Thermally conductive adhesive tape
- 3M Scotch-weld, DP760 Epoxy adhesive
- KS200, Fischerelektronik Heat sink
- HTSP50T Silicone Heat transfer compound plus
- GMxxx, Metasistema support insulator

Ferrite LV 1/3

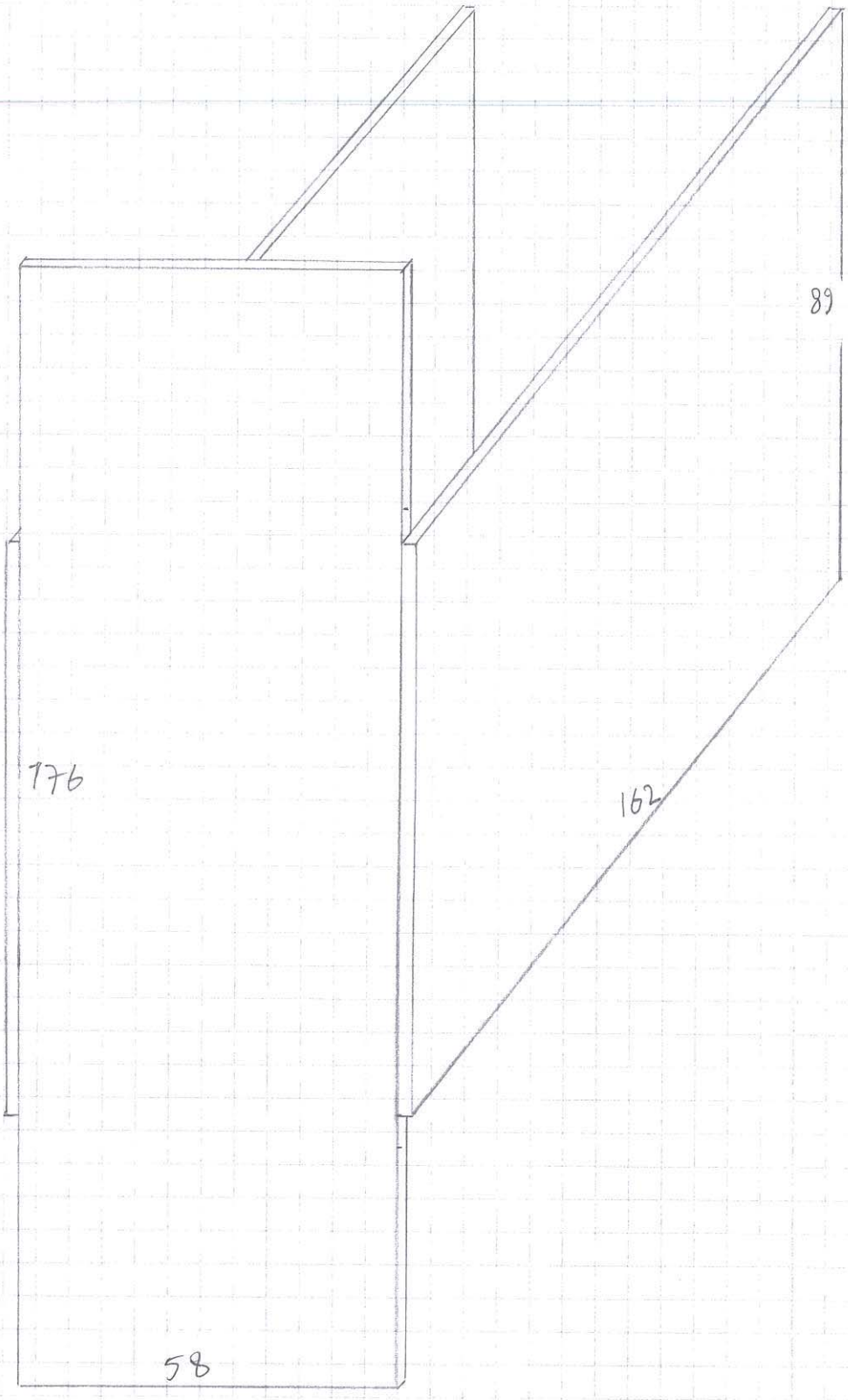

Ferrite LV2/3

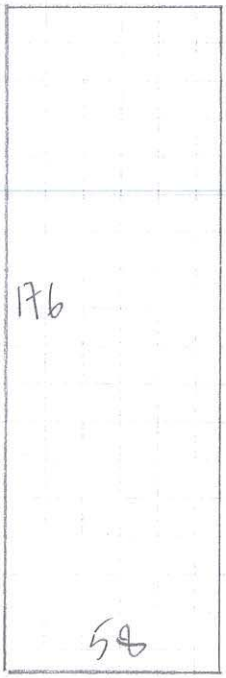

x2

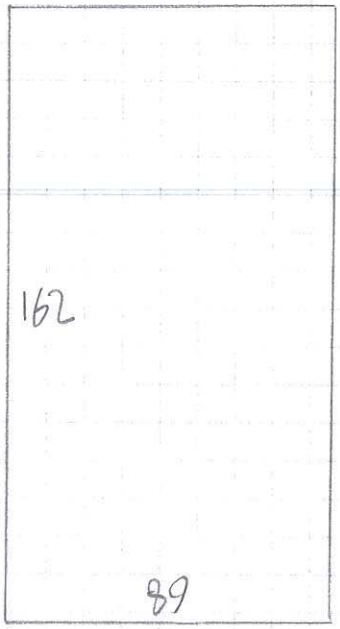

x2

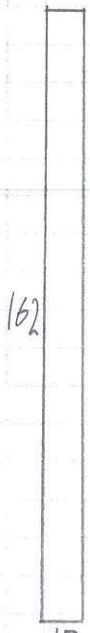

x4

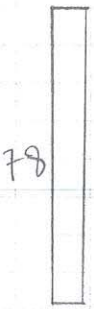

x4

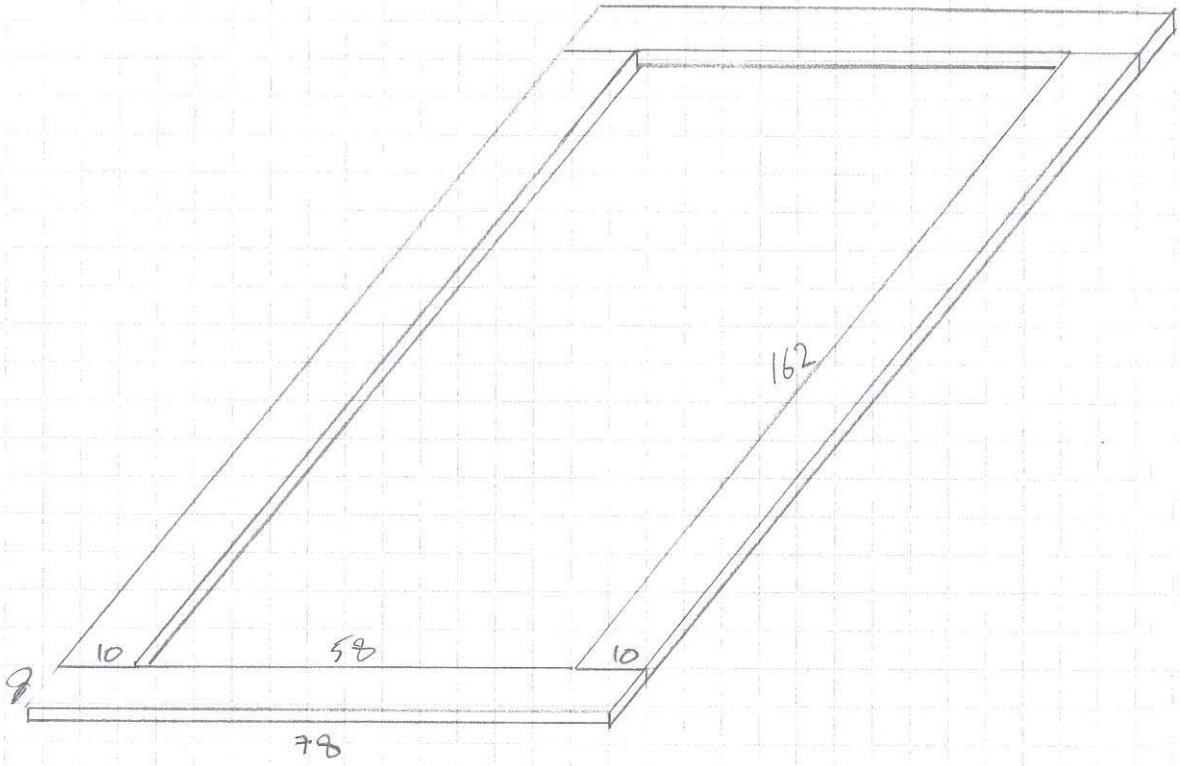

Ferrite LV 3/3
Cutting

176x58 mm² x2

162x89 mm² x2

162x10 mm² x4

78x9 mm² x4

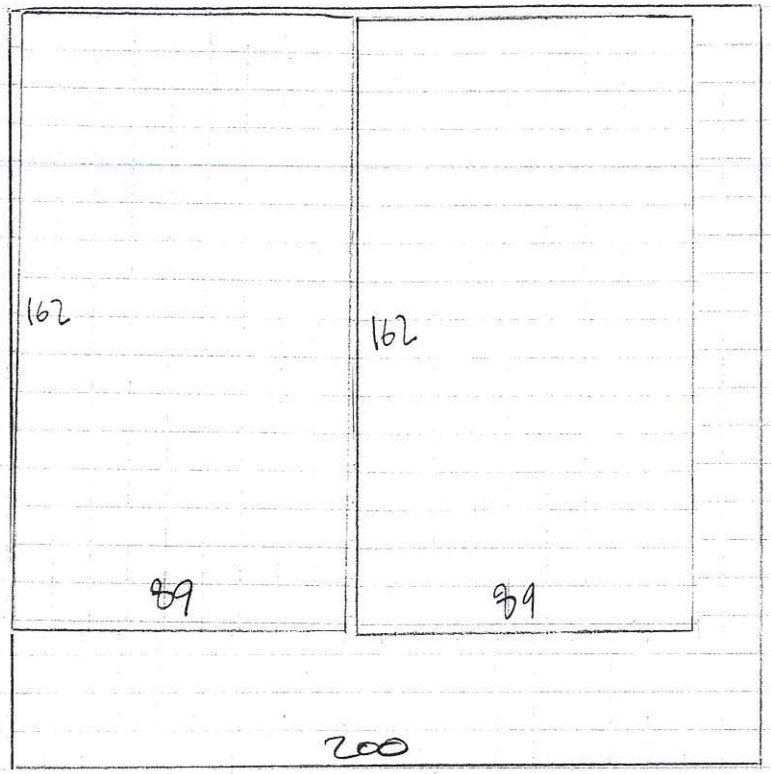

[mm]

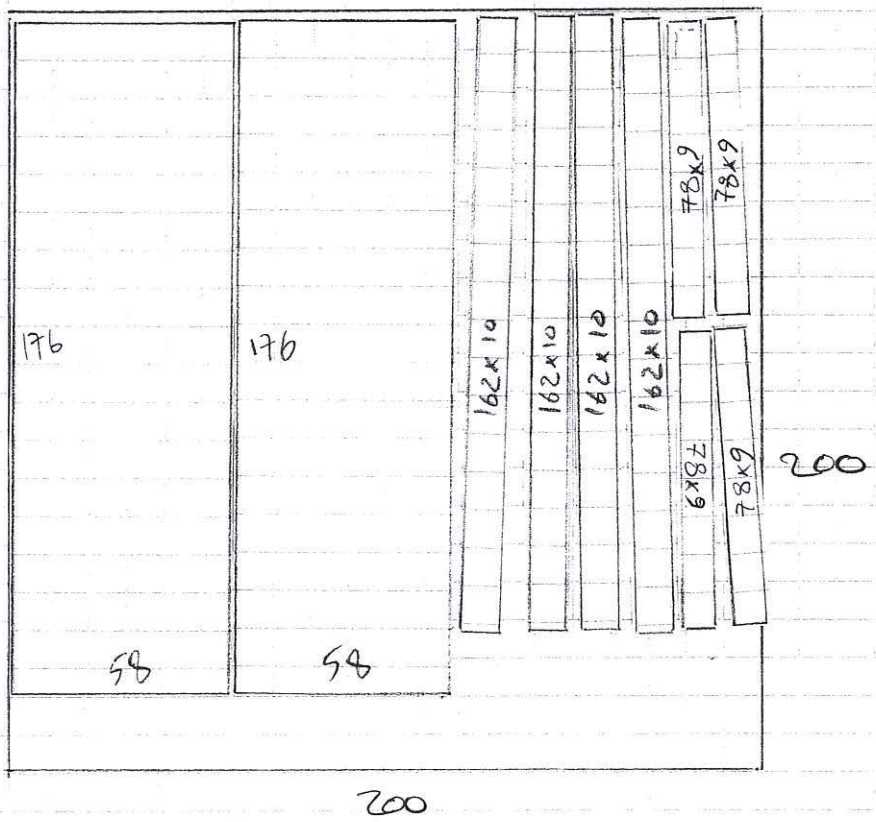

30x5+8=158

Ferrite LV
Cutting

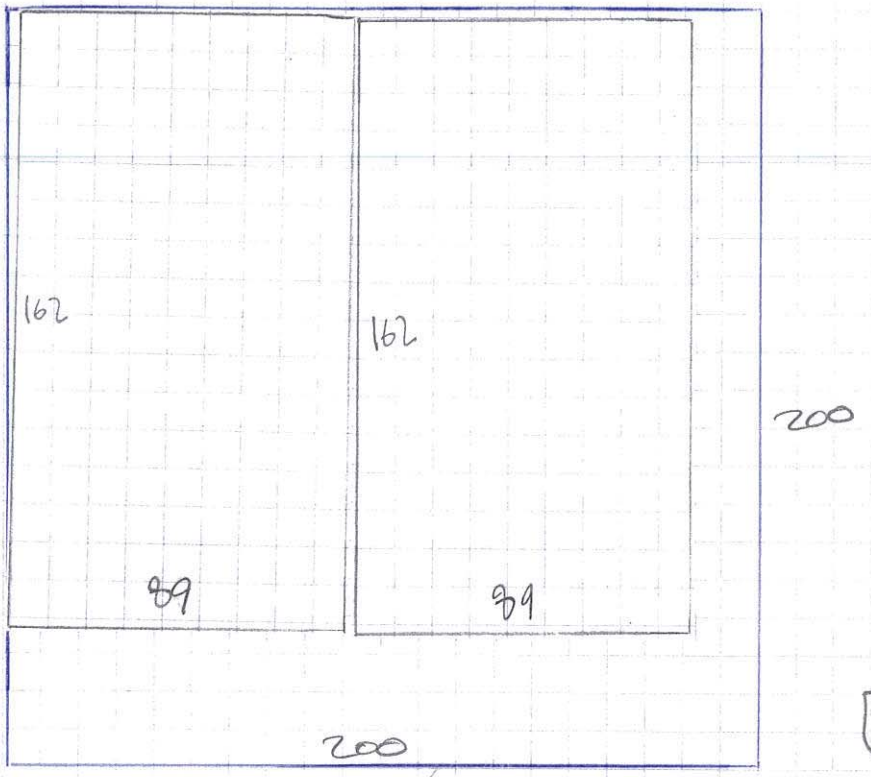

[mm]

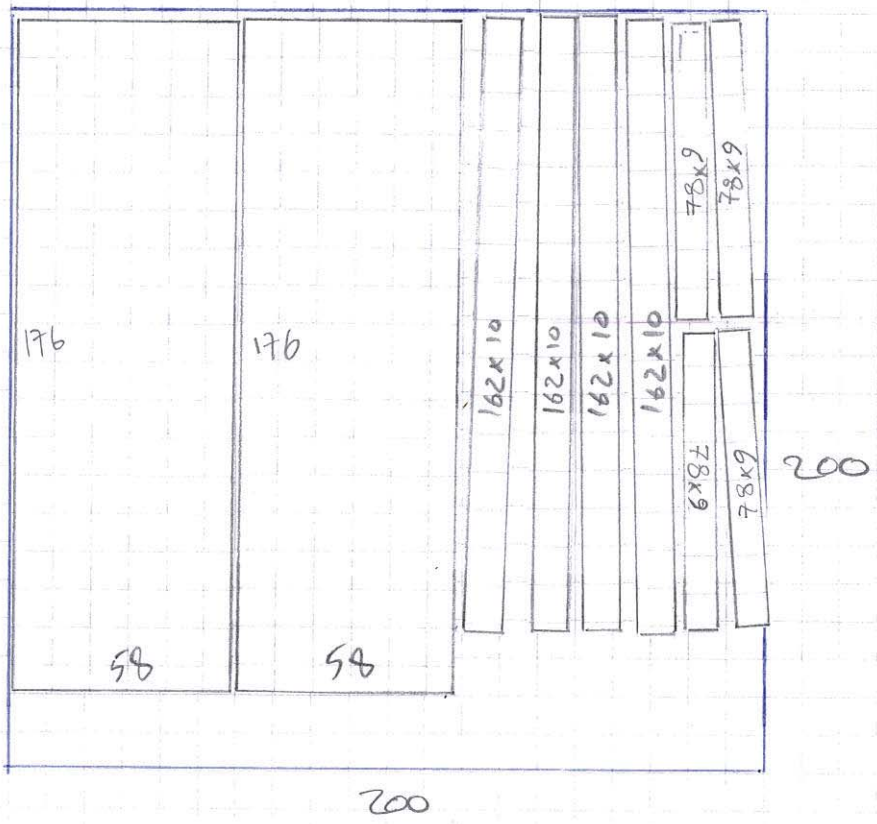

HV Ferrite 1/2

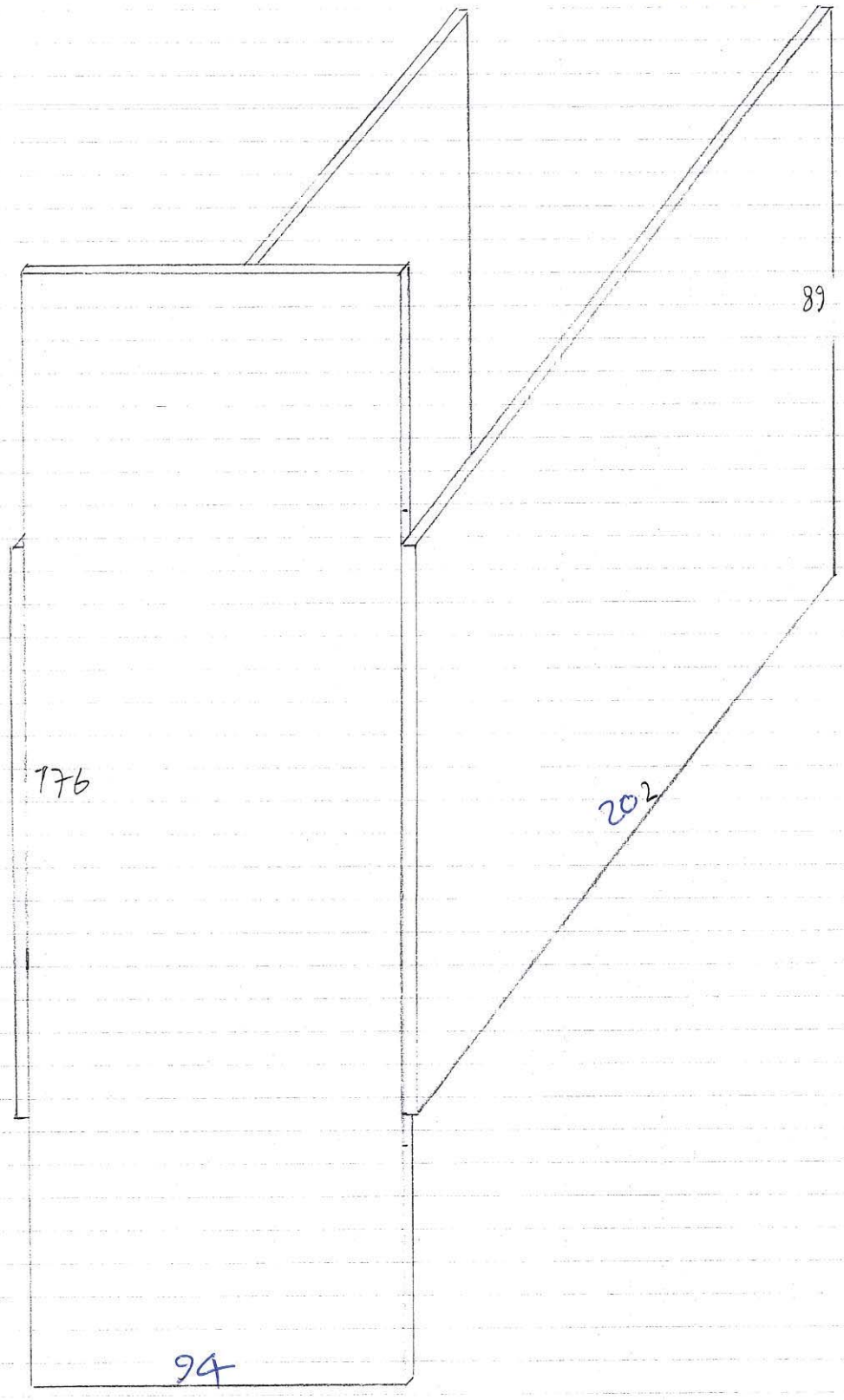

HV 2/2
Ferrite

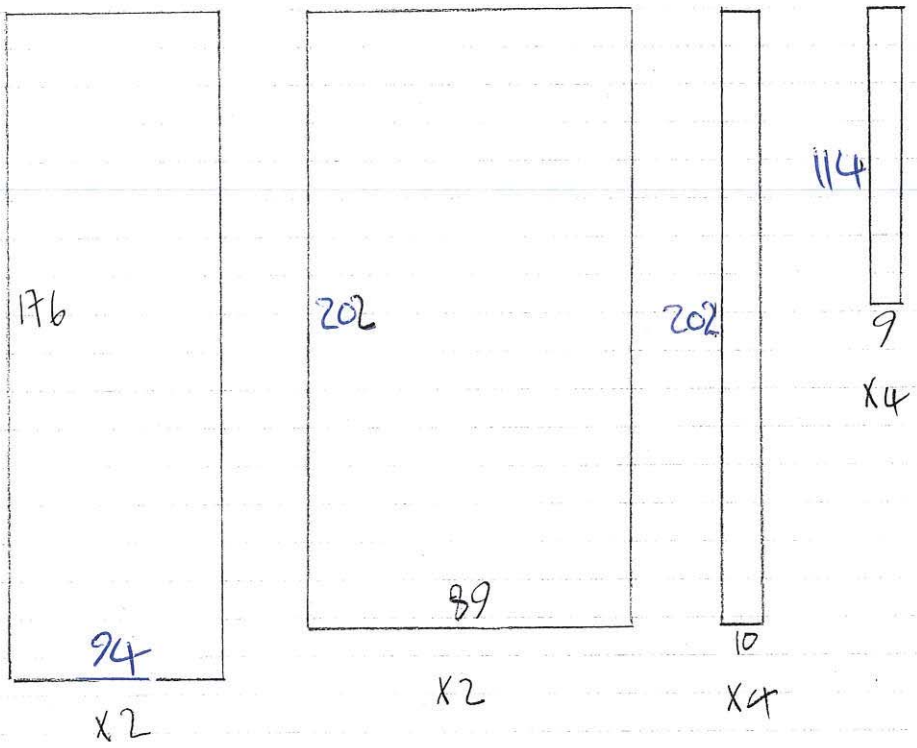

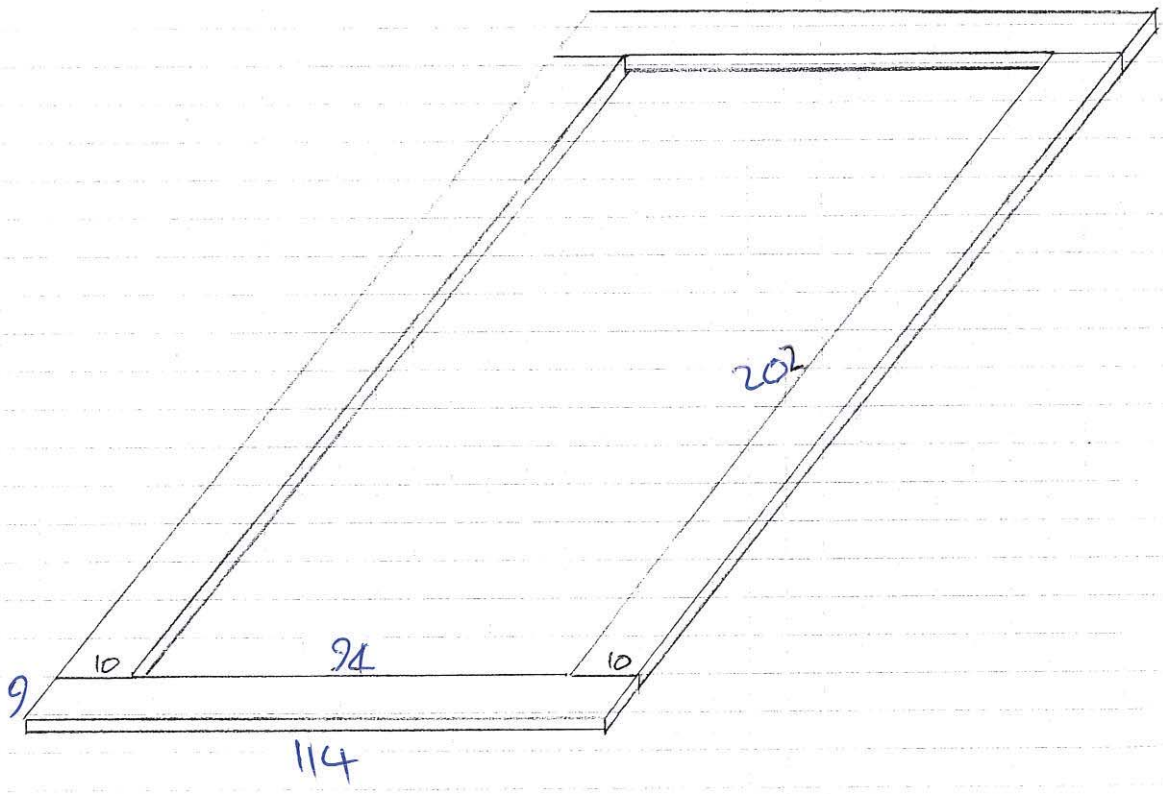

Ferrite HV
Calculations
A1

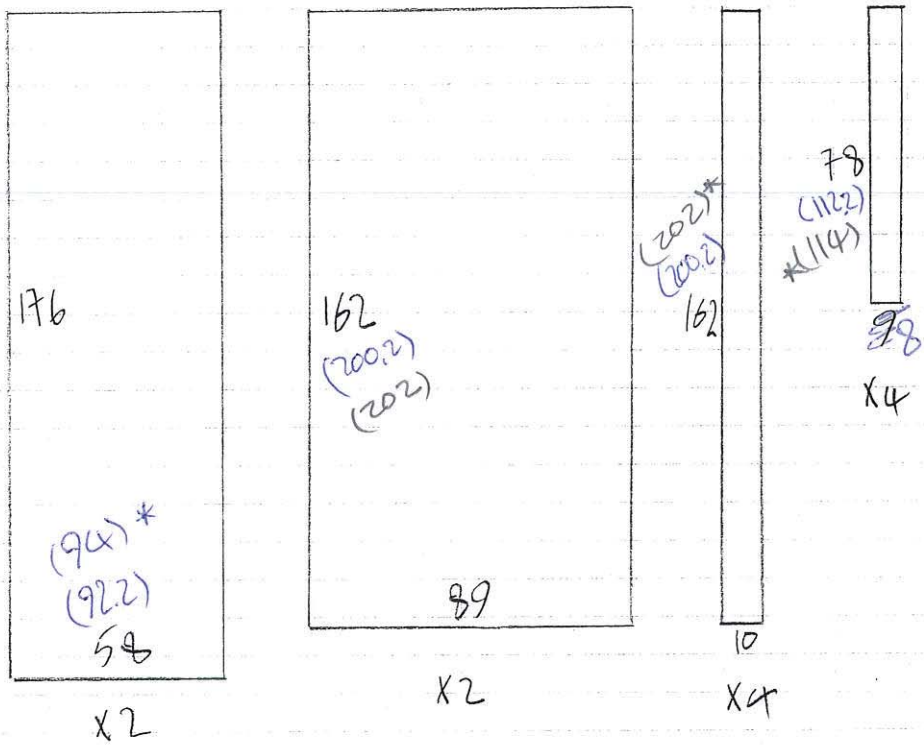

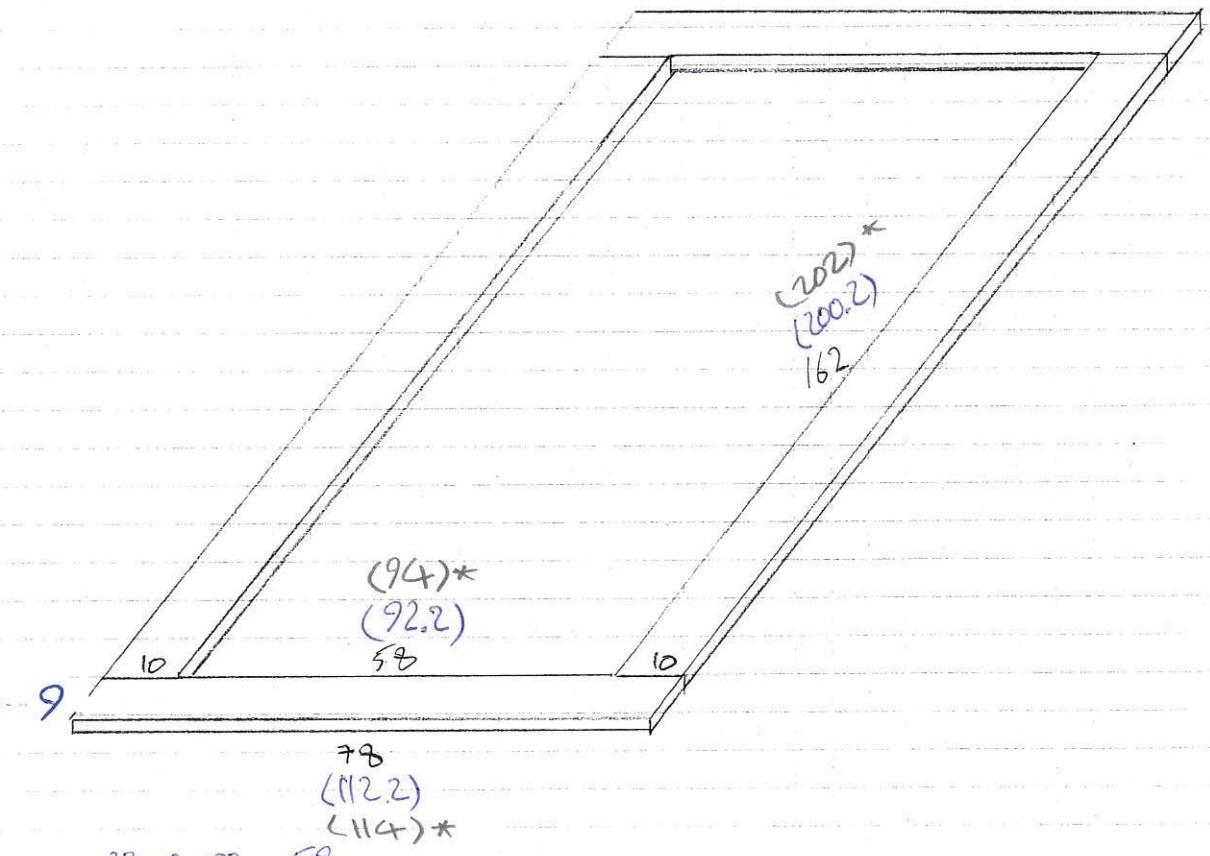

LV: 28+2+28 = 58

HV: 2+9.6+3x2.5+2+28+2+28+2+3x2.5+9.6-2 = 92.2 = 2+9.6+7.5+2+58+2+7.5+9.6-2

HV, LV: 3x2.5+0.5 = 8 mm

LV: 2+30+2+30+2+30+2+30+2+30+2 = 162

HV: 2+9.6+3x2.5+2+30+2+30+2+30+2+30+2+30+2+3x2.5+9.6+2 = 2+9.6+7.5+162+7.5+9.6+2
= 200.2

Ferrite HV
Calculations A2

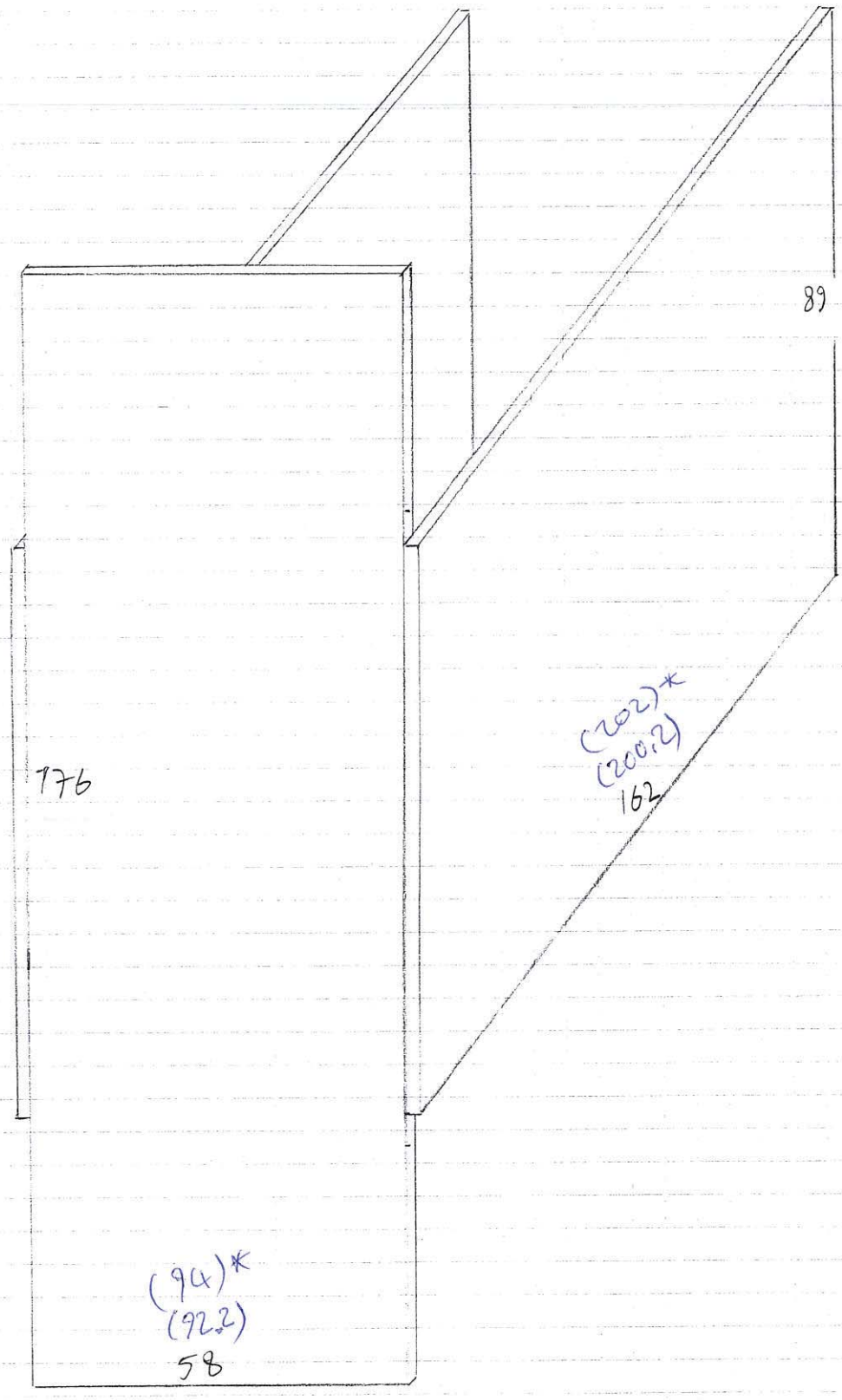

Mohammad 1/2 HV+Cover HV LV
MTe 4P00711-01 Ferrite

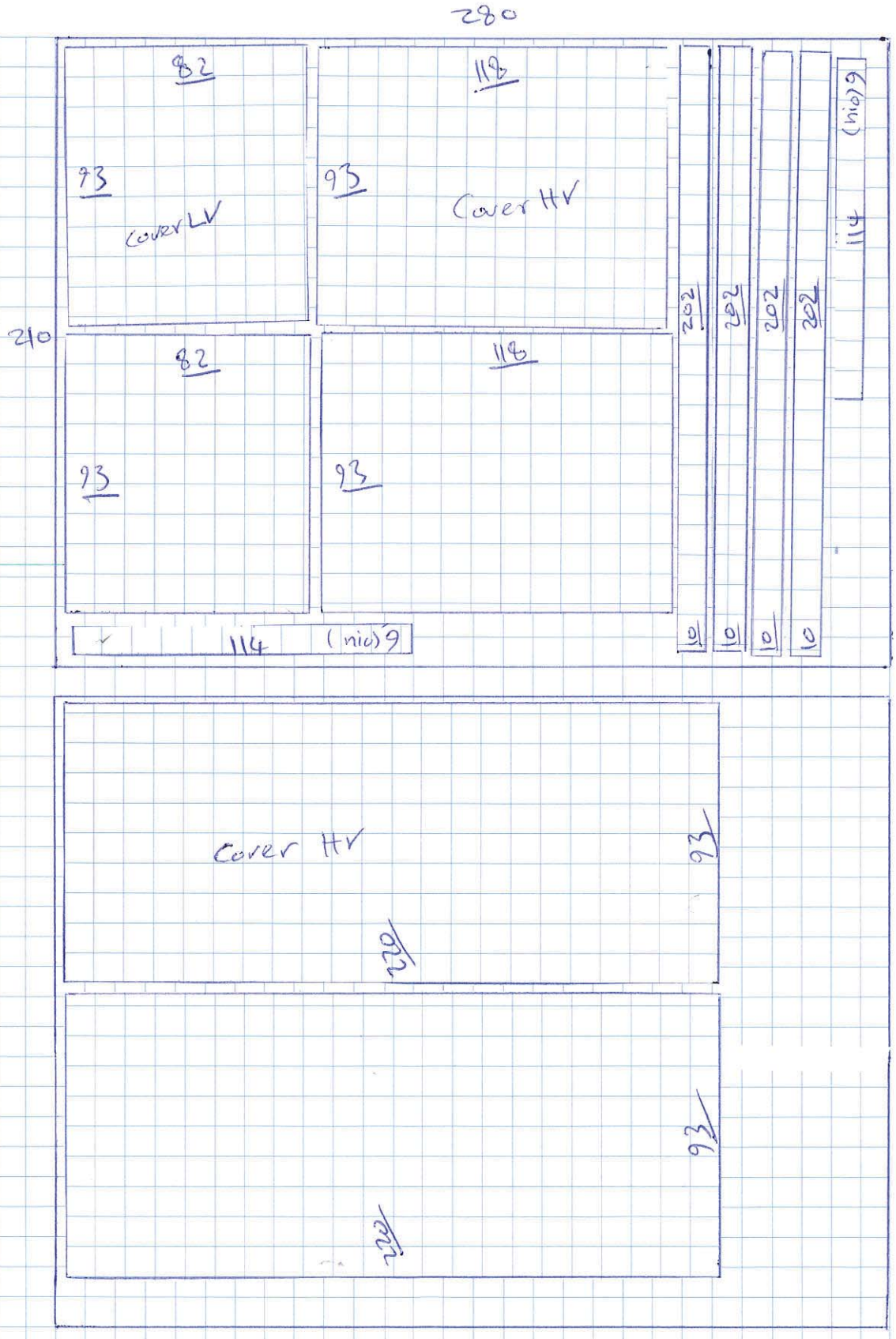

Mohammed 2/2 HV+CoverLV

MTe 4PC0711-01 Ferrite

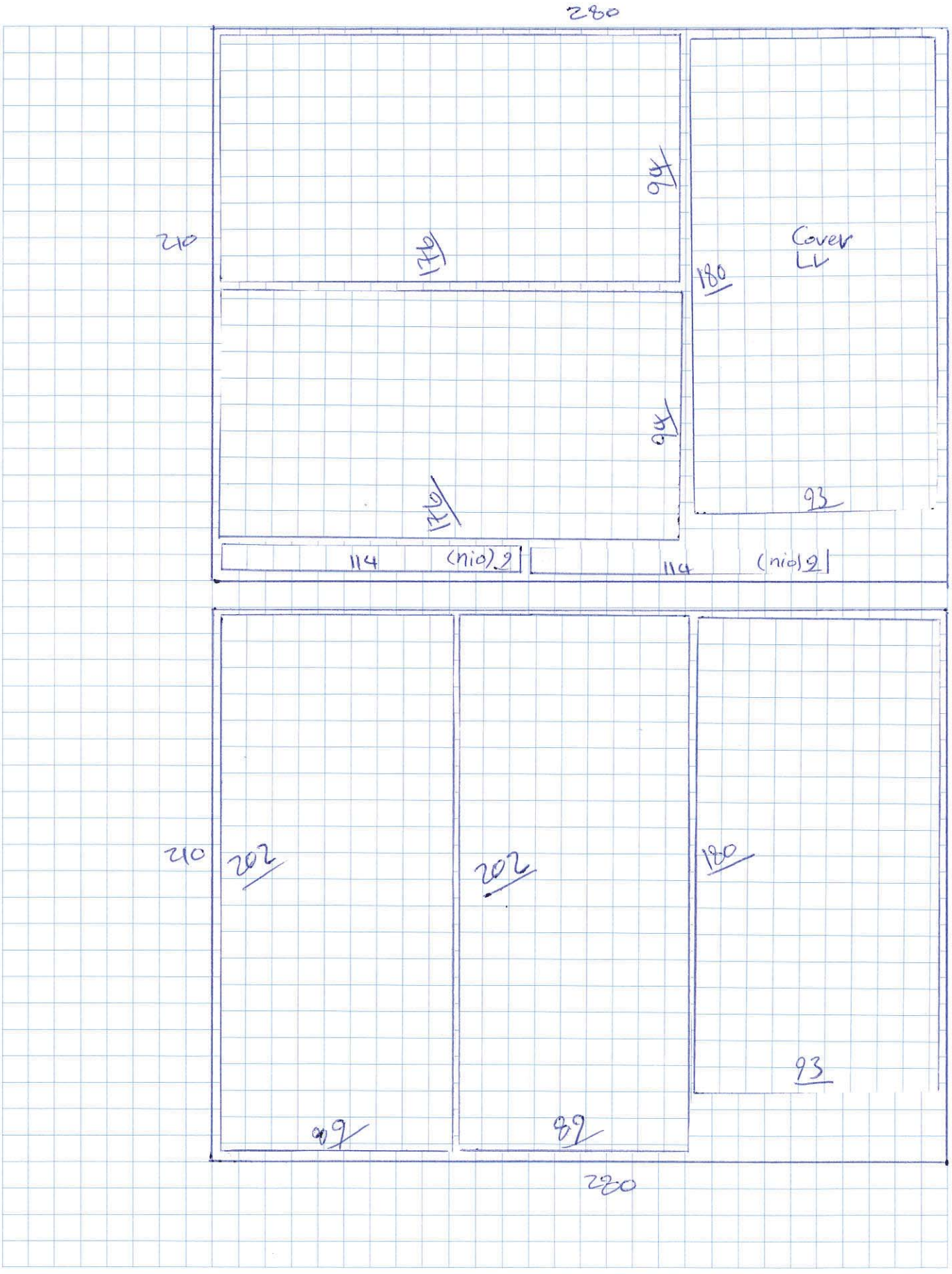

Ferrite Covers

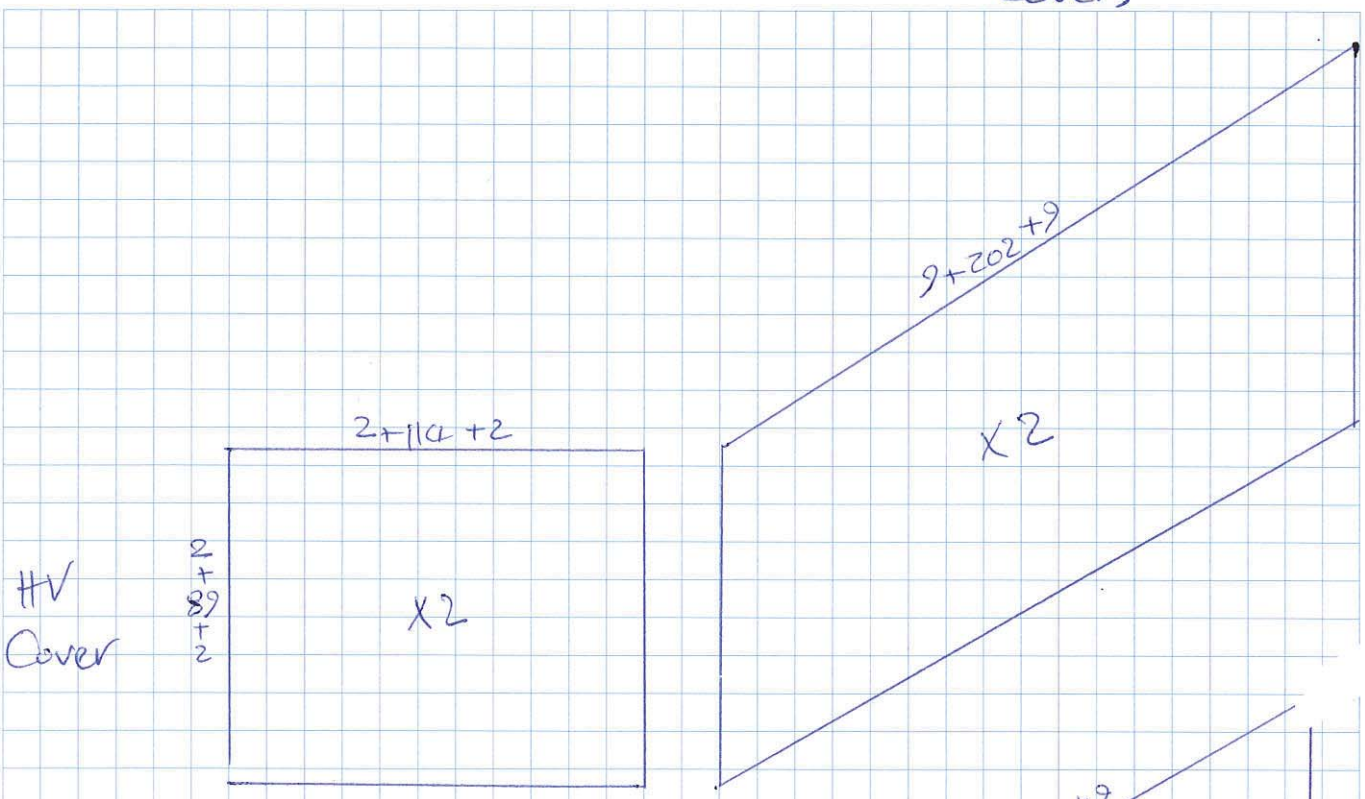

HV Cover

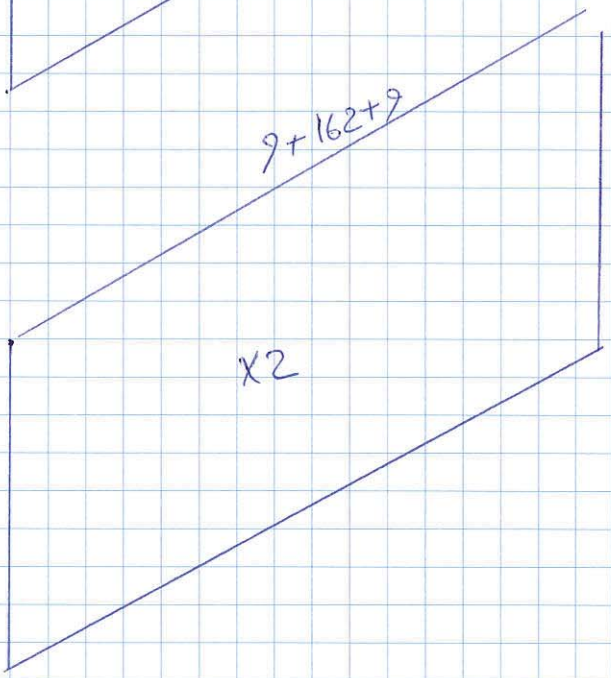

LV Cover

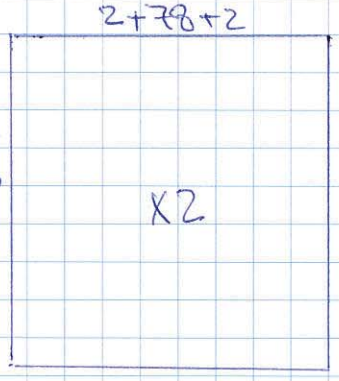

Nano
Bobbines

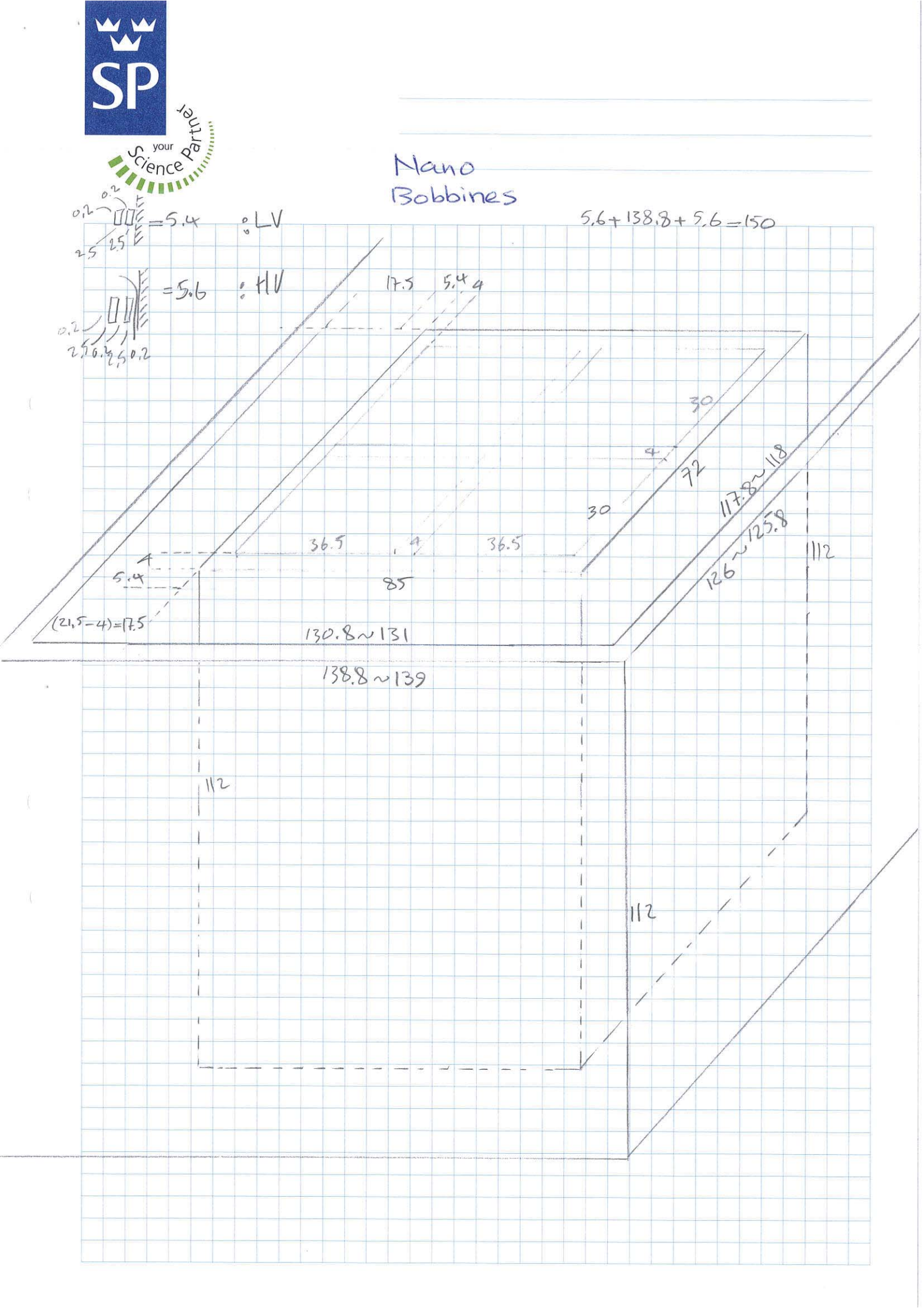

Nano HV

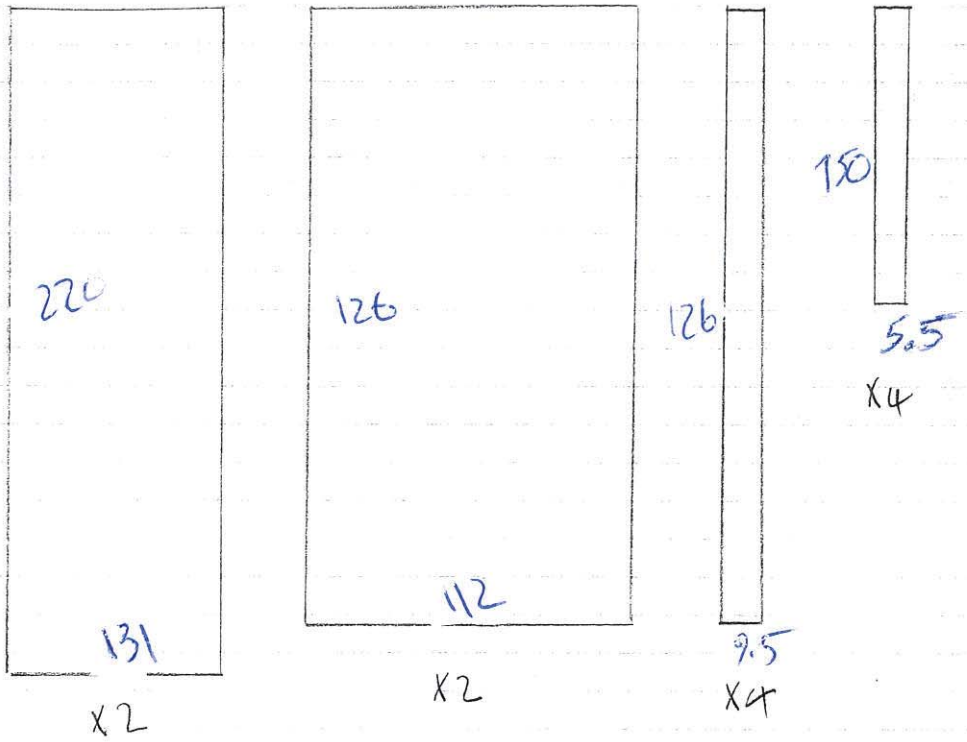

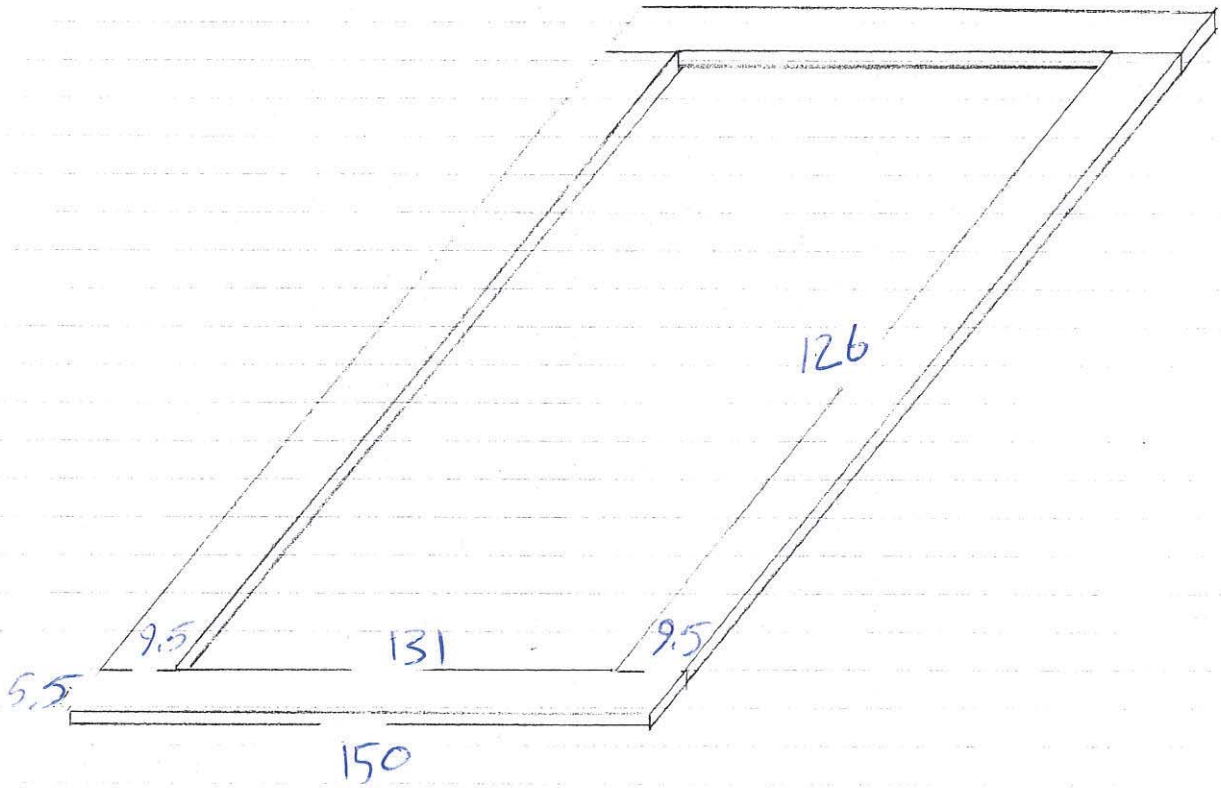

5.6 ~ 5.5

4 + 5.6 ~ 9.5

Thickness : 4 mm

Nano HV

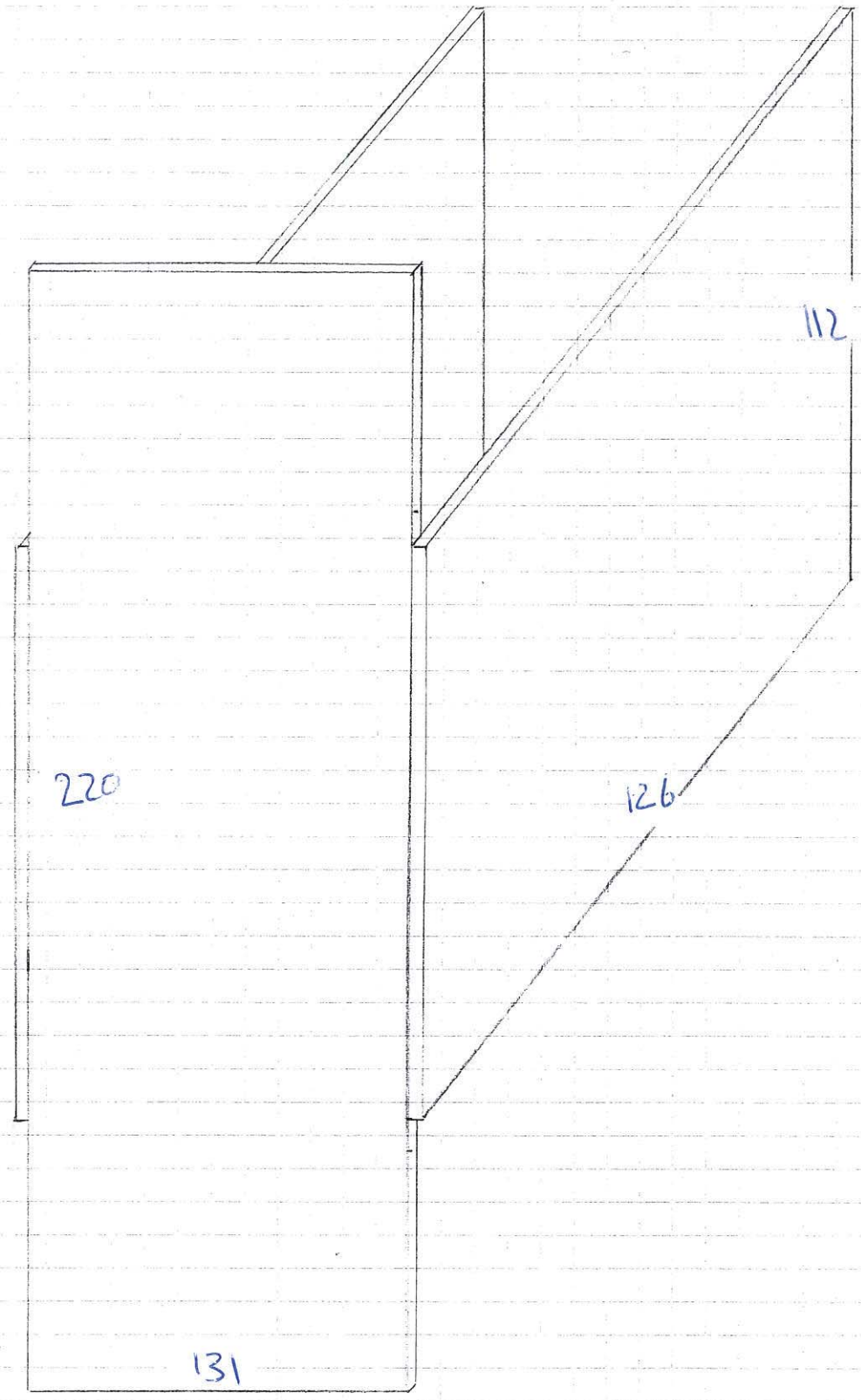

15+35+4+112+35+15=220

Thickness: 4mm

Nano LT mm

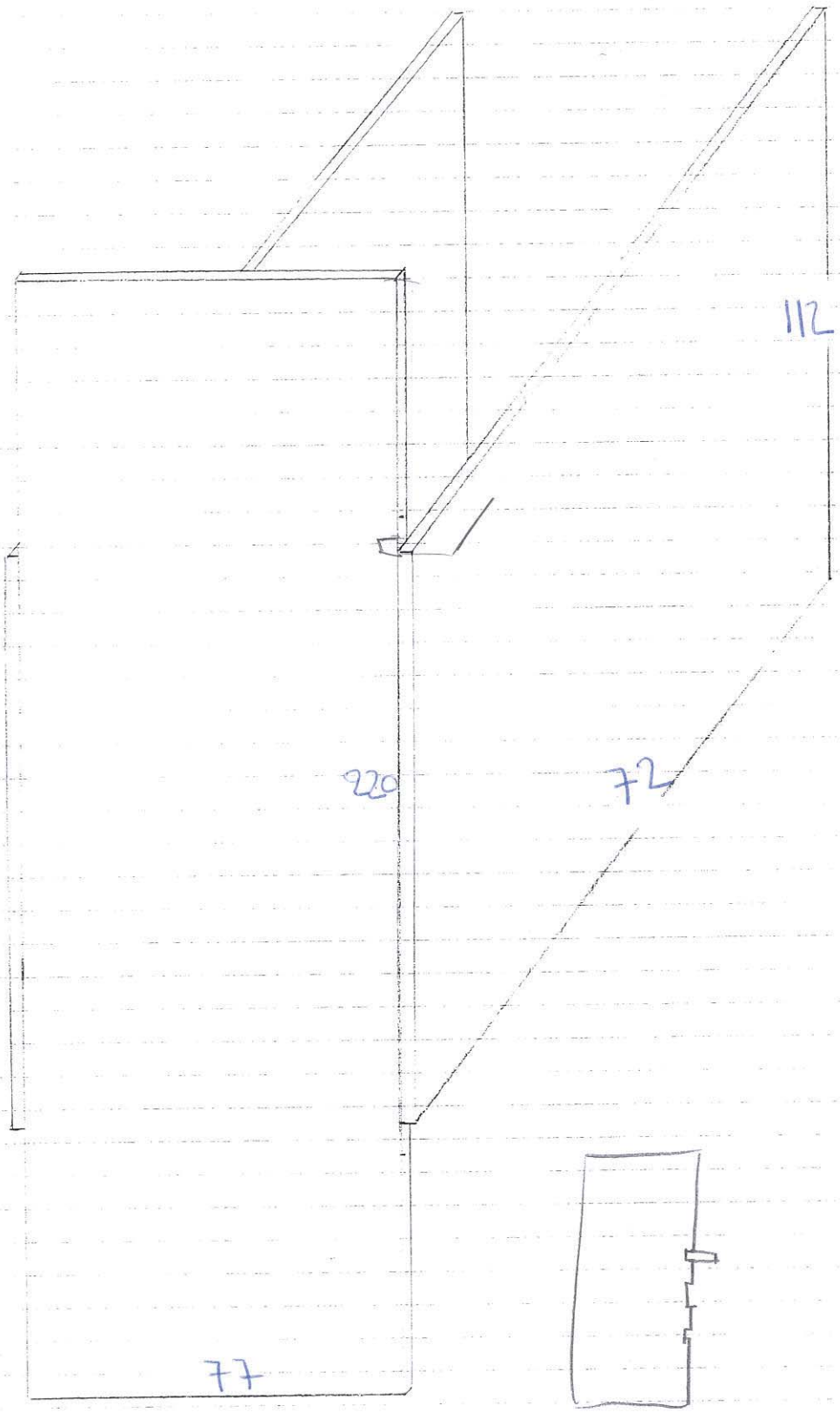

15 + 35 + 4 + 112 + 4 + 35 + 15 = 220

Thickness : 4 mm

Nano LV mm

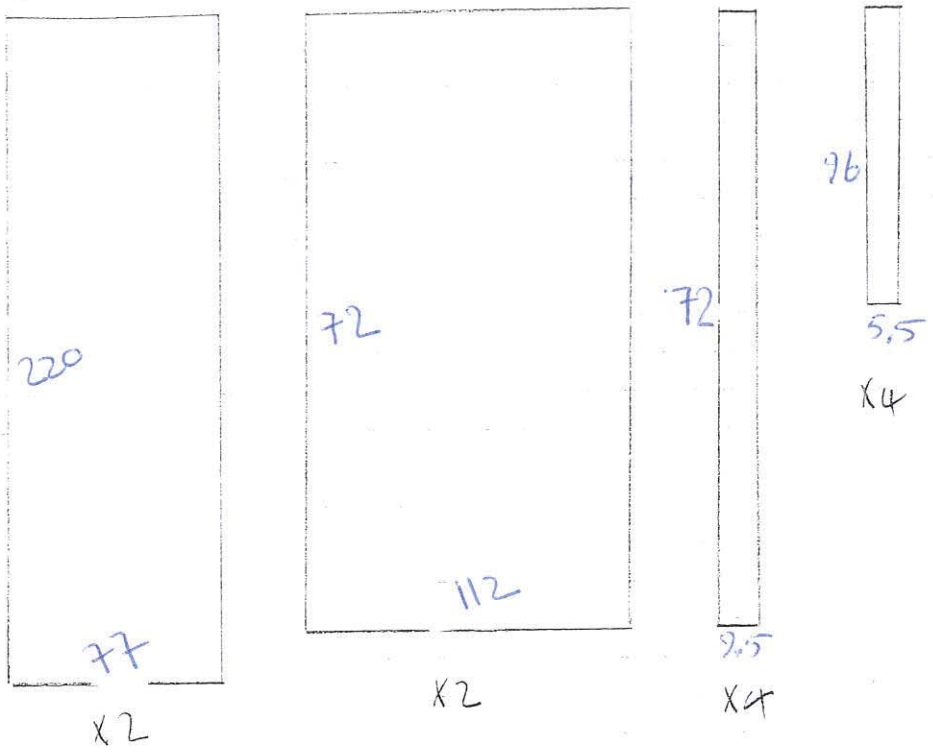

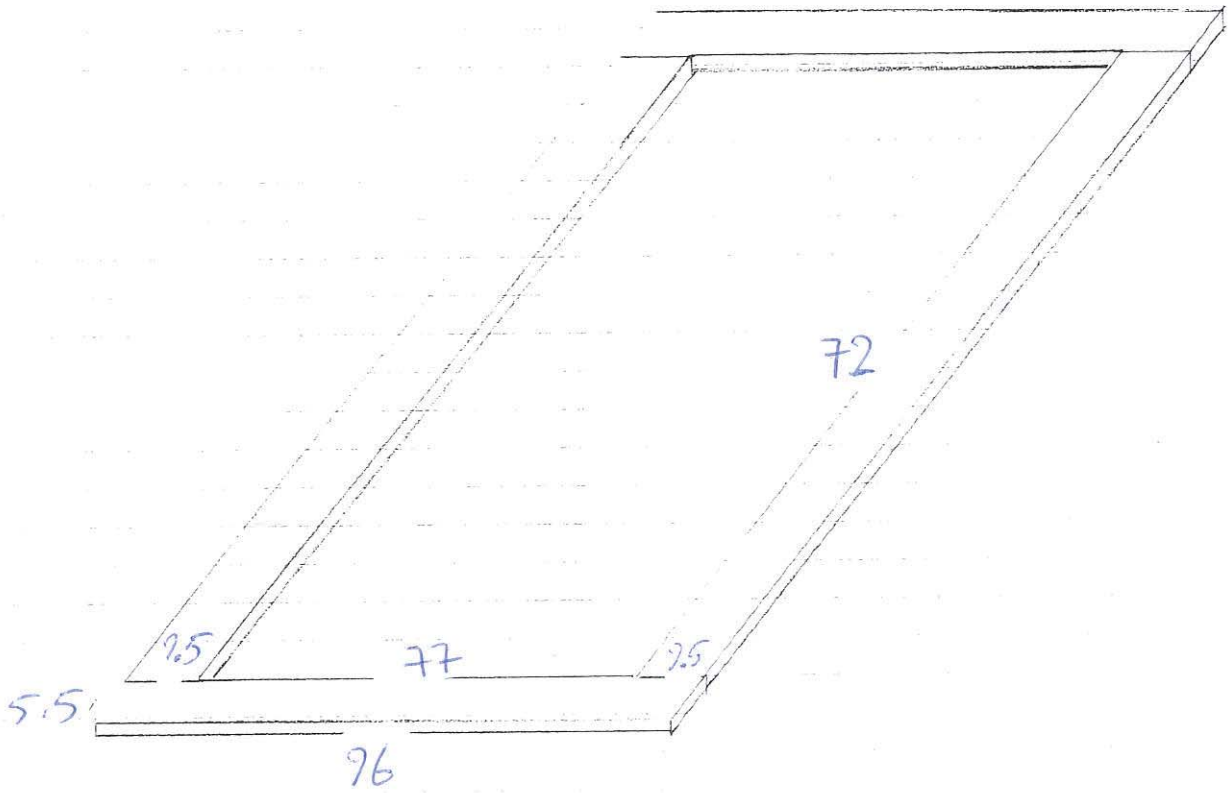

4 + 5.4 = 9.4 ~ 9.5

5.4 ~ 5.5

Thickness : 4 mm

Cover HV & LV
Nano

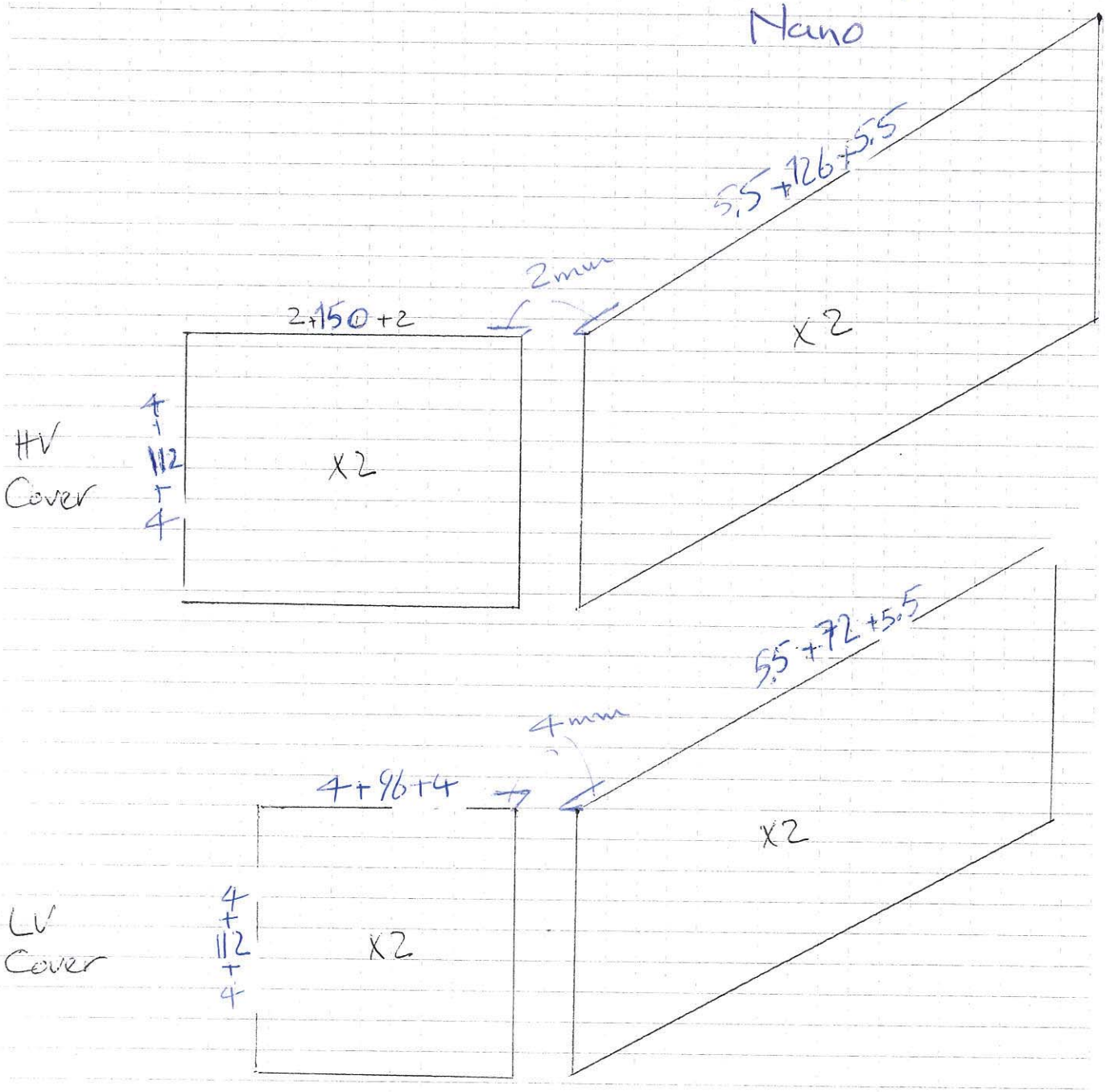

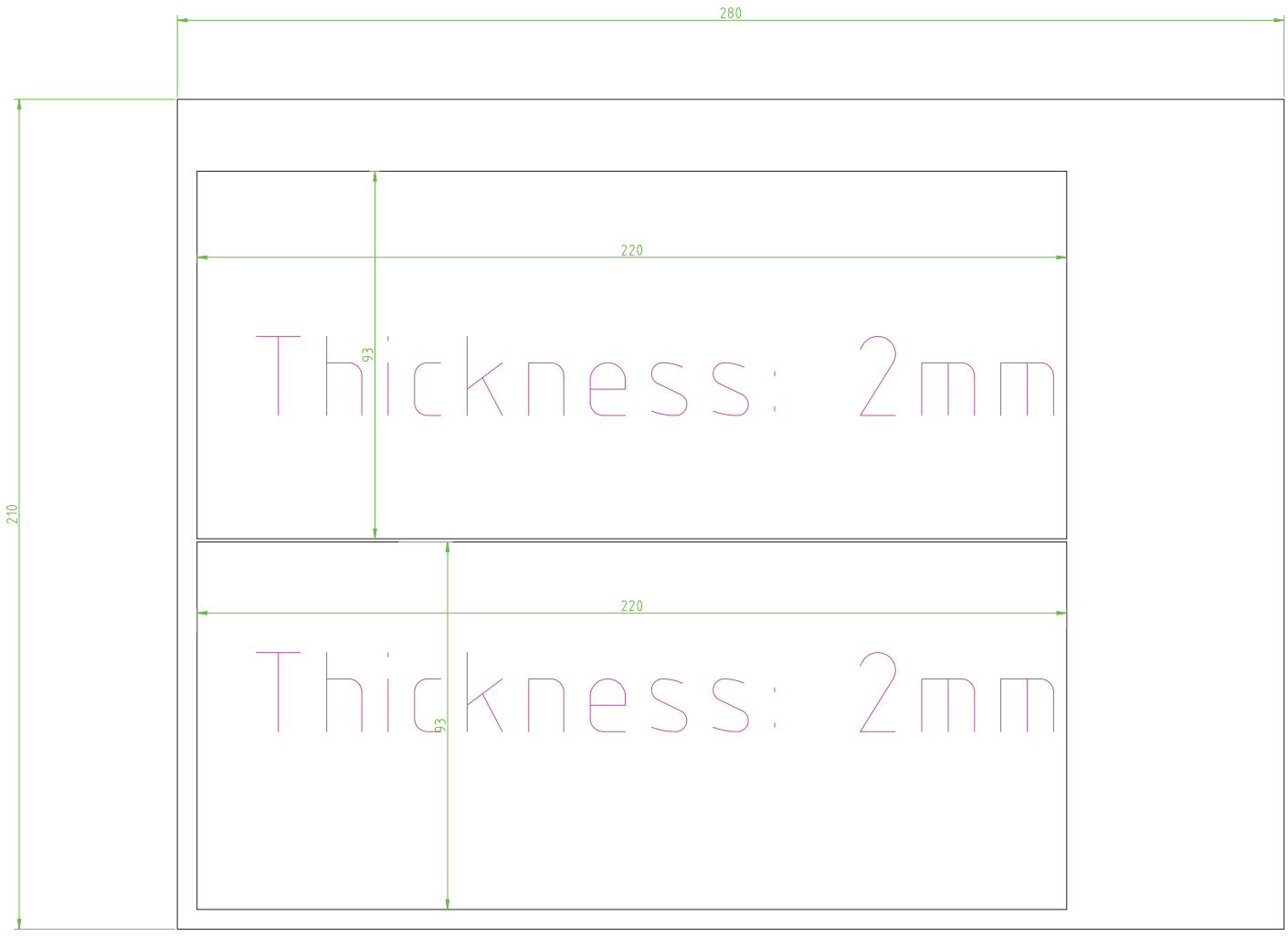
280
210
220
93
Thickness: 2mm
220
93
Thickness: 2mm

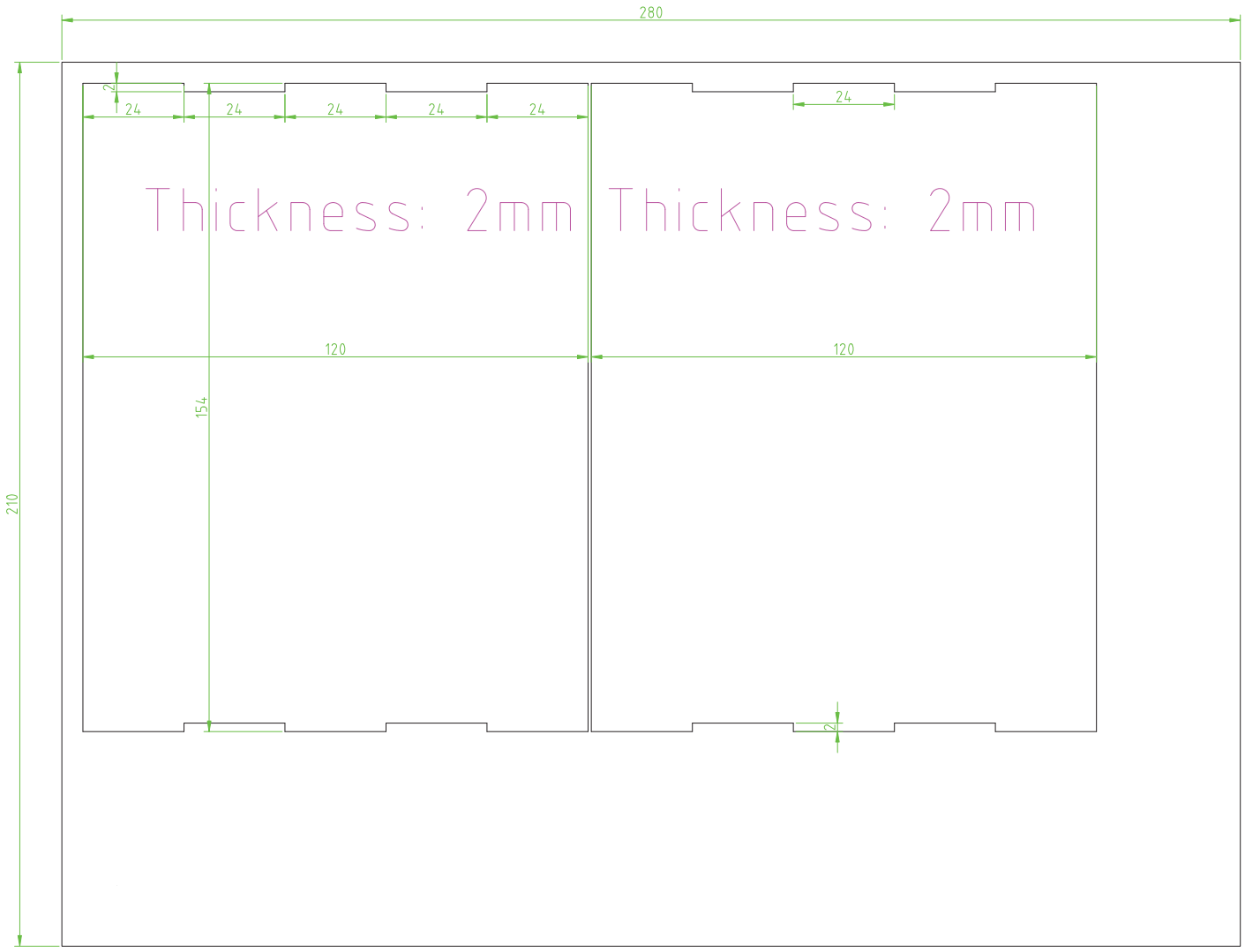
280
210
2
24
24
24
24
24
24
Thickness: 2mm
Thickness: 2mm
120
120
154
2

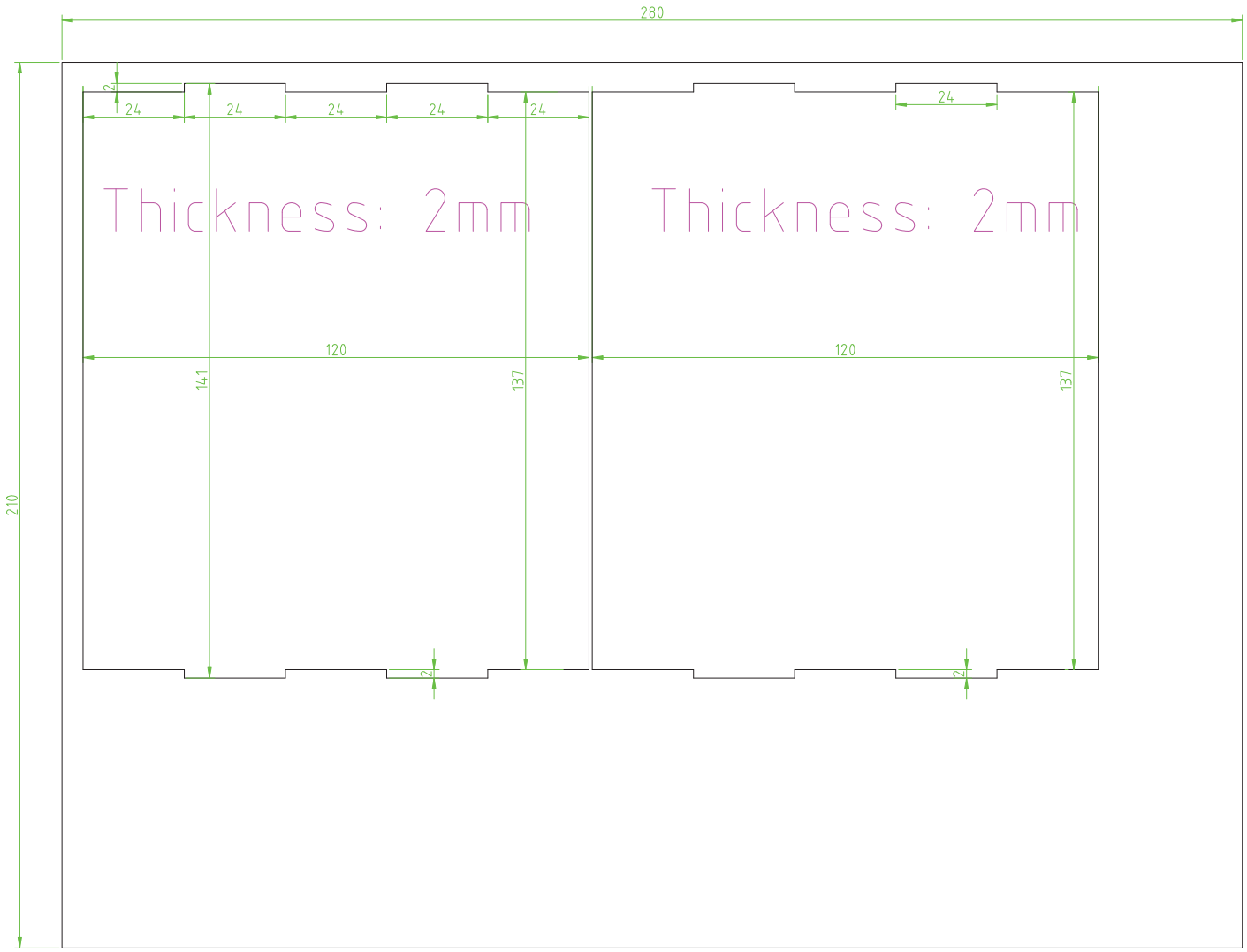
280
210
2
24
24
24
24
24
Thickness: 2mm
120
141
137
2
24
Thickness: 2mm
120
137
2

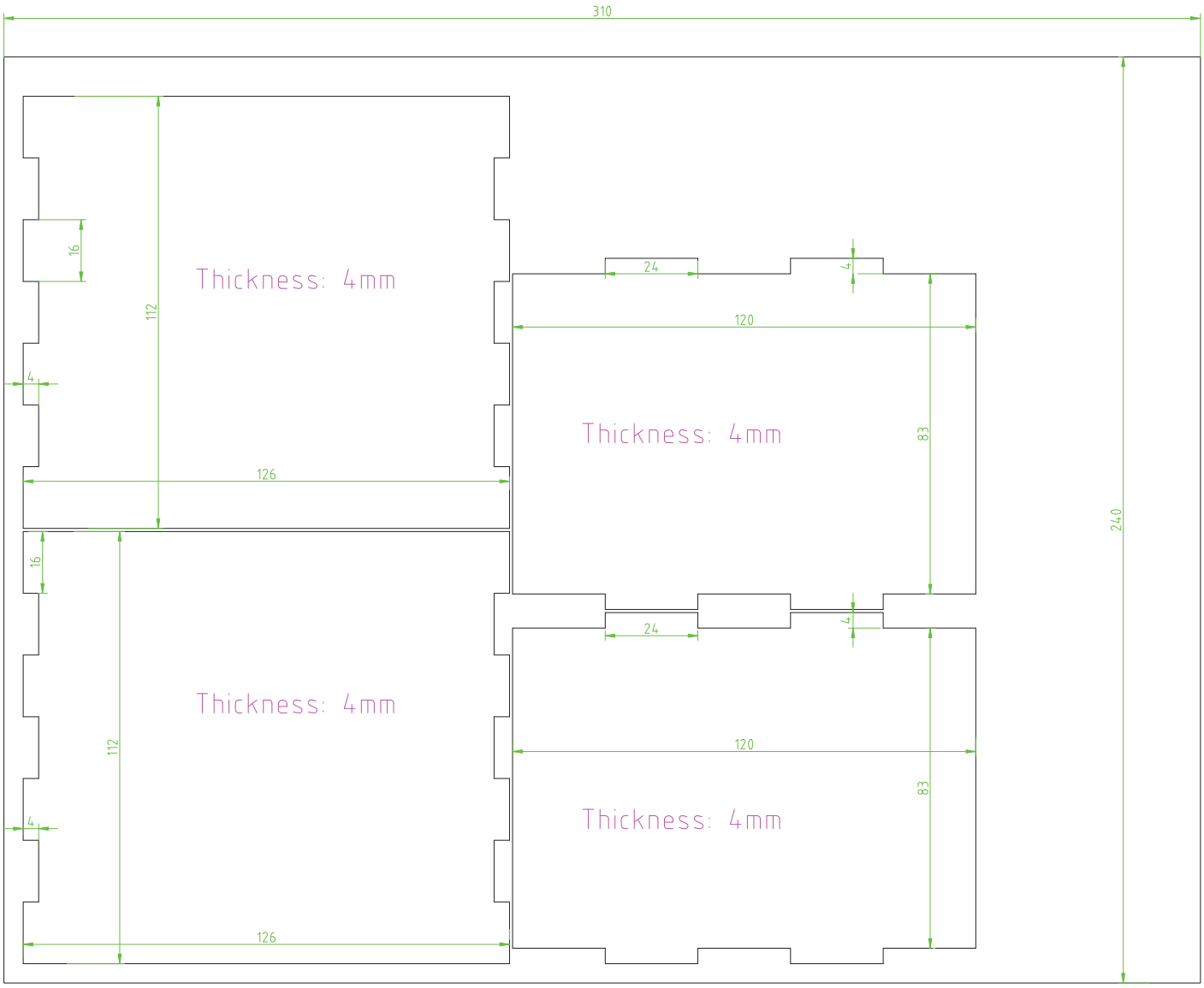
310
240
16
112
4
126
Thickness: 4mm
24
4
120
83
Thickness: 4mm
16
112
4
126
Thickness: 4mm
24
4
120
83
Thickness: 4mm

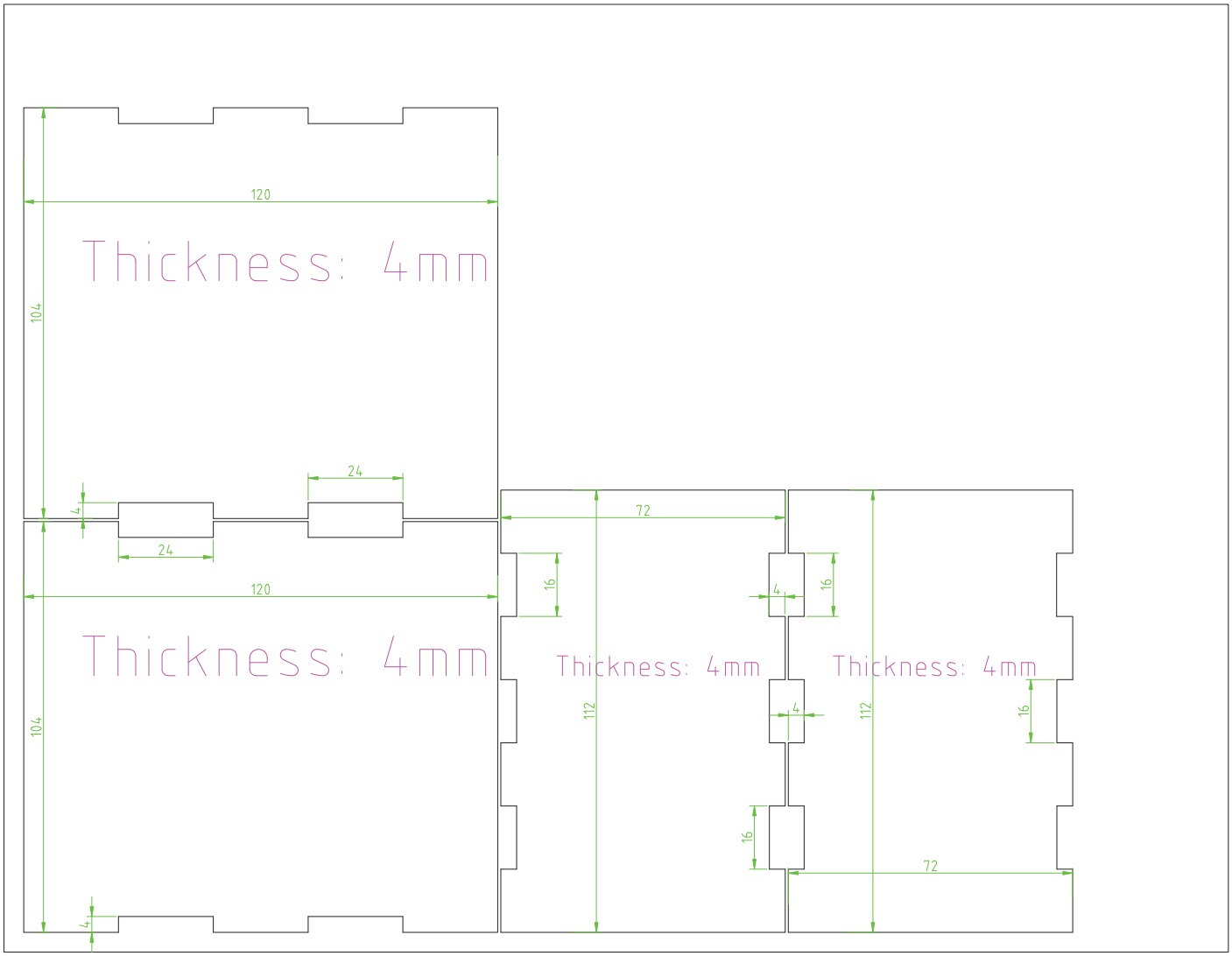
120
Thickness: 4mm
104
24
4
24
120
Thickness: 4mm
104
4
72
16
112
4
16
Thickness: 4mm
4
112
16
16
72
Thickness: 4mm

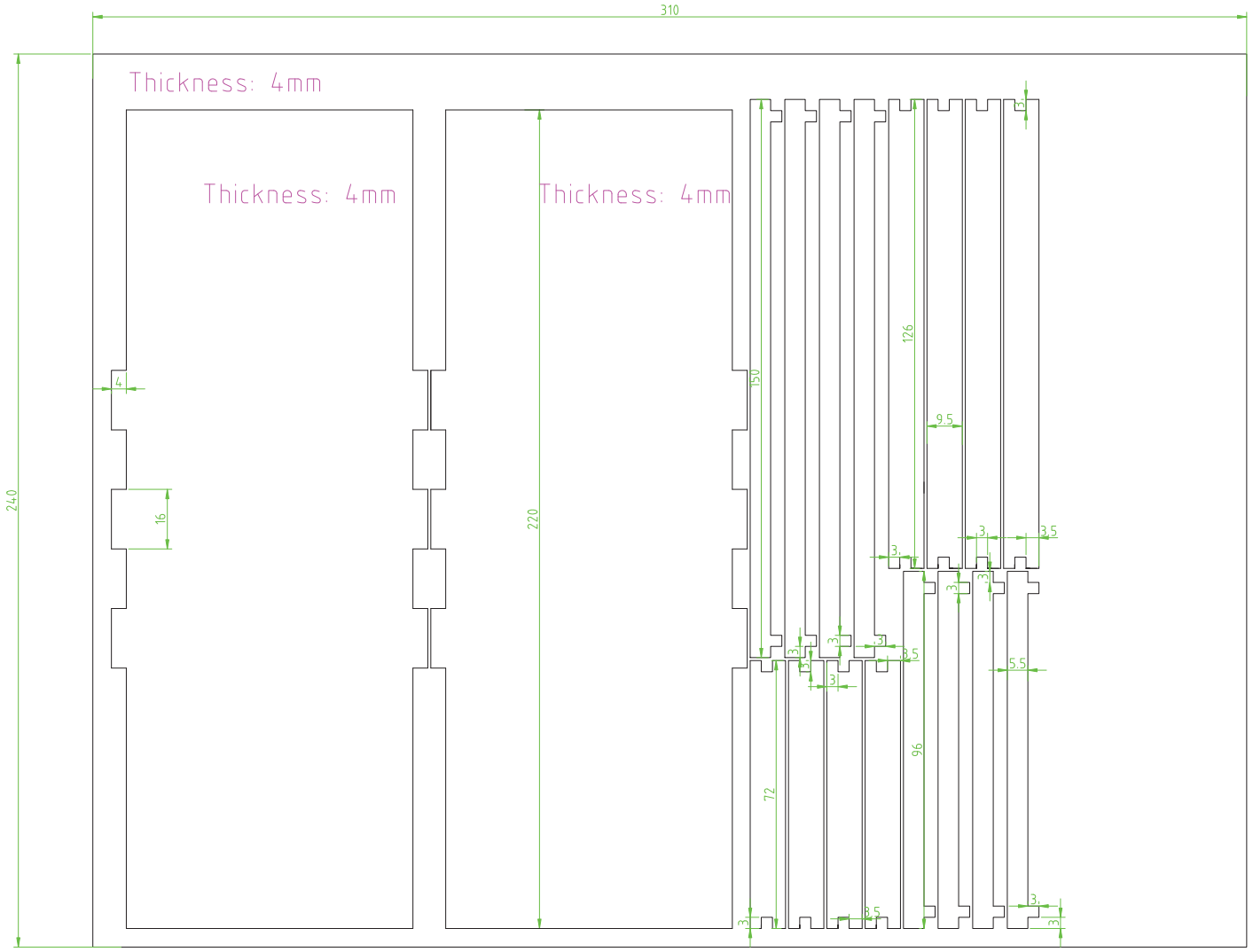
310
240
Thickness: 4mm
Thickness: 4mm
Thickness: 4mm
4
16
220
150
126
9.5
3
3.5
5.5
96
72
13

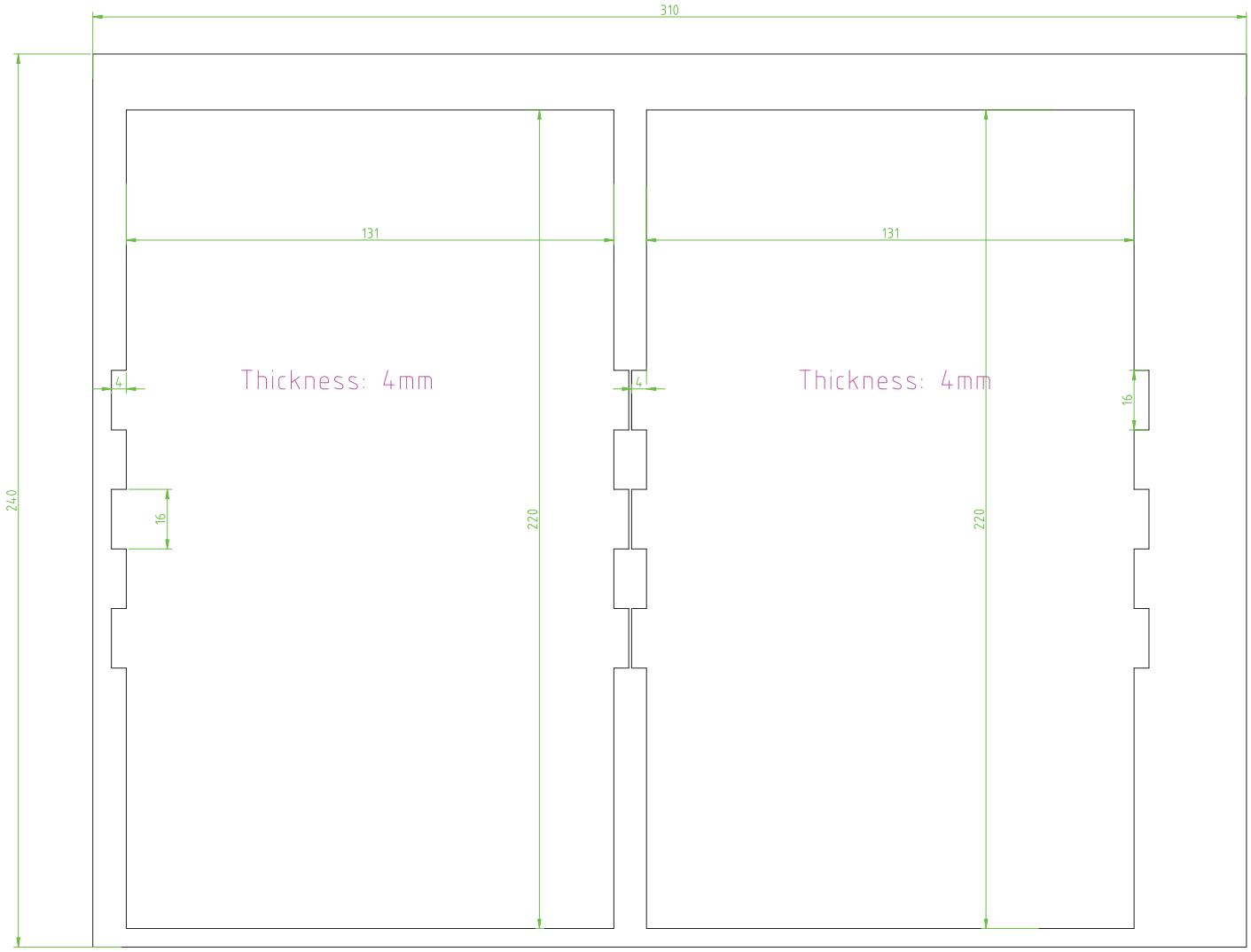
310
240
131
131
Thickness: 4mm
Thickness: 4mm
4
4
16
16
220
220

Ferrite
Pressing sheets

4P00711-01
Mohammadkh
5228

Scale 1:2
Length : mm

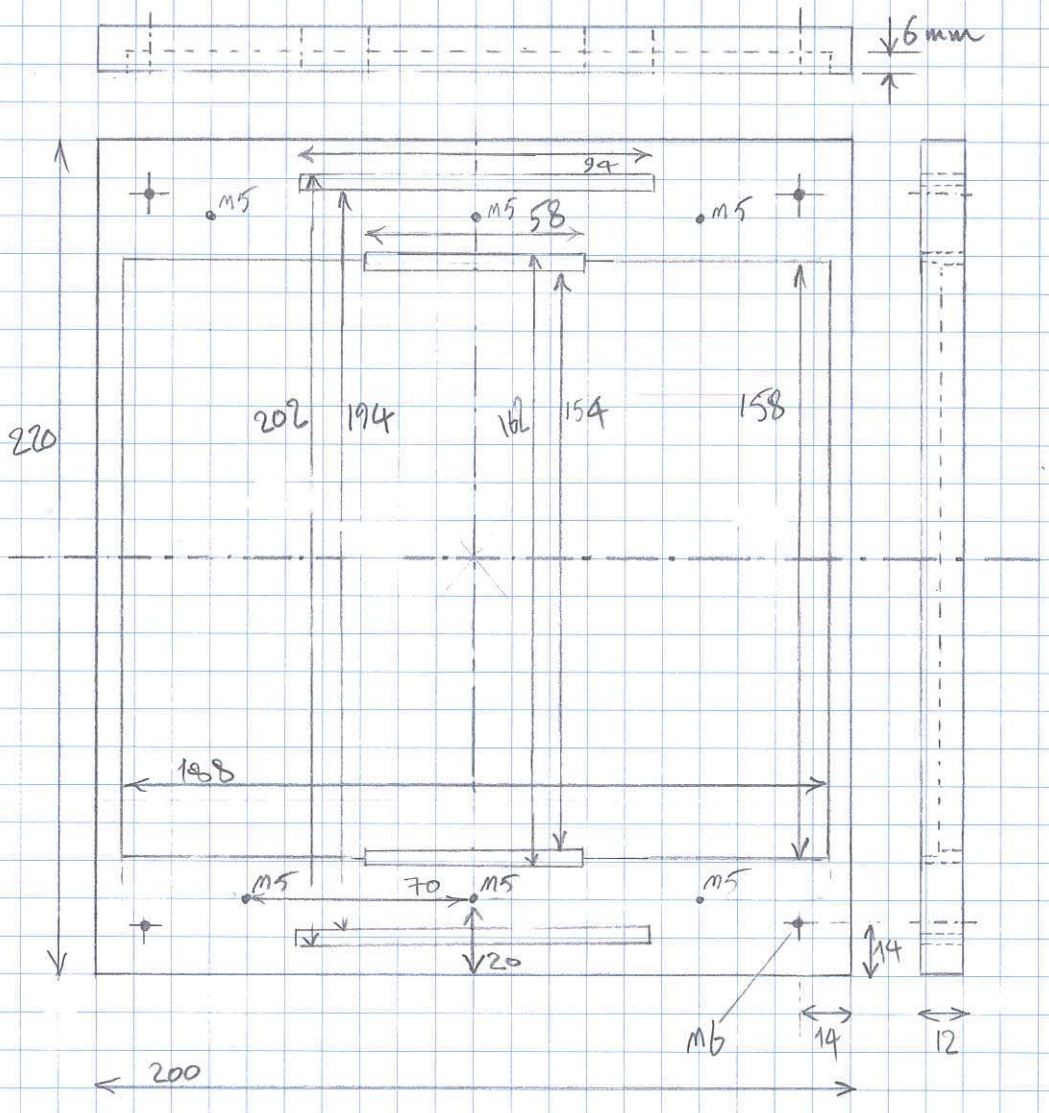

Wiring exit side

2 pieces !
Aluminium

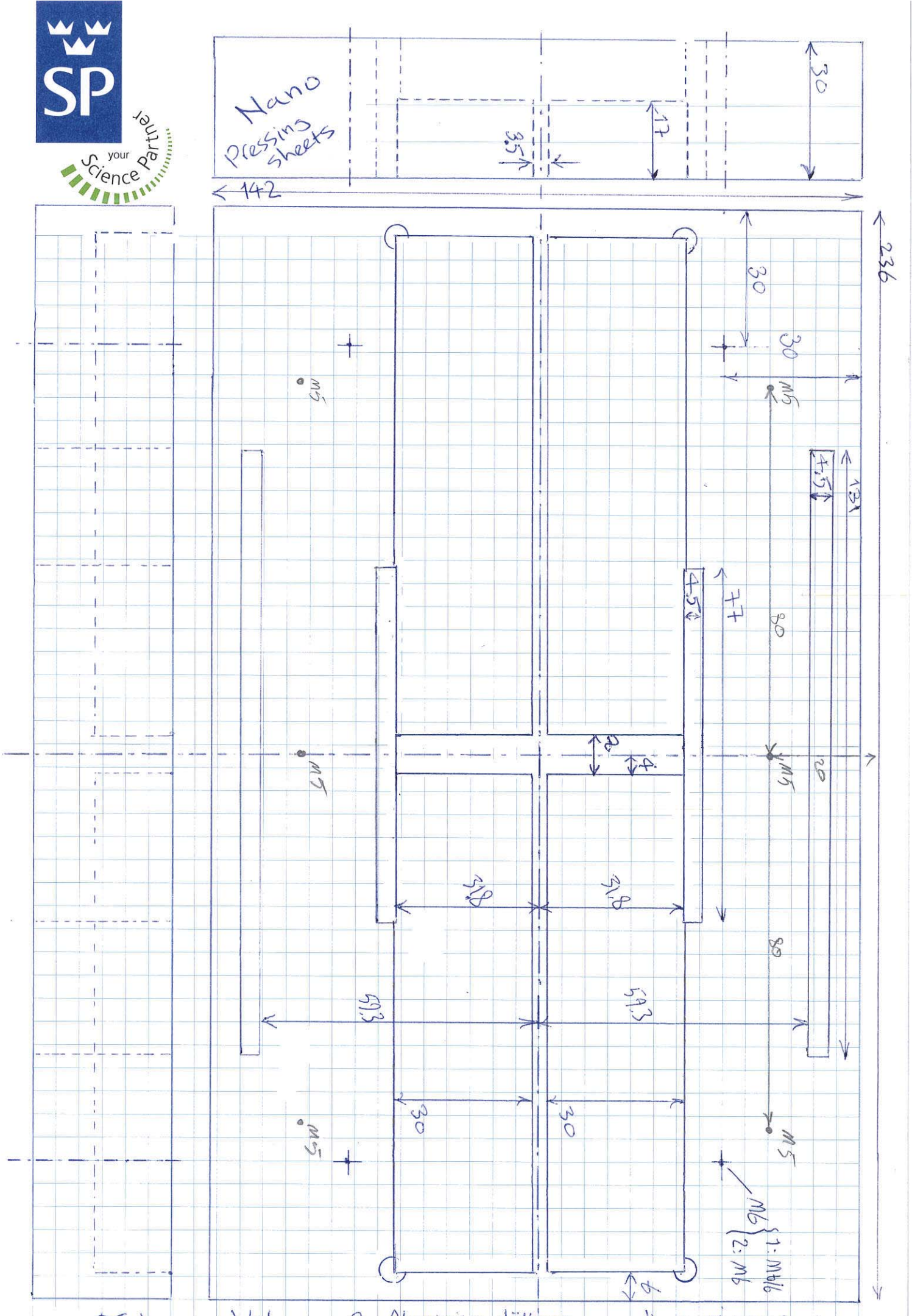

Mohammad kh
5228

2 Aluminiumplåtar
4100711-01

dimensioner : mm

Enamelled Copper Wire acc to IEC - Europe

General

Product-Code (Show all)	P155 ☑
Product-Name	Polysol155
General Description	mod. Polyurethane
IEC (including the following norms)	IEC 60317-20, IEC 60317-4
NEMA (including the following norms)	MW 79, MW 2, MW 75
UL-approval	yes
Diameters available	0,010 - 0,50 mm
Properties	Very good solderability and high thermal properties.
Applications	Small transformers, linear motors, relais, solenoids, small motors, clock coils, watch coils, transformers, magnetic heads, instruments

Thermal Values

Product-Code (Show all)	P155 ☑
Temperature index 20.000 h acc. to IEC 60172	158°C
Cut through temperature	
0.05mm: acc. to IEC 60851-6.4	≥ 200°C
Elektrisola typical value	225°C
0.25mm: acc. to IEC 60851-6.4	≥ 200°C
Elektrisola typical value	230°C
Heat Shock	
0.05mm: acc. to IEC 60851-6.3	≥ 175°C
Elektrisola typical value	190°C
0.25mm: acc. to IEC 60851-6.3	≥ 175°C
Elektrisola typical value	180°C

>> Click here to see a Thermal Stability Chart

Electrical Values

Product-Code (Show all)	P155 ☑
Low voltage continuity for Grade 1 wires	
0.05mm: acc. to IEC 60851-5.1	≤ 60
Elektrisola typical value	0

Enamelled Copper Wire acc to IEC - Europe

⊟General

Product-Code Show all	P155 ☑
Product-Name	Polysol155
General Description	mod. Polyurethane
IEC (including the following norms)	IEC 60317-20, IEC 60317-4
NEMA (including the following norms)	MW 79, MW 2, MW 75
UL-approval	yes
Diameters available	0,010 - 0,50 mm
Properties	Very good solderability and high thermal properties.
Applications	Small transformers, linear motors, relais, solenoids, small motors, clock coils, watch coils, transformers, magnetic heads, instruments

⊞Thermal Values

⊟Electrical Values

Product-Code Show all	P155 ☑
Low voltage continuity for Grade 1 wires	
0.05mm: acc. to IEC 60851-5.1	≤ 60
Elektrisola typical value	0
High voltage continuity for Grade 1 wires	
0.05mm: acc. to IEC 60851-5.2	≤ 60
0.05mm: Elektrisola typical value	2
0.25mm: acc. to IEC 60851-5.2	≤ 25
Elektrisola typical value	1
Breakdown voltage (at 20 °C, 35% humidity)	
0.05mm: Elektrisola typical value	220 V/µm
0.25mm: Elektrisola typical value	180 V/µm
Decrease of breakdown voltage for Grade 1 wires	
0.05mm: Elektrisola typical value	25% / 155°C
0.25mm: Elektrisola typical value	25% / 155°C

>> Click here to see the Calculation Method for Breakdown Voltage

⊞Mechanical Values

⊞

VITROPERM :

extending the possibilities of iron

Nanocrystalline VITROPERM alloys are based on Fe with Si and B with Nb and Cu additives. VAC pioneered the development of rapid solidification technology resulting in the production of thin tapes or ribbons approximately 20 µm thick. Special slitting and core winding machines produce tape-wound cores with external diameters ranging from 2 mm to 600 mm. A subsequent heat treatment at around 500 – 600 °C transforms the initially amorphous microstructure of the tape into the desired nanocrystalline state. This being a two-phase structure with fine crystalline grains (average grain diameter of 10-40 nm) embedded in an amorphous residual phase.

VITROPERM nanocrystalline alloys are optimized to combine highest permeability and lowest coercive field strength. The combination of very thin tapes and the relatively high electrical resistance (1.1 – 1.2 µΩm) ensure minimal eddy current losses and an outstanding frequency vs. permeability behaviour. Along with saturation flux density of 1.2 T and wide operational temperature range, these features combine to make VITROPERM a universal solution for most common EMC problems and vastly superior in many aspects to commonly used ferrite and amorphous materials.

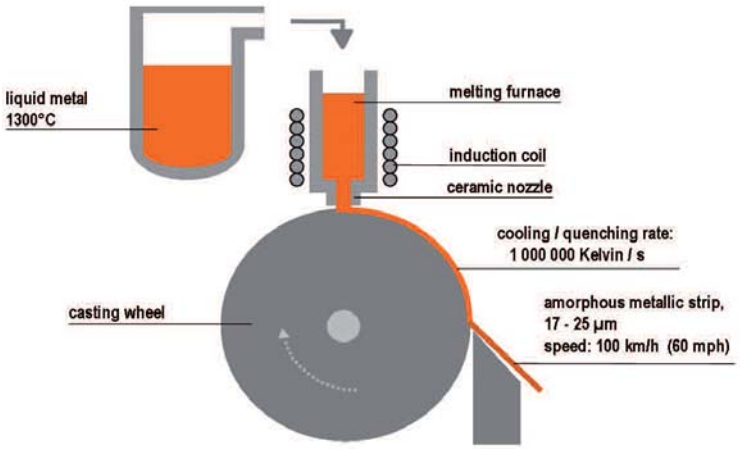

Fig. 1: Rapid solidification technology is used to produce thin metal tapes with an amorphous structure (metallic glass).

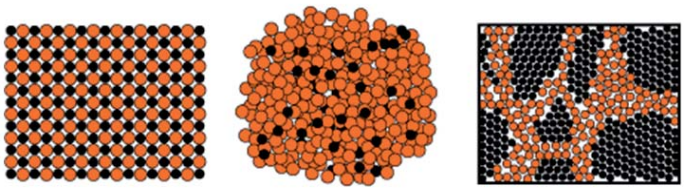

Fig 2: Crystalline structure, amorphous structure, nanocrystalline microstructure

COMMON MODE CHOKES & tape-wound cores

Nanocrystalline cores are widely used in common mode choke (CMC) applications due to their unique combination of properties. By utilising low-cost raw materials (Fe-based) and modern, large-scale production, VITROPERM is a very competitive solution for a wide range of applications. Key areas of application are:

- Switched-mode power supplies (SMPS)
- Solar inverters
- Frequency converters
- EMC filters
- Welding equipment
- Wind generators
- Inductive cooking
- Automotive applications
- Uninterruptable power supplies (UPS)

Our CMCs feature high attenuation which is maintained across a wide frequency range offering extremely broadband attenuation. In many cases, this characteristic can allow a reduction of the number of filter stages in multistage EMC filter configurations to reduce complexity, cost and filter volume. Ohmic (copper) losses are also reduced increasing the efficiency and lowering component temperature.

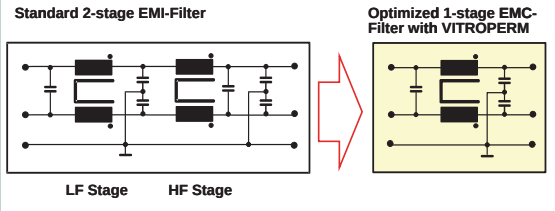

Fig. 3: Nanocrystalline chokes allow a reduction of filter stages

VACUUMSCHMELZE has extensive practical and theoretical expertise in the design of CMCs and filter configuration using nanocrystalline cores and components. At higher frequencies, the winding configuration has a major effect on the parameters of winding capacitance and leakage inductance and is therefore carefully considered in our choke designs. Figure 4 shows a comparison of insertion loss for two chokes which differ only in their winding configuration (core material, number of turns and wire thickness are identical in both cases). This illustrates how our design expertise can improve filter efficiency, maximize reliability and reduce costs.

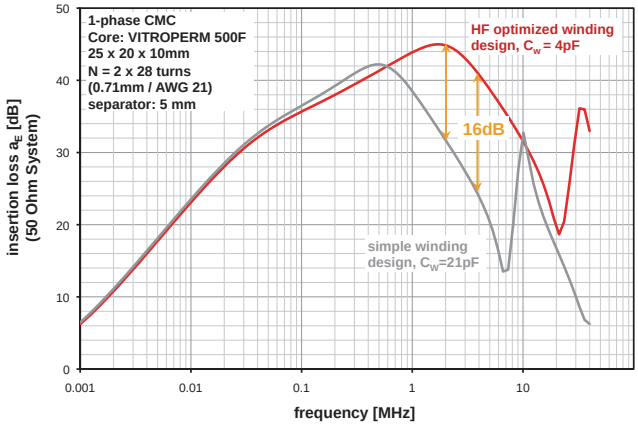

Fig. 4 : Optimized choke design: improved attenuation of up to 16 dB (or more) at 4 MHz.

Features & benefits of VITROPERM nanocrystalline chokes

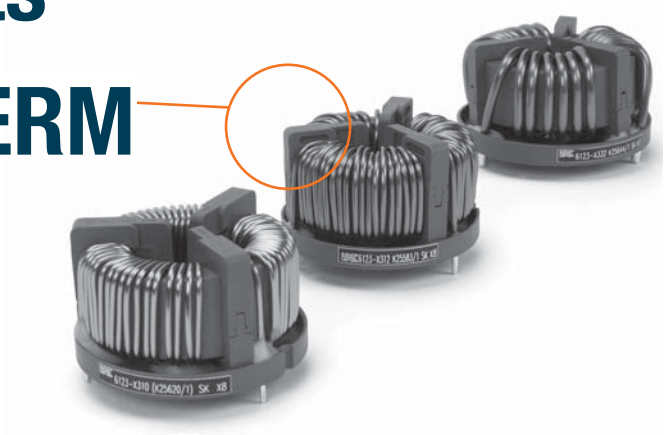

• Small size	High μ, high B_S
• Suitable for high currents and/or high voltages	High μ, high B_S, suitable core geometries
• Single stage filter designs possible	Extremely broadband attenuation behaviour, high permeability, low-capacitance design, moderate reduction of μ up to high frequencies, low Q-factor in 150 kHz range
• High efficiency, low power loss	Low number of turns required for high L, reduction of filter stages
• "Green", environmentally friendly	Low power loss, reduced use of material
• Suitable for high and low ambient temperatures and high operating temperatures	High Curie temperature, material properties (μ, Bs, λ_S) nearly independent of temperature
• "Easy filter design"	Material properties (μ, B_S, λ_S) nearly independent of temperature, linear magnetization curve delivers stable impedance across a broad range of common mode currents – VAC choke design software available
• UL-compliant designs	Suitable plastic materials meet UL1446 insulation requirements
• Optimized solutions for a variety of different applications	A range of μ levels and VITROPERM alloys available
• No operating noise	Material is practically magnetostriction-free
• Best suited for winding of thick wires	Material is practically magnetostriction-free, coatings/casings are resistant against mechanical stress

VITROPERM

vs. ferrite

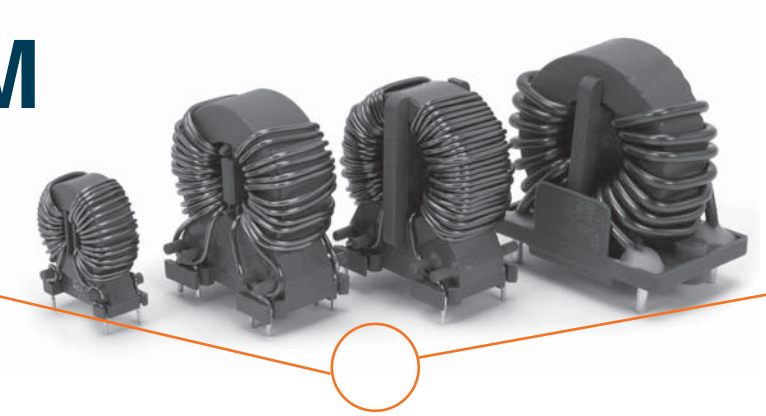

Due to the optimized high-frequency properties the insertion loss of our nanocrystalline common mode chokes is superior compared to that of a typical ferrite choke in the relevant frequency range.

The properties of VITROPERM are very different to conventional ferrites. This has to be considered in the filter design for optimal solutions. The main physical and magnetic characteristics are illustrated in the following diagrams.

Insertion loss

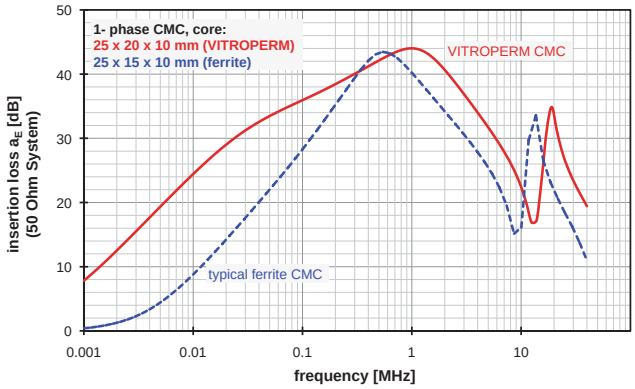

Fig. 5: Comparison of insertion loss of VITROPERM and ferrite

The permeability of VITROPERM 500F is significantly higher than ferrite in the low frequency range. At higher frequencies the μ of both nanocrystalline materials remains above that of ferrites. A high choke impedance is preferred for a high attenuation. This can be achieved more effectively by using high permeability core materials than by increasing the number of turns, as a lower number of turns results in lower winding capacitance and hence improved HF properties.

Permeability

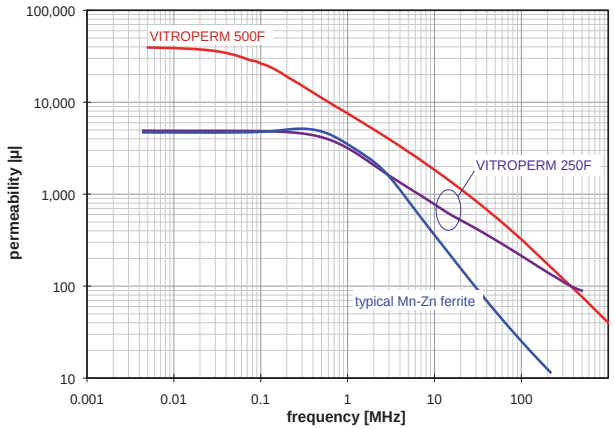

Fig. 6: Frequency response of the permeability of VITROPERM 500F (μ=40 000) and VITROPERM 250F (μ=5 000) in comparison to a typical MnZn ferrite (μ=5 000).

Permeability & magnetization curve

The frequency dependence of the permeability, μ(f) of VITROPERM 500F and ferrites differ fundamentally. μ(f) of μ=5 000 ferrites offer a flat and linear characteristic up to approximately 1 MHz (ferrites with μ=10 000 range up to approximately 200 kHz). In this flat range, the attenuation properties are determined by μ' and the impedance IZI is dominated by the inductance L. If the self resonance of the choke is within this frequency range, the attenuation curve is narrow-band and attenuation is primarily caused by reflection of the interference signal. Above 1 MHz (or 200 kHz) Re(Z) takes the major share of attenuation and μ'' becomes the dominant factor. If the self resonance of the choke is in this frequency range, the attenuation characteristic becomes increasingly broadband.

VITROPERM is basically similar in this respect. The flat sector of μ(f) of VITROPERM 500F ranges (depending on the initial permeability level) to frequencies of several 10 kHz (20 kHz in this example), only. Consequently, attenuation (or IZI) is already dominated by Re(Z) and is always broadband in the whole EMC-relevant range above 150 kHz. Inductance plays a minor role and describes the attenuation only partially. The determining factor is the total impedance. The approximation IZI=ωL is valid for ferrite chokes. For VITROPERM chokes IZI>>ωL applies. Attenuation primarily does not result from a reflection of the interference signal, but from its absorption.

It is only when these different characteristics are taken into consideration that the design of optimized, compact and low-cost nanocrystalline chokes is possible. However, VITROPERM 250F is an exception, because the flat μ(f) sector range is similar to μ=5 000 ferrites to frequencies of up to 1 MHz and the attenuation is primarily inductive.

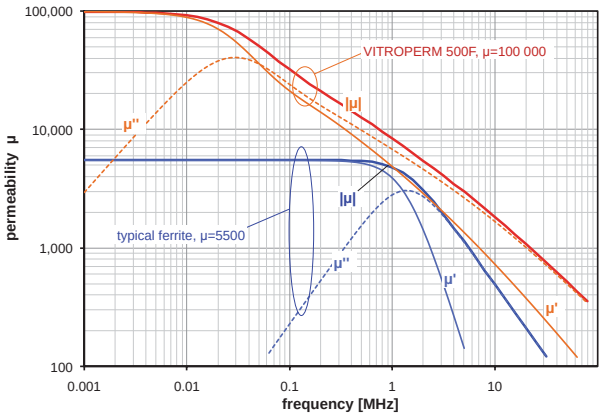

Fig. 7: Differences in the balance between μ' and μ'' for VITROPERM and ferrite lead to different attenuation mechanisms

Magnetization curve

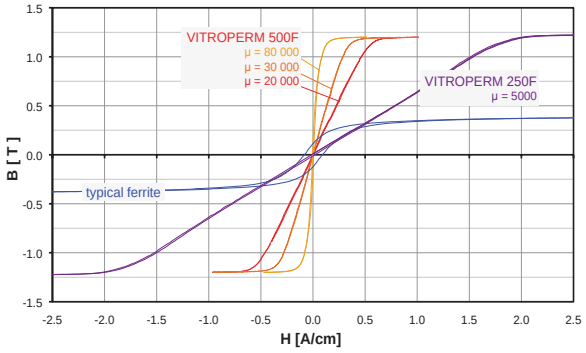

Fig. 8a: Hysteresis loops for various types of VITROPERM and typical MnZn ferrite.

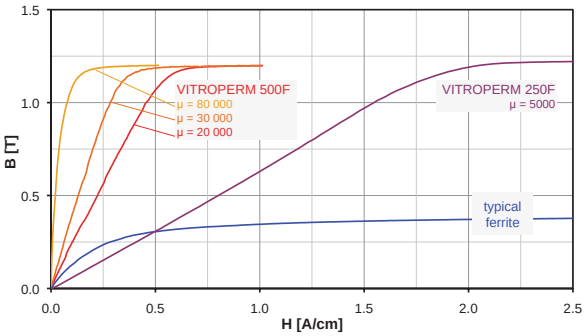

Fig. 8b: Magnetization curve of VITROPERM 500F and VITROPERM 250F in comparison to typical MnZn ferrite, showing noticeable differences in permeability (slope of the curve) and saturation flux density (B_S)

Thermal properties

Thermal behaviour

The saturation flux density of VITROPERM changes by only a few percent in the operating temperature range of up to 150 °C, while MnZn ferrites decline by up to 40 % at temperatures above 100 °C. The high Curie temperature of VITROPERM alloys (above 600 °C), allows short term maximum operating temperatures as high as 180 – 200 °C [1]).

[1] Maximum continuous temperature depends on the casing / coating materials used. Please contact VAC for more detailed information.

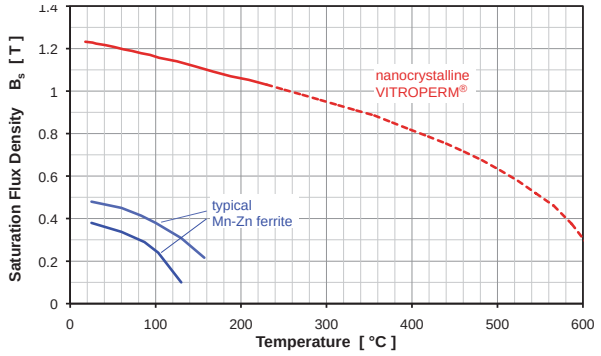

Fig. 9: Temperature dependence of saturation flux density $B_S(T)$

The permeability of VITROPERM typically changes by less than 10 % in the temperature range from -40 °C to 120 °C, while the permeability of MnZn ferrites can drift in a range of ± 40 – 60 % around the room temperature value.

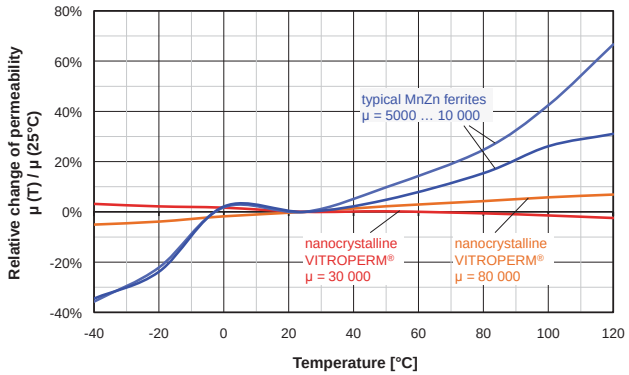

Fig. 10: Relative change of μT) at f = 100 kHz, normalized for room temperature

Insertion loss (and impedance) of a CMC made of VITROPERM 500F is almost temperature-independent in the temperature range of – 40 °C to above 150 °C. In contrast, ferrite chokes feature a significant drop of insertion loss with increasing temperature.

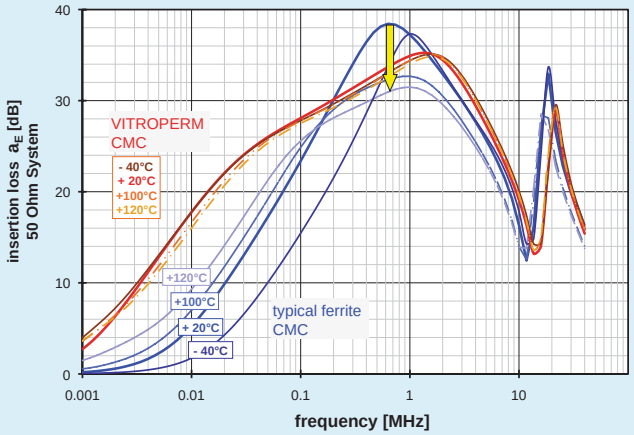

Fig. 11a: Comparison of temperature dependence of insertion loss of a VITROPERM CMC and a choke with standard MnZn ferrite core

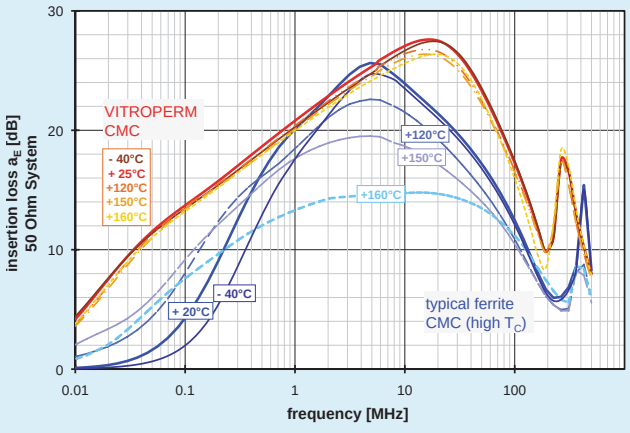

Fig. 11b: Comparison of temperature dependence of insertion loss up to 160 °C of a VITROPERM CMC and a MnZn choke using a high Curie temperature ferrite material

Saturation behaviour

High permeability nanocrystalline cores enable very high inductance levels in extremely compact core or choke dimensions. However, an increased sensitivity to asymmetric magnetization conditions caused by common mode, unbalanced or leakage currents has to be considered. These currents may occur as low-frequency leakage currents (50/60 Hz) or as medium or high-frequency interference currents. These are caused for example by long motor cables with different capacitance of the individual conductors to earth, or by resonances which occur (commonly due to bearing currents) in such cables leading to short, extremely high and rapidly declining current peaks with amplitudes of up to several 10 A_{peak} and pulse widths in the nanosecond range (1 … several 100 ns). If these common mode currents exceed the saturation level of the choke or core, the attenuation of the choke breaks down and the choke becomes less effective.

The saturation behaviour of ferrite is less sensitive due to its lower permeability. For applications with higher unbalanced currents, the advantages of VITROPERM with 1.2 T saturation flux density (approximately 3 times higher than ferrites) can still be realised since VITROPERM is available in a range of permeability levels between 4 000 and 150 000. In these cases, a lower µ level may have to be selected in order to find the optimum saturation-resistant solution. Fig. 12a shows a comparison of saturation currents for different VITROPERM designs with a typical ferrite core of similar dimensions. It can be seen that the saturation behaviour of the MnZn ferrite (µ=6 000) is comparable with that of VITROPERM 500F (µ=17 000) up to frequencies of approximately 50 kHz.

At higher frequencies, however, the VITROPERM design is becoming more advantageous. The VITROPERM solution offers a 50 % higher A_L value at 100 kHz and a significantly higher impedance (note that the impedance of VITROPERM is determined to a small part by inductance L in this frequency range). High permeability VITROPERM 500F cores are characterized by an extremely high attenuation or impedance at low frequencies, and they are clearly superior against ferrites at high frequencies. However, the price of this superior performance is a more sensitive saturation behaviour, which is improving with increasing frequency but still more critical than that of other core materials. It should be noted that Fig. 12a shows the saturation currents of the cores without winding. Depending on the number of turns, the I_{cm} values of chokes are some 10 mA to several 100 mA, only (see tables of standard series).

Fig. 12b shows permeability characteristics under DC bias field for a VITROPERM 500F core (µ=20 000) and 2 typical MnZn ferrites (µ=5 000 and µ=8 000, respectively). The diagram shows the significantly higher permeability and a square µ(H_{DC}) characteristic of the nanocrystalline material in comparison to the rounded properties of the two ferrite cores. This behaviour complies to the linear magnetization curve of VITROPERM (Figs. 8a / 8b) and leads to nearly constant inductance over a wide range of the DC bias fields.

VITROPERM 250F is always used where highly saturation-resistant solutions are required for applications with very high common mode or unbalanced currents. However, it cannot equal the high attenuation of VITROPERM 500F.

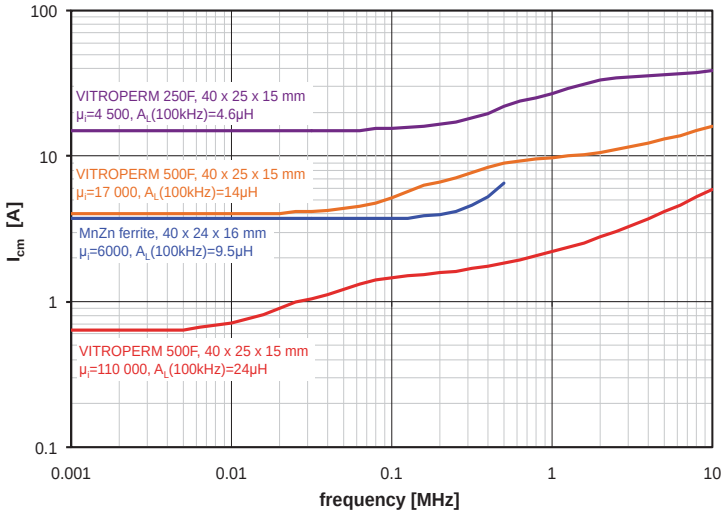

Fig. 12a: Comparison of saturation behaviour of VITROPERM 500F, VITROPERM 250F and MnZn ferrite

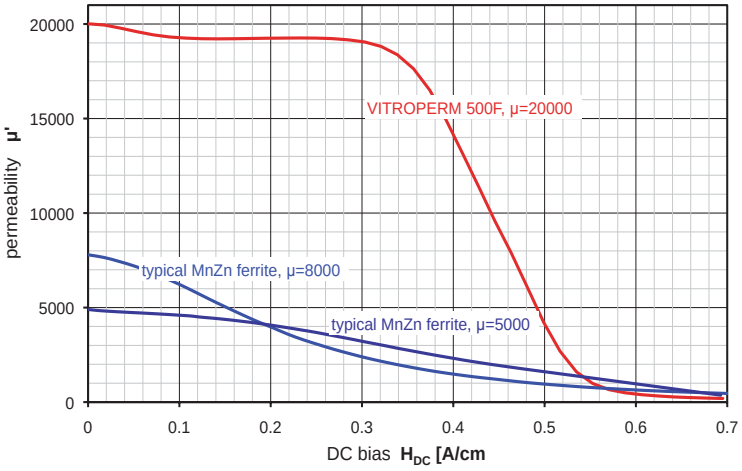

Fig. 12b: Comparison of permeability characteristics under DC bias fields for VITROPERM 500F and two typical MnZn ferrites.

Design advantages with VITROPERM

The superior material properties of nanocrystalline VITROPERM enable common mode chokes with high inductance/impedance with a small number of turns, resulting in reduced copper losses, low winding capacitance and excellent HF performance.

Due to the high initial permeability, low winding capacitance and a low Q-factor (above 100 kHz) VITROPERM CMCs offer a broadband insertion loss curve ranging from 10 kHz up to several MHz and improved attenuation behaviour at both low and high frequencies in comparison to conventional ferrite chokes with similar core dimensions and identical windings (see Fig. 13).

Better attenuation properties and an extended operating temperature range allow a reduction of the component volume by a factor of up to 3 or more under similar conditions. Note that the insertion loss curve of the small VITROPERM choke in Fig. 14 is similar to that of ferrite materials at frequencies of about 600 kHz – 1 MHz and is superior below 500 kHz and above 1 MHz.

The excellent attenuation of VITROPERM CMCs simplifies the filter design in a wide frequency range. For laboratory tests, VAC offers different sample kits with selected standard cores and chokes.

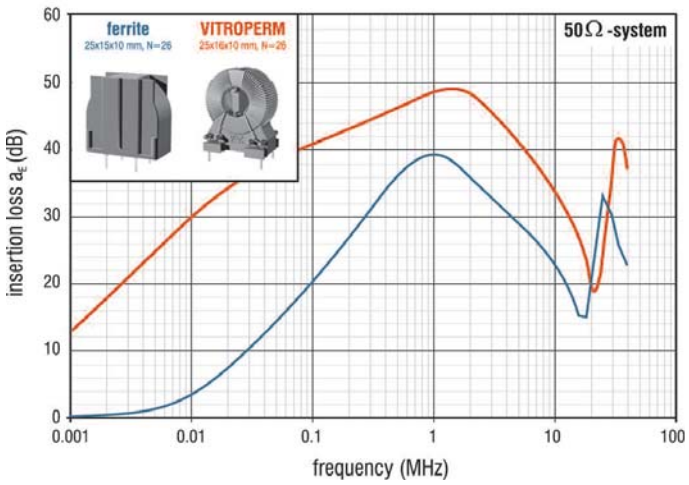

Fig. 13: Comparison of insertion loss curve of a VITROPERM 500F CMC (red curve) and ferrite CMC (blue curve) of similar size and with the same number of turns.

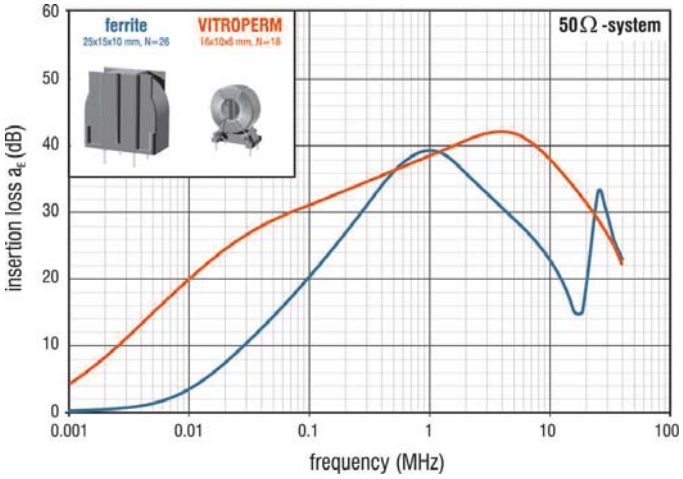

Fig. 14: Comparison of the dimensions of a VITROPERM 500F CMC (red curve) and ferrite CMC (blue curve) with similar attenuation properties in the 1 MHz range

VITROPERM – typical data

Saturation flux density	B_S = 1.2 T	Max. operational temperature	T_{max} =
Coercivity (static)	H_C < 3 A/m	Continuous-epoxy	120 °C [1]
Saturation magnetostriction	λ_S=	Continuous-plastic casing	130/155 °C [1]
VITROPERM 500F	10^{-8}....10^{-6}	short-term	180 °C [1]
VITROPERM 250F	≈ 8 x 10^{-6}	Permeability	μ_i=
Specific electrical resistance	≈115 µΩcm	VITROPERM 500F	15 000...150 000
Curie temperature	T_C > 600 °C	VITROPERM 250F	4 000... 6 000
		Core losses (100 kHz, 0.3 T)	P_{Fe} = 80 W/kg (typ.)

[1] *Please contact VAC for more detailed information about the temperature limits of our casing and coating materials.*

STANDARD SERIES
OF VITROPERM CORES

Our VITROPERM cores are available with different A_L-levels for many core sizes. Thus, saturation-resistant solutions are available for various fields of applications. Common mode currents may occur as interference currents, bias currents or, primarily, unbalanced currents. If the common mode currents exceed the saturation currents (I_{cm}) of the cores or chokes, cores with higher saturation resistance must be used. High A_L values (high µ) are more suitable for typical single-phase applications with low unbalanced current (e.g. switched-mode power supplies), while cores with lower A_L values are often used in 3-phase applications with high unbalanced currents (e.g. frequency converters with long motor cables).

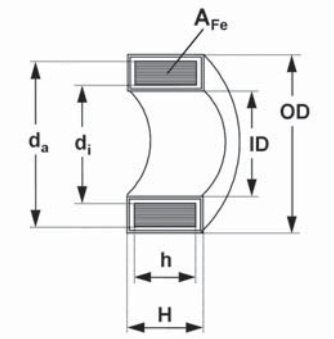

Nanocrystalline VITROPERM cores with epoxy resin coating

Although the epoxy resin coating is suitable for direct winding, we recommend additional insulation between core and winding for enhanced insulation requirements. The epoxy resin is suitable for continuous operational temperatures of up to 120 °C and complies with the UL94-V0 standard (UL file number: E214934), class A (105 °C).

nominal core dimensions	limiting dimensions (incl. coating)			iron cross section	mean path length	weight	A_L*		saturation current Icm**, typical		
							10 kHz	100 kHz	10 kHz	100 kHz	
d_a x d_i x h	OD	ID	H	A_{Fe}	l_{Fe}	m_{Fe}	nominal				part number
mm x mm x mm	mm	mm	mm	cm^2	cm	g	µH		A		
16 x 12.5 x 6	17,8	10,7	8	0,08	4,5	2,6 2,6	15,0 6,0	4,8 3,9	0,5 1,1	0,8 1,7	T60004-L2016-W620 T60004-L2016-W619
22 x 17 x 6	24,0	15,2	8,0	0,12	6,1	5,4	16,4	4,3	0,6	1,2	T60004-L2022-W867
25 x 20 x 10	27,3	17,5	12,3	0,19	7,1	9,9 9,9	22,5 9,0	7,2 5,8	0,7 1,7	1,4 2,7	T60004-L2025-W622 T60004-L2025-W621
30 x 25 x 15	32,3	22,7	17,5	0,27	8,6	17,4	26,5	8,5	0,9	1,7	T60004-L2030-W676
30 x 20 x 10	32,5	17,8	12,5	0,40	7,9	23,1	56,0	13,4	0,6	1,2	T60004-L2030-W911
40 x 32 x 15	42,3	29,1	17,8	0,44	11,3	36 36	32,5 13,0	10,3 8,4	1,1 2,8	2,2 4,3	T60004-L2040-W624 T60004-L2040-W623
45 x 32 x 15	47,3	29,8	17,8	0,71	12,1	63,3	19,7	12,8	3,0	4,6	T60004-L2045-W886
50 x 40 x 20	52,3	37,1	22,8	0,73	14,1	76 76	43,0 17,0	13,8 11,2	1,4 3,6	2,7 5,4	T60004-L2050-W626 T60004-L2050-W625
63 x 50 x 20	65,5	46,6	22,8	0,95	17,8	124 124	18,0 11,5	11,6 10,4	4,4 6,9	6,7 8,7	T60004-L2063-W627 T60004-L2063-W721
80 x 63 x 20	83	59,5	22,8	1,24	22,5	205 205	18,5 11,9	12,0 10,7	5,6 8,7	8,5 11,0	T60004-L2080-W628 T60004-L2080-W722
100 x 80 x 20	104	75	23	1,46	28,3	303 303	17,3 11,2	11,2 10,0	7,1 10,9	10,7 13,8	T60004-L2100-W629 T60004-L2100-W723
130 x 100 x 25	134,5	95,0	28,5	2,85 2,74 2,74	36,1 36,1 36,1	757 727 727	50,0 25,4 16,4	19,4 16,5 14,7	4,8 9,0 14,0	8,5 13,6 17,7	T60004-L2130-W567 T60004-L2130-W630 T60004-L2130-W587
160 x 130 x 25	165	125	28,5	2,74	45,6	917 917	20,1 13,0	13,1 11,7	11,3 17,6	17,1 22,3	T60004-L2160-W631 T60004-L2160-W720
194 x 155 x 25	200	149	28,5	3,71	54,8	1490 1490	45,3 14,7	14,7 13,2	6,9 20,7	12,5 26,4	T60004-L2194-V105 T60004-L2194-W908

Nanocrystalline VITROPERM cores in plastic casing

The plastic cases are suitable for direct winding and offer good mechanical protection of the nanocrystalline core material. This enables the best magnetic properties and highest permeability levels to be maintained. Additional winding protection is optional for heavy wire windings, where there may be a danger of core damage. The plastic materials comply with the standards UL94-V0 (UL file number: E41871), class B (130 °C) and UL94-V0 (UL file number E41938), class F (155 °C).

nominal core dimensions	limiting dimensions (incl. case)			iron cross section	mean path length	weight	A_L*		saturation current I_{cm}**, typical		part number
							10 kHz	100 kHz	10 kHz	100 kHz	
d_a x d_i x h	OD	ID	H	A_{Fe}	l_{Fe}	m_{Fe}	nominal				
mm x mm x mm	mm	mm	mm	cm^2	cm	g	µH		A		
9.8 x 6.5 x 4.5	11,2	5,1	5,8	0,06	2,6	1,1	25,5	6,4	0,2	0,4	T60006-L2009-W914
12 x 8 x 4.5	14,1	6,6	6,3	0,07	3,1	1,7	28,0	6,8	0,2	0,4	T60006-L2012-W902
12.5 x 10 x 5	14,3	8,5	7,0	0,05	3,5	1,3	10,0	3,6	0,4	0,8	T60006-L2012-W498
15 x 10 x 4.5	17,1	7,9	6,5	0,09	3,9	2,6	27,0	6,7	0,3	0,5	T60006-L2015-W865
16 x 10 x 6	17,9	8,1	8,1	0,14	4,1	4	43,0	10,1	0,3	0,6	T60006-L2016-W403
						4	11,7	6,5	1,2	1,7	T60006-L2016-W308
17.5 x 12.6 x 6	19,0	11,0	8,0	0,12	4,7	4,1	30,0	6,9	0,3	0,7	T60006-L2017-W515
19 x 15 x 10	21,2	13,0	12,3	0,16	5,3	6,3	36,1	8,8	0,4	0,7	T60006-L2019-W838
20 x 12.5 x 8	22,6	10,3	10,2	0,24	5,1	9,0	55,2	13,6	0,4	0,7	T60006-L2020-W409
						9,0	14,3	9,1	1,4	2,1	T60006-L2020-W450
25 x 20 x 10	27,6	17,4	12,8	0,20	7,1	10,4	28,4	7,3	0,6	1,1	T60006-L2025-W523
25 x 16 x 10	27,9	13,6	12,5	0,36	6,4	17	65,5	15,5	0,4	0,9	T60006-L2025-W380
						17	17,0	11,5	1,7	2,6	T60006-L2025-W451
						17	3,2	3,1	9,3	9,6	T60006-L2025-W980
30 x 20 x 10	32,8	17,6	12,5	0,40	7,9	23	59,3	14,0	0,5	1,0	T60006-L2030-W423
						23	15,5	11,1	2,1	3,1	T60006-L2030-W358
						23	2,9	2,8	11,4	11,8	T60006-L2030-W981
30 x 20 x 15	32,8	17,5	17,8	0,57	7,9	33	88,0	20,0	0,5	1,1	T60006-L2030-W514
40 x 32 x 15	43,1	28,7	18,5	0,46	11,3	38	47,2	11,1	0,8	1,5	T60006-L2040-W422
						38	12,2	7,9	3,7	5,1	T60006-L2040-W452
						38	2,3	2,2	16,6	17,1	T60006-L2040-W964
40 x 25 x 15	43,1	22,5	18,5	0,86	10,2	64	101,0	23,1	0,7	1,4	T60006-L2040-W424
						64	25,4	17,2	2,9	4,2	T60006-L2040-W453
45 x 30 x 15	48,3	26,4	18,2	0,86	11,8	74	87,5	20,3	0,8	1,6	T60006-L2045-V102
						74	24,3	15,9	3,0	4,5	T60006-L2045-V118
						74	15,7	14,3	4,6	5,8	T60006-L2045-V101
50 x 40 x 20	53,5	36,3	23,4	0,76	14,1	79	45,3	14,0	1,4	2,7	T60006-L2050-W516
						79	18,0	10,0	3,5	5,3	T60006-L2050-W565
63 x 50 x 25	67,3	46,5	28,6	1,24	17,8	161	58,6	18,1	1,8	3,5	T60006-L2063-W517
						161	23,3	13,5	4,4	6,7	T60006-L2063-V110
						163	3,3	3,2	30,2	30,9	T60006-L2063-W985
80 x 50 x 20	86,0	44,7	25,7	2,28	20,4	342	35,0	24,0	5,5	8,2	T60006-L2080-W531
						347	9,6	9,2	26,4	27,3	T60006-L2080-V091
90 x 60 x 20	95,4	54,7	24,7	2,28	23,6	395	81,0	25,1	2,4	4,5	T60006-L2090-W518
						400	4,6	4,5	40,9	41,8	T60006-L2090-W984
100 x 80 x 25	105,5	75,0	29,6	1,90	28,3	379	56,3	16,9	2,8	5,3	T60006-L2100-V082
						379	14,5	13,1	10,9	13,8	T60006-L2100-V081
102 x 76 x 25	108,1	70,0	30,3	2,47	28,0	508	68,8	21,6	3,8	6,7	T60006-L2102-W468
						508	19,1	17,2	10,7	13,6	T60006-L2102-V080
						515	4,3	4,2	47,4	48,5	T60006-L2102-W947
160 x 130 x 25	166,9	123,9	30,5	2,74	45,6	917	26,8	13,7	8,4	13,6	T60006-L2160-V074
				2,74	45,6	917	20,1	13,1	11,3	17,1	T60006-L2160-V088
				2,74	45,6	917	12,9	11,7	17,6	22,3	T60006-L2160-V066
				2,85	45,6	967	3,0	2,9	79,3	81,1	T60006-L2160-W982

* A_L = inductance for N = 1 (tolerance +45 % / -25 %) ** I_{cm} : the listed saturation currents are guidelines, only. They are calculated for nominal core dimensions at room temperature and for approx. 70 % saturation flux density. The frequency-dependent saturation behaviour is demonstrated in Fig. 12.

Core stack assemblies
with nanocrystalline cores

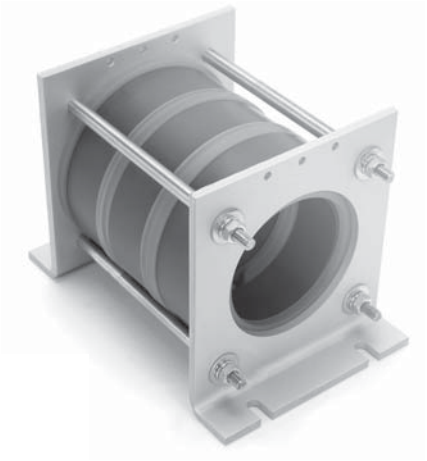

Single-turn chokes employing a number of nanocrystalline cores assembled in a stack are an effective solution for bearing current problems or extremely high common mode noise from other causes in large-scale variable speed drives, wind generators and other applications in which resonance phenomena cause high-amplitude interference currents (with peak values ranging from several 10 A to over 100 A). These generally take the form of short and thus high-frequency current peaks. For these applications, VAC offers assembled core stacks which can be easily and securely integrated into existing applications with the minimum of effort.

The core stacks are available in two sizes with two different through-hole diameters. They are custom-designed, allowing an individual selection of core type and the number of stacked cores (up to 7 pieces) depending on the required saturation level and the required inductance.

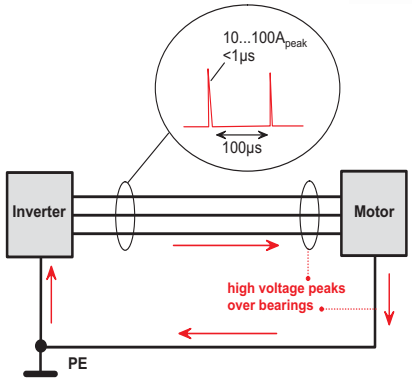

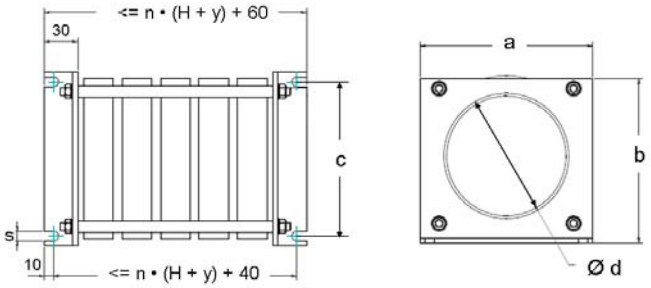

Dimensions of the core stack assemblies

	Size 1	Size 2
a (mm)	120	180
b (mm)	130	190
c (mm)	70	130
d (mm)	~ 70	> 118
s (mm)	7	10

n = number of stacked cores
H = maximum core height
y = 9.5 for epoxy coated cores, T60004...
y = 10.2 for cased cores, T60006...
The inductance L of a core stack can be calculated by multiplying the number of stacked cores with the AL-value of the single core.
A_L : inductance of single core
I_{cm} : maximum permissible leakage or common mode current. Calculated guideline for nominal core dimensions at room temperature and for approximately 70 % saturation flux density.

core data							data of core stack example for 5 stacked cores				
	nominal core dimensions	limit core dimensions (incl. Case/coating)			A_L (10 kHz)	A_L (100 kHz)		$I_{cm\ (10\ kHz)}$	$I_{cm(100\ kHz)}$	L (10 kHz)	L (100 kHz)
core part number	d_a x d_i x h	OD	ID	H	nominal	nominal	size	typical	typical	nominal	nominal
	mm x mm x mm	mm	mm	mm	µH	µH		A	A	µH	µH
T60004-L2100-W629	100 x 80 x 20	104,0	75,0	23,0	17,3	11,2	1	7,1	10,7	86,5	56,0
T60004-L2100-W723	100 x 80 x 20	104,0	75,0	23,0	11,2	10,0	1	10,9	13,8	56,0	50,0
T60006-L2100-V082	100 x 80 x 25	105,5	75,0	29,6	56,3	16,9	1	2,8	5,3	281,5	84,5
T60006-L2100-V081	100 x 80 x 25	105,5	75,0	29,6	14,5	13,1	1	10,9	13,8	72,5	65,5
T60006-L2102-W468	102 x 76 x 25	108,1	70,0	30,3	68,8	21,6	1	3,8	6,7	344,0	108,0
T60006-L2102-V080	102 x 76 x 25	108,1	70,0	30,3	19,1	17,2	1	10,7	13,6	95,5	86,0
T60006-L2102-W947	102 x 76 x 25	108,1	70,0	30,3	4,3	4,2	1	47,4	48,5	21,5	21,0
T60006-L2160-V074	160 x 130 x 25	166,9	123,9	30,5	26,8	13,7	2	8,4	13,6	134,0	68,5
T60006-L2160-V088	160 x 130 x 25	166,9	123,9	30,5	20,1	13,1	2	11,3	17,1	100,5	65,5
T60006-L2160-V066	160 x 130 x 25	166,9	123,9	30,5	12,9	11,7	2	17,6	22,3	64,5	58,5
T60006-L2160-W982	160 x 130 x 25	166,9	123,9	30,5	3,0	2,9	2	79,3	81,1	15,0	14,3

Common mode chokes

UL1446 STANDARD SERIES

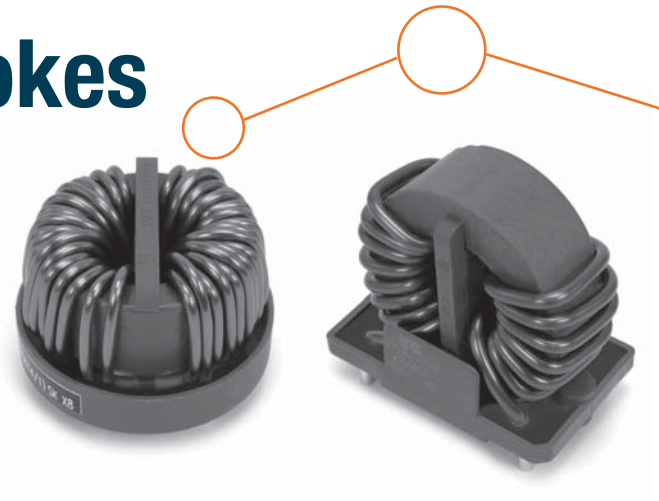

General information

Chokes are designed, manufactured and tested in compliance with EN50178.

Plastic materials comply with the following UL standards:
UL94 (file number E41871)
UL1446 (file number OBJY2.E329745)

Temperature class B (130 °C)
I_N = nominal current in each winding
$U_{N\ OVCat\ III\ /\ II}$ = operating voltage for overvoltage category III / II
L_N = nominal inductance, tolerance +50 % / -30 %
Ambient temperature T_a = – 40 °C...+70 °C (short-term +90 °C)
Operating temperature T_{op} = – 40 °C...+130 °C (short-term +150 °C)

The standard chokes are designed for a temperature rise of ΔT = 45….60 K at T_a=70 °C and I=I_N in each winding. Data derating is necessary for deviating ambient temperature or deviating nominal current. Please contact VAC for further detailed information.

Standard series CMCs for single-phase applications

I_N	design	U_N	L_N		R_{Cu}	|Z|	f_R	I_{cm}	dimensions			part number
		OVCat III / II	10 kHz	100 kHz	typ.	100kHz	typ.	10 kHz	l	b	h	
A		V	mH		mΩ	Ω	MHz	mA	mm	mm	mm	
2	upright	300 / 600	2x12.1	2x2.8	101	3000	3,6	17	22	12	25	T60405-R6131-X402
4	upright	300 / 600	2x10.8	2x2.5	27,5	2320	1.2	12	22	12	25	T60405-R6131-X204
4.5	upright	300 / 600	2x28.3	2x6.6	36	6500	0,4	18	27	17	29	T60405-R6161-X504
6	upright	300 / 600	2x29.1	2x6.7	37,6	8500	0,25	14	35	21	37	T60405-R6166-X206
8	upright	300 / 600	2x16.4	2x3.7	19,1	4200	0,5	20	35	21	36,5	T60405-R6166-X208
10	low profile	300 / 600	2x11.4	2x2.6	12,2	3200	0,7	16	35	35	23	T60405-R6123-X210
10	upright	300 / 600	2x11.4	2x2.6	12,7	3150	0.7	16	35	21	37	T60405-R6166-X210
12	upright	300 / 600	2x11.4	2x2.6	8.9	2950	0,7	22	38	22	35	T60405-R6126-X212
12	low profile	300 / 600	2x11.4	2x2.6	8,8	2950	0,7	22	35	35	25	T60405-R6123-X213
13	low profile	300 / 600	2x8.6	2x2.2	6,3	2250	1,1	28	35	35	22	T60405-R6122-X100
16	low profile	300 / 600	2x12.9	2x3.1	5,7	3000	3.0	37	40	40	24	T60405-R6123-X616
16	upright	300 / 600	2x6	2x1.5	4,6	1600	1.0	35	38	21	38	T60405-R6166-X033
16	upright	300 / 600	2x2.9	2x0.7	3,9	830	3,3	60	36	21	38	T60405-R6166-X039
20	low profile	300 / 600	2x1.8	2x0.4	3,2	500	11,5	40	35	35	23,5	T60405-R6123-X220
20	low profile	300 / 600	2x6.6	2x1.6	2.9	1470	5,7	35	43	43	24	T60405-R6123-X221
25	low profile	300 / 600	2x4.2	2x1	1.9	970	7,1	50	42,5	42,5	25	T60405-R6123-X226
25	low profile	600 / 1000	2x12	2x2.8	3,5	2900	2,4	55	52	52	32	T60405-R6123-X227
25	upright	300 / 600	2x4.2	2x1	1.9	970	4,9	50	42	27	40	T60405-R6128-X225
30	low profile	600 / 1000	2x3.9	2x0.9	2.4	920	7.0	50	52	52	29	T60405-R6123-X232
30	upright	600 / 1000	2x3.9	2x0.9	2,3	900	4.0	65	51	27	50	T60405-R6128-X031
40	low profile	600 / 1000	2x3.6	2x0.8	1.4	870	8,2	90	52	52	32	T60405-R6123-X241
48	low profile	600 / 1000	2x2.5	2x0.6	0.75	660	6,7	110	52	52	32	T60405-R6123-X248
63	low profile	600 / 1000	2x1.6	2x0.4	0,5	390	9,3	150	53,5	53,5	32	T60405-R6123-X263
85	low profile	600 / 1000	2x1.6	2x0.5	0.6	510	1,6	200	73	73	40	T60405-R6123-X285

R_{Cu}: winding resistance per winding IZI : choke impedance f_R : choke resonance frequency

For more detailed technical information please see our product data sheets at **www.vacuumschmelze.com.** Custom CMCs for other nominal currents, in different designs and with other properties are available on request.

3- and 4-phase CMCs

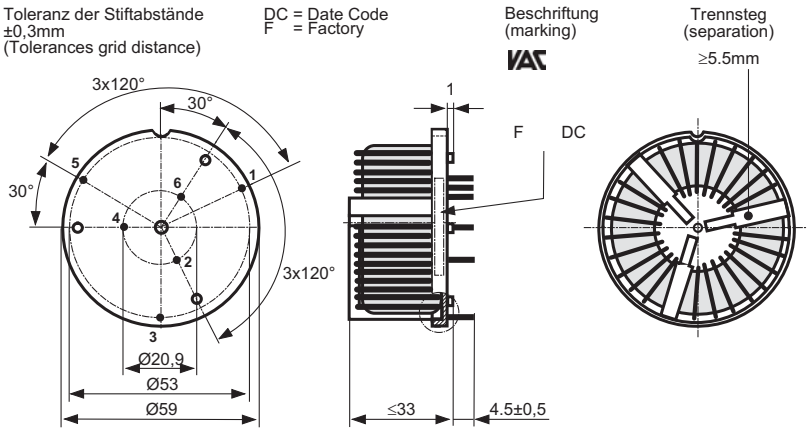

We provide more detailed technical information (data sheets) for all standard products on our web-page **www.vacuumschmelze.com.** Example outline of the 3-phase CMC T60405-S6123-X332.

Standard series 3-phase chokes for 3-phase applications

I_N	design	U_N	L_N		R_{Cu}	|Z|	f_R	I_{cm}	dimensions			part number
		OVCat III / II	10 kHz	100 kHz		100kHz		10 kHz	l	b	h	
A		V	mH		mΩ	Ω	MHz	mA	mm	mm	mm	
7	low profile	600 / 1000	3x31.8	3x7.4	24,6	8650	0,23	27	40,5	40,5	32,5	T60405-S6123-X306
10	low profile	600 / 1000	3x13.9	3x3.2	14	3500	1,5	30	51	51	32	T60405-S6123-X310
11	low profile	600 / 1000	3x10.6	3x2.5	8,5	2600	0,8	40	42	42	32	T60405-S6123-X308
12	low profile	600 / 1000	3x5.7	3x3.7	11,8	2650	0,48	150	51	51	32	T60405-S6123-X312
16	low profile	600 / 1000	3x4.8	3x3.1	6,5	2500	0,65	200	59	59	32	T60405-S6123-X316
16	low profile	600 / 1000	3x9.4	3x2.2	5,9	2400	1,45	35	51,5	51,5	34	T60405-S6123-X317
20	low profile	600 / 1000	3x10.6	3x2.4	4,1	2650	0,9	60	59	59	33	T60405-S6123-X320
25	low profile	600 / 1000	3x2	3x1.3	2,27	1000	2,8	380	60	60	33	T60405-S6123-X325
25	low profile	600 / 1000	3x4.9	3x1.1	2,1	1150	2	60	51,5	51,5	32	T60405-S6123-X326
32	low profile	600 / 1000	3x1.2	3x0.8	1,4	600	4,9	480	59	59	33	T60405-S6123-X332
40*	low profile	600 / 1000	3x2.5	3x0.6	1,2	600	4,7	100	52	52	33	T60405-S6123-X140
40*	low profile	600 / 1000	3x1.5	3x0.8	1,72	680	4	380	70	70	37	T60405-S6123-X240
63	low profile	600 / 1000	3x1.6	3x0.5	0,72	500	1	190	70	70	42	T60405-S6123-X363
70	low profile	600 / 1000	3x0.8	3x0.5	0,86	415	1,45	900	85	85	53	T60405-S6123-X370
110	low profile	600 / 1000	3x0.7	3x0.6	0,63	430	1,4	1750	135	135	57	T60405-S6123-X311

Standard series 4-fold chokes

10** 12	low profile	600 / 1000	4x6.9	4x1.6	7,66	1500	1,7	40	51	51	33	T60405-S6123-X400
16** 20	low profile	600 / 1000	4x3.6	4x0.8	2,75	860	3,4	90	51,5	51,5	33	T60405-S6123-X401
24** 30	low profile	600 / 1000	4x3.2	4x0.7	1,5	750	3,5	100	60	60	33,5	T60405-S6123-X402
32** 40	low profile	600 / 1000	4x1.4	4x0.3	0,82	360	7	160	60	60	33	T60405-S6123-X403

* for $T_a \leq 60°C$ ** for $T_a \leq 85°C$

MATERIAL INFORMATION

NANOCRYSTALLINE CUT CORES

MADE OF VITROPERM® 500 FOR TRANSFORMERS

Applications:

- High frequency, high power transformers for converters in drives, traction, power supplies, welding, induction heating

Key Properties:

- Lower losses than other materials, due to nanocrystalline rapid solidified alloy with thickness of approx. 18 µm
- Low audible noise due to lower magnetostriction compared to other materials
- High flux density material (1.2 Tesla)

VITROPERM – typical data

Saturation flux density	B_S = 1.2 T
Coercivity (static)	H_C < 3 A/m
Saturation magnetostriction	$\lambda_S = 10^{-8} \ldots 10^{-6}$
Electrical resistivity	ρ ~ 115 µΩcm
Curie temperature	T_C > 580 °C
Material permeability	μ_i = 20000... 50000*
Core losses (2500Hz, 0.5 T)	$P_{Fe} \leqslant$ 1 W/kg*
Tape thickness:	approx. 18 µm
Material Composition:	$(FeSi)_{89}(BNbCu)_{11}$ At.-%

* Toroidal core without air gap

VACUUMSCHMELZE

ADVANCED MATERIALS – THE KEY TO PROGRESS

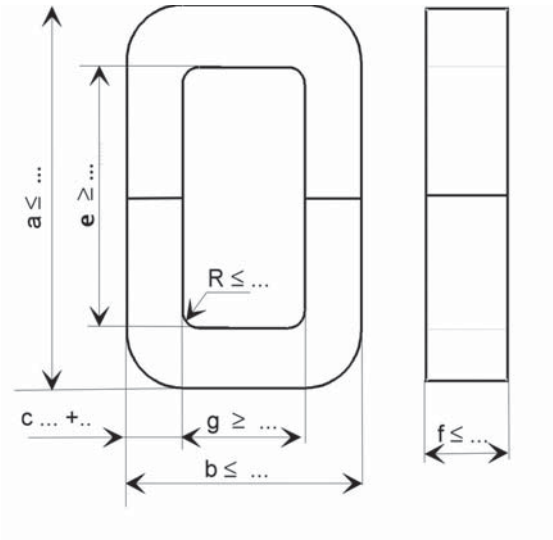

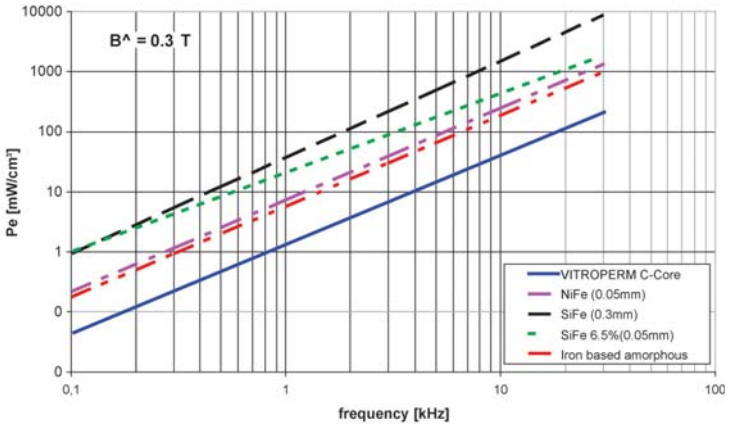

Fig. 1: Losses vs. frequency of cut cores (airgap closed) made of different materials.

Part number	Weight	Iron cross section A_{Fe}	Mean iron path length l_{Fe}	Limiting dimensions (for 2 U-shaped halves)					
T60102-L2…	g	cm^2	cm	Length a / mm	Width b / mm	Window length e / mm	Window width g / mm	Leg width c / mm	Height f / mm
…083-W156	378	2.8	18.2	83.7	48.4	50.5	16	15.8	26.6
…130-W157	941	4.5	28.4	130.0	76.0	78.0	25.0	24.7	26.6
…198-W171	1,680	5.3	43.2	198.0	115.0	118.0	38.0	37.6	21.6
…157-W159	1,360	5.4	34.2	157.5	90.0	95.0	30.0	29.6	26.6
…157-W158	1,570	6.2	34.2	157.5	90.0	95.0	30.0	29.6	31.6
…198-W160	2,520	7.95	43.2	198.0	115.0	118.0	38.0	37.6	31.6

VACUUMSCHMELZE GmbH & Co. KG
Grüner Weg 37
D-63450 Hanau
Tel.: +49 6181/38-0
Fax: +49 6181/38-2645
info@vacuumschmelze.com
www.vacuumschmelze.com

VACUUMSCHMELZE	**Spezifikation für weichmagnetische Kerne** *Specification for Soft Magnetic Cores*	**S-No.:** T60**102**-L2198- **W160**-02-
HFG: IAO	Kunde/*Customer:*	Datum: 48/10 Seite: 1 von 1

Rev.

Ausführung / ***Core design*:**
Schnittbandkern / *Cut core:*
Ähnlich / *Similar to* SU 114/30
(2 Kerne je Trafo "114 b" erforderlich /
2 cores for a transformer "114 b" necessary)

Legierung / ***Core Material*:**
VITROPERM 500

Bezugswerte / ***Rated Dimensions:***

A_{Fe} = 7,95 cm²
l_{Fe} = 43,2 cm
m_{Fe} = 2,52 kg

Maßbild / ***Drawing:***
ohne Maßstab / *without scale*
Maße in mm / *Dimensions in mm*

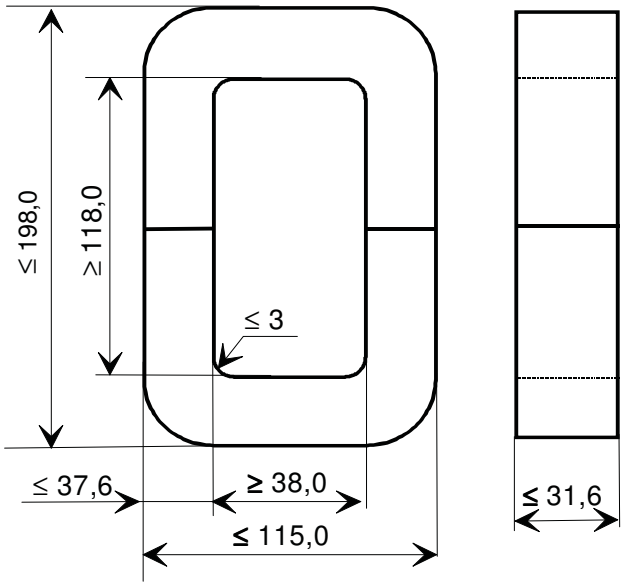

-02-
-02-
-02-
-02-

Endprüfung / ***Final Inspection:***
(100% Prüfung, AQL...: IEC 410 / DIN ISO 2859)

1. Mechanische Prüfung (AQL 4,0) / ***Mechanical Test*** *(AQL 4,0)*
Grenzmaße nach Maßbild / *Limited dimensions according to drawing*
Prüfmittel: Meßschieber / *Test instrument: caliper gauge*

2. Magnetische Prüfung (AQL 0,65) / ***Magnetical Test*** *(AQL 0,65)*

Verlust- und Scheinleistungsprüfung gemäß A60092-Y3022-K005 /
Measurement of core losses and apparent core losses according to A60092-Y3022-K005

Einstellwerte / *Setting values:*
f = 20 kHz
$\hat{B}$ = 0,3 T (entspr. / *corresp.* U_2 = 21,2 V/Wdg.)

Prüfwerte / *Specified values:*
p_{Fe} ≤ 15,0 W/kg (entspr. / *corr.* P_{Fe} ≤ 37,8 W) -02-
p_S ≤ 410 VA/kg (entspr. / *corr.* I_{eff} x N ≤ 49,0 A) -02-

Hinweis / *Remark:* Bau-Nr. / *Part-No.*: 97000555 -02-

Herausgeber	Bearbeiter	KB-PM	KB-E IN		Datum	freigegeben
KB-OP K FT	Till	Lehmann	Petzold		10.12.10	Günther

Ferrites and accessories

SIFERRIT material N87

Date: September 2006

Material properties

Preferred application			Power transformers
Material			N87
Base material			MnZn
	Symbol	Unit	
Initial permeability (T = 25 °C)	μ_i		2200 ±25%
Flux density (H = 1200 A/m, f = 10 kHz)	B_S (25 °C) B_S (100 °C)	mT mT	490 390
Coercive field strength (f = 10 kHz)	H_c (25 °C) H_c (100 °C)	A/m	21 13
Optimum frequency range		kHz	25 … 500
Hysteresis material constant	η_B	10^{-6}/mT	<1.0
Curie temperature	T_C	°C	>210
Mean value of α_F at 25 … 55 °C		10^{-6}/K	4
Density (typical values)		kg/m³	4850
Relative core losses (typical values)	P_V		
25 kHz, 200 mT, 100 °C		kW/m³	57
100 kHz, 200 mT, 100 °C		kW/m³	375
300 kHz, 100 mT, 100 °C		kW/m³	390
500 kHz, 50 mT, 100 °C		kW/m³	215
Resistivity	ρ	Ωm	10
Core shapes			RM, P, PM, ETD, EFD, E, ER, EP, EQ, ELP, U, Toroid

Complex permeability
versus frequency
(measured on R34 toroids, $\hat{B} \leq 0.25$ mT)

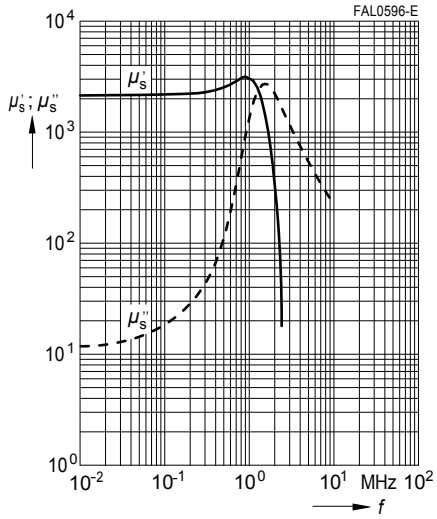

Initial permeability μ_i
versus temperature
(measured on R34 toroids, $\hat{B} \leq 0.25$ mT)

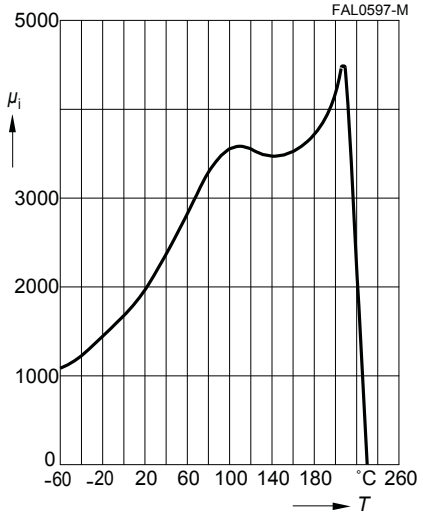

Amplitude permeability
versus AC field flux density
(measured on R34 toroids, $\hat{B} \leq 0.25$ mT)

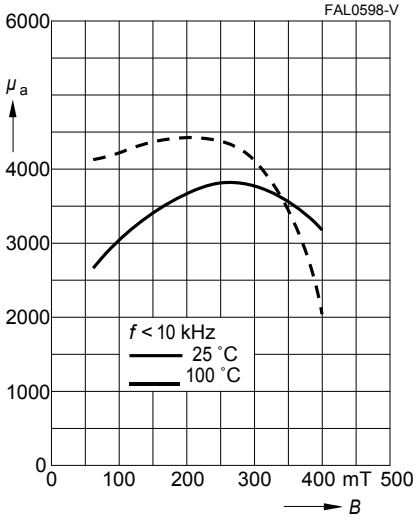

Dynamic magnetization curves
(typical values)
(f = 10 kHz, T = 25 °C)

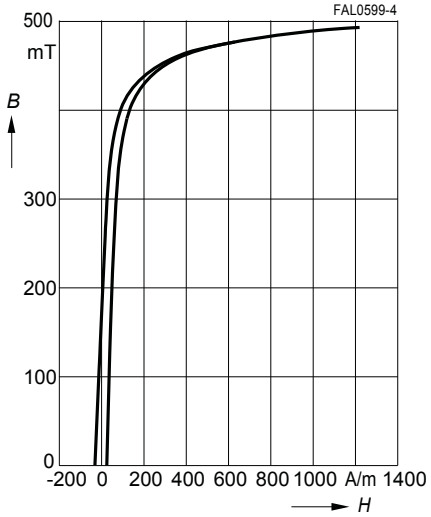

Dynamic magnetization curves
(typical values)
(f = 10 kHz, T = 100 °C)

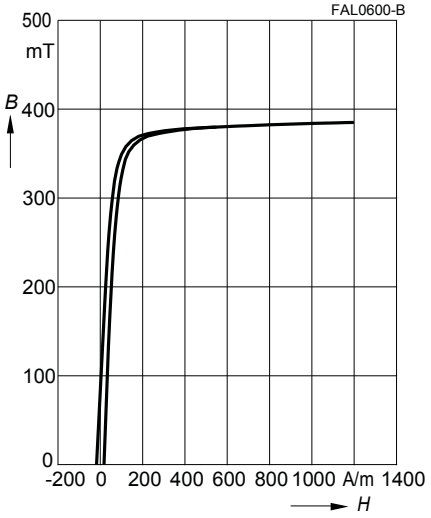

DC magnetic bias
of P, RM, PM and E cores
($\hat{B} \leq 0.25$ mT, f = 10 kHz, T = 25 °C)

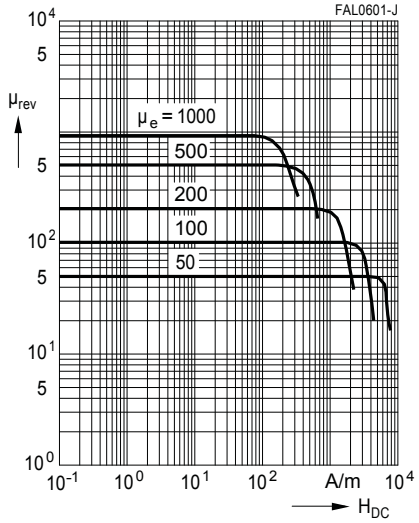

DC magnetic bias
of P, RM, PM and E cores
($\hat{B} \leq 0.25$ mT, f = 10 kHz, T = 100 °C)

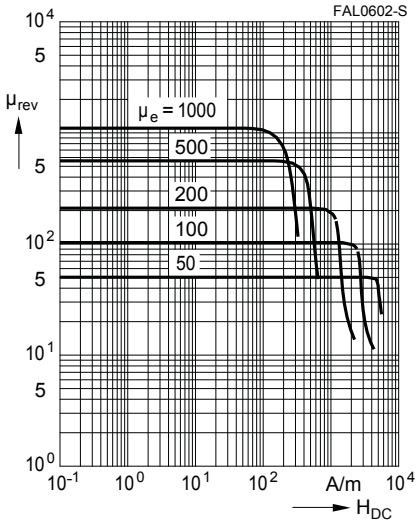

Relative core losses
versus AC field flux density
(measured on R34 toroids)

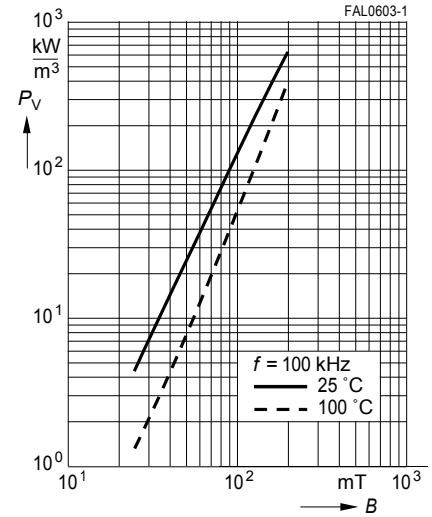

Relative core losses versus
temperature (measured on
R34 toroids)

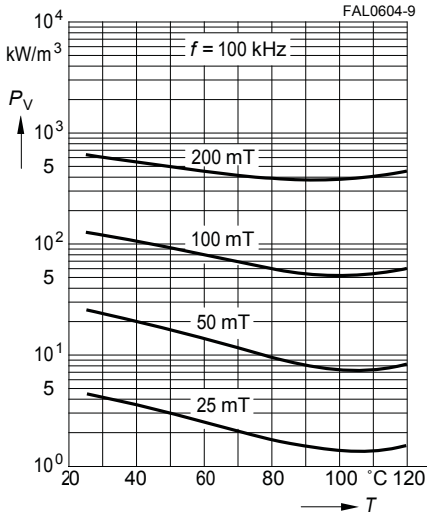

Relative core losses versus
frequency (measured on
R34 toroids)

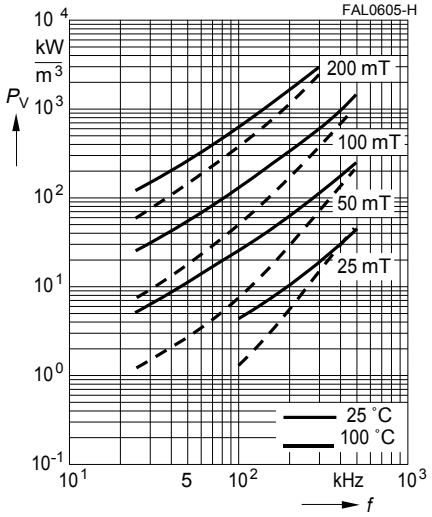

General

Based on IEC 60401-3, the data specified here are typical data for the material in question, which have been determined principally on the basis of toroids (ring cores).

The purpose of such characteristic material data is to provide the user with improved means for comparing different materials.

There is no direct relationship between characteristic material data and the data measured using other core shapes and/or core sizes made of the same material. In the absence of further agreements with the manufacturer, only those specifications given for the core shape and/or core size in question are binding.

Effects of core combination on A_L value

Stresses in the core affect not only the mechanical but also the magnetic properties. It is apparent that the initial permeability is dependent on the stress state of the core. The higher the stresses are in the core, the lower is the value for the initial permeability. Thus the embedding medium should have the greatest possible elasticity.

For detailed information see Data Book 2007, chapter “General – Definitions, 8.2”.

Heating up

Ferrites can run hot during operation at higher flux densities and higher frequencies.

Ferrites and accessories

UU 93/152/30, UI 93/104/30
Core set

Series/Type: **B67345B0001, B67345B0002**
Date: September 2006

■ For power transformers >1 kW (20 kHz)

Magnetic characteristics (per set)

	UU 93/152/30	UI 93/104/30	
©l/A	0.42	0.31	mm^{-1}
l_e	354	258	mm
A_e	840	840	mm^2
A_{min}	840	840	mm^2
V_e	297000	217000	mm^3
m	1500	1100	g/set

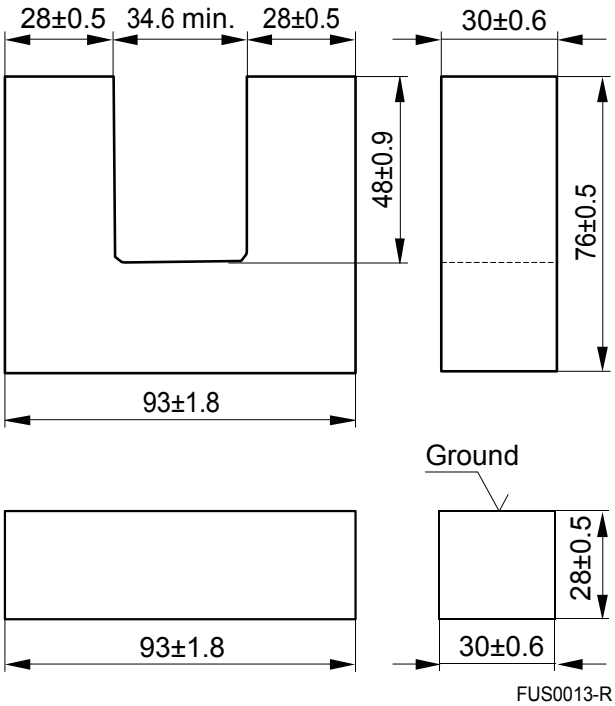

U and I cores are supplied as single units. The A_L value in the table applies to a core set comprising two ungapped cores.

Material	A_L value nH	α_e	P_V W/set	Ordering code
Combination UU 93/152/30				
N27	5400 +30/–20%	1800	< 16 (100 mT, 25 kHz, 100 °C)	B67345B0001X027
N87	5700 +30/–20%	1900	< 5.5 (100 mT, 25 kHz, 100 °C)	B67345B0001X087
Combination UI 93/104/30				
N27	7400 +30/–20%	1850	< 12 (100 mT, 25 kHz, 100 °C)	B67345B0001X027 (U) B67345B0002X027 (I)
N87	7900 +30/–20%	1930	< 4 (100 mT, 25 kHz, 100 °C)	B67345B0001X087 (U) B67345B0002X087 (I)

Cautions and warnings

Mechanical stress and mounting

Ferrite cores have to meet mechanical requirements during assembling and for a growing number of applications. Since ferrites are ceramic materials one has to be aware of the special behavior under mechanical load.

As valid for any ceramic material, ferrite cores are brittle and sensitive to any shock, fast changing or tensile load. Especially high cooling rates under ultrasonic cleaning and high static or cyclic loads can cause cracks or failure of the ferrite cores.

For detailed information see Data Book 2007, chapter “General – Definitions, 8.1”.

Effects of core combination on A_L value

Stresses in the core affect not only the mechanical but also the magnetic properties. It is apparent that the initial permeability is dependent on the stress state of the core. The higher the stresses are in the core, the lower is the value for the initial permeability. Thus the embedding medium should have the greatest possible elasticity.

For detailed information see Data Book 2007, chapter “General – Definitions, 8.2”.

Heating up

Ferrites can run hot during operation at higher flux densities and higher frequencies.

NiZn-materials

The magnetic properties of NiZn-materials can change irreversible in high magnetic fields.

Processing notes

– The start of the winding process should be soft. Else the flanges may be destroid.

– To strong winding forces may blast the flanges or squeeze the tube that the cores can no more be mount.

– To long soldering time at high temperature (>300 °C) may effect coplanarity or pin arrangement.

– Not following the processing notes for soldering of the J-leg terminals may cause solderability problems at the transformer because of pollution with Sn oxyd of the tin bath or burned insulation of the wire. For detailed information see Data Book 2007, chapter “Processing notes, 2.2”.

– The dimensions of the hole arrangement have fixed values and should be understood as a recommendation for drilling the printed circuit board. For dimensioning the pins, the group of holes can only be seen under certain conditions, as they fit into the given hole arrangement. To avoid problems when mounting the transformer, the manufacturing tolerances for positioning the customers’ drilling process must be considered by increasing the hole diameter.

Important notes

The following applies to all products named in this publication:

1. Some parts of this publication contain **statements about the suitability of our products for certain areas of application**. These statements are based on our knowledge of typical requirements that are often placed on our products in the areas of application concerned. We nevertheless expressly point out **that such statements cannot be regarded as binding statements about the suitability of our products for a particular customer application.** As a rule, EPCOS is either unfamiliar with individual customer applications or less familiar with them than the customers themselves. For these reasons, it is always ultimately incumbent on the customer to check and decide whether an EPCOS product with the properties described in the product specification is suitable for use in a particular customer application.
2. We also point out that **in individual cases, a malfunction of passive electronic components or failure before the end of their usual service life cannot be completely ruled out in the current state of the art, even if they are operated as specified.** In customer applications requiring a very high level of operational safety and especially in customer applications in which the malfunction or failure of a passive electronic component could endanger human life or health (e.g. in accident prevention or life-saving systems), it must therefore be ensured by means of suitable design of the customer application or other action taken by the customer (e.g. installation of protective circuitry or redundancy) that no injury or damage is sustained by third parties in the event of malfunction or failure of a passive electronic component.
3. **The warnings, cautions and product-specific notes must be observed**.
4. In order to satisfy certain technical requirements, **some of the products described in this publication may contain substances subject to restrictions in certain jurisdictions (e.g. because they are classed as "hazardous")**. Useful information on this will be found in our Material Data Sheets on the Internet (www.epcos.com/material). Should you have any more detailed questions, please contact our sales offices.
5. We constantly strive to improve our products. Consequently, **the products described in this publication may change from time to time**. The same is true of the corresponding product specifications. Please check therefore to what extent product descriptions and specifications contained in this publication are still applicable before or when you place an order.

   We also **reserve the right to discontinue production and delivery of products**. Consequently, we cannot guarantee that all products named in this publication will always be available.
6. Unless otherwise agreed in individual contracts, **all orders are subject to the current version of the "General Terms of Delivery for Products and Services in the Electrical Industry" published by the German Electrical and Electronics Industry Association (ZVEI)**.
7. The trade names EPCOS, EPCOS-JONES, Baoke, Alu-X, CeraDiode, CSSP, MLSC, PhaseCap, PhaseMod, SIFI, SIFERRIT, SIKOREL, SilverCap, SIMID, SIOV, SIP5D, SIP5K, UltraCap, WindCap are **trademarks registered or pending** in Europe and in other countries. Further information will be found on the Internet at www.epcos.com/trademarks.

Product Data
Rev. 8/8/2007

CoolPoly® D5108 Thermally Conductive Polyphenylene Sulfide (PPS)

CoolPoly D series of thermally conductive plastics transfers heat, a characteristic previously unavailable in injection molding grade polymers. CoolPoly is lightweight, netshape moldable and allows design freedom in applications previously restricted to metals. The D series is electrically non-conductive and can be used for its dielectric properties.

Thermal	SI/Metric	Testing Standard
Thermal Conductivity	10 W/mK	ASTM E1461
Thermal Diffusivity	0.07 cm²/sec	ASTM E1461
Specific Heat	1.00 J/g°C	ASTM E1461
Coefficient of Linear Thermal Expansion		
Parallel	6.5 ppm/°C	ISO 11359-2
Normal	5 ppm/°C	ISO 11359-2
Temperature of Deflection		
@ 0.45MPa	276 °C	ISO 75-1,2
@ 1.80MPa	239 °C	ISO 75-1,2
Flammability	V-0 @ 1.0mm	UL 94

Mechanical	SI/Metric	English	Testing Standard
Tensile Modulus	23600 MPa	3422 ksi	ISO 527-1
Tensile Strength	37 MPa	5365 psi	ISO 527-1
Nominal Strain @ Break	0.16 %	0.16 %	ISO 527-1
Flexural Modulus	19400 MPa	2813 ksi	ISO 178
Flexural Strength	69 MPa	10005 psi	ISO 178
Impact Strength			
Charpy Unnotched	2.50 kJ/m²	1.19 ft-lb/in²	ISO 179-1
Charpy Notched	1.10 kJ/m²	0.523 ft-lb/in²	ISO 179-1

Electrical	SI/Metric		Testing Standard
Surface Resistivity	4.50E14 ohm/square		ASTM D257
Volume Resistivity	2.50E16 ohm - cm		ASTM D257
Dielectric Constant			
@ 100Hz	4.8		ASTM D150
@ 1MHz	3.7 kV/mm	V/mil	ASTM D150
Dissipation Factor			
@ 100Hz	0.022		ASTM D150
@ 1MHz	0.0023		ASTM D150
Dielectric Strength	29 kV/mm	727 V/mil	ASTM D149
Comparative Tracking Index	580 volts		ASTM D3638
High Voltage Arc Resistance to Ignition	>300 sec		UL-746A

CoolPoly® D5108 Thermally Conductive Polyphenylene Sulfide (PPS)

CoolPoly D series of thermally conductive plastics transfers heat, a characteristic previously unavailable in injection molding grade polymers. CoolPoly is lightweight, netshape moldable and allows design freedom in applications previously restricted to metals. The D series is electrically non-conductive and can be used for its dielectric properties.

Electrical	SI/Metric	Testing Standard
High Voltage Arc Tracking Rate	DID NOT TRACK	UL-746A
Arc Resistance	300 sec	ASTM D495
Hot Wire Ignition	>120 sec	ASTM D3874

Physical	SI/Metric	English	Testing Standard
Density	1.82 g/cc	0.0658 lb/in³	ISO 1183
Mold Shrinkage			
Flow	0.2 %	0.002 in/in	ASTM D551
Cross-Flow	0.4 %	0.004 in/in	ASTM D551

CoolPoly® D5108 Thermally Conductive Polyphenylene Sulfide (PPS)

CoolPoly D5108 is a thermally conductive injection molding resin based on a polyphenylene sulfide (PPS) matrix. CoolPoly D5108 is electrically insulative. Thermally conductive polymers like CoolPoly D5108 cool faster than standard injection molding grade resins.

Typical Injection Molding Conditions

Temperature Settings	SI /Metric	English
Rear Zone	270 - 300 °C	520 - 570 °F
Center Zone	295 - 320 °C	560 - 610 °F
Front Zone	305 - 330 °C	580 - 630 °F
Nozzle	307 - 330 °C	585 - 630 °F
Melt	310 - 330 °C	590 - 625 °F
Mold	135 - 180 °C	275 - 350 °F

Pressure Settings		
Injection	6.2 - 13.8 MPa	900 - 2000 psi
Hold	2.1 - 6.9 MPa	300 - 1000 psi
Back	0.2 - 0.7 MPa	25 - 100 psi

Injection Settings		
Fill	moderate - fast mm/sec	moderate - fast in/sec
Screw	40 - 150 rpm	40 - 150 rpm
cushion	0.5 - 1.3 cm	0.2 - 0.5 inch

Drying Conditions		
Time & Temperature	4-6hrs @ 120 °C	4-6hrs @ 250 °F
Dew Point	-40 °C	-40 °F
Moisture Content	0.1 %	0.1 %

Additional Information

A Screw compression ratio 2.5 or less is recommended.
A reverse taper nozzle is recommended.
A mold surface temperature between 190F and 275F should be avoided as parts will have a varying degree of crystallinity leading to poor dimensional and long-term thermal stability.
A2 or D2 mold steel is recommended (Rc 60 or higher).

3M™ Thermally Conductive Adhesive Tape 8940 / 8943

Product Information Sheet 11.04.2007

Supersedes Version 01.10.2005

Product Description

3M™ Thermally Conductive Adhesive Tapes 8940 / 8943 are designed to provide an efficient heat transfer path between heat generating components and heat sinks or other cooling devices.

The tapes consist of a carrier, highly loaded with thermally conductive fillers, coated on either one side (3M™ 8943) or both sides (3M™ 8940) with a high temperature resistance acrylic pressure sensitive adhesive.

The specialized construction securely bonds the heat generating components to heat sinks and offer both, good thermal conductivity and excellent electrical insulation properties.

Product Construction

	3M 8940	3M 8943
Color	Beige	
Carrier	Filled Copolymer	
Adhesive type	Modified Acrylic Adhesive	
Tape type	Double coated	Single coated
Tape Thickness	0.190mm	0.170 mm
Liner Thickness	0,075 mm	

The film liner is a double sided siliconized Polyester Film with a differential release system.

Typical Applications

Applications requiring good thermal transfer and thin bonding.
Typical applications are assembling of power devices as bare dies in chip on board technique or flip chip assemblies with a directly mounted heat sink.
The tape performance properties have been primarily adapted to fit thermal requirements in applications such as Engine Control Units bonding, ABS Systems, High power LED's, and other electronic increased power devices.

3M™ Thermally Conductive Adhesive Tapes 8940 / 8943

Typical Properties and Performance Characteristics

Note: The following technical information for 3M™ Thermally Conductive Tape 8940 / 8943 should be considered representative or typical only and should not be used for specification purposes.

Thermal Properties

Test	Unit	Value	Test Method
Thermal Conductivity at 25 °C	W/m*K	0,9	ASTM D 5470
Coefficient of Thermal Expansion (-40 to 150°C)	mm/°C	140 E -06	TMA

Electrical Properties

Test	Unit	Value 8940	Value 8943	Test Method
Breakdown Voltage typical value *	kV	10.3	9.8	IEC 60243-1
Dielectric Strength typical value *	kV/mm	55	52	IEC 60243-1
Volume Resistivity	Ω*cm	$2,5 \times 10^{13}$		ASTM D257

* Average value (not for specification purposes)

Mechanical Properties

	Test	Unit	Value	Test Method
90° Peel Adhesion to Aluminium Substrate ($AlMg_3$; R_a: 0,48 µm; R_z:)µm)	20 min dwell time at room temp.	N/cm	5,0	AFERA 5001
	24 h dwell time room temp.	N/cm	6,0	AFERA 5001
	at 150 °C	N/cm	4,9	AFERA 5001
	at 180 °C	N/cm	2,4	AFERA 5001
Overlap Shear	20 min dwell time at room temp.	MPa	5,3	ASTM D 1002
	24 h dwell time room temp.	MPa	9,0	ASTM D 1002
	After 24 h @ 150 °C	MPa	6,8	ASTM D 1002
	After 24 h @ - 40 °C	MPa	9,0	ASTM D 1002
Holding Power	1000 g load @ room temp.	Minutes	10000+	AFERA 4012
	500 g load @ 70 °C	Minutes	10000+	AFERA 4012
Tensile strength	Tensile Strength	N/mm²	6-7	EN ISO 527-2
	Elongation at break	%	80-120	EN ISO 527-2
Liner properties	Liner release	cN/25,4 mm	15	FINAT TM3
Temperature Performance	Thermal Stability 225 °C Dwell @ 60 min (Tape was applied between a glass and an aluminium panel)	Visual	No Change	3M
	Solder Reflow process according to JEDEC J-STD-020C (Level 1)	Visual	Test in process	3M
	Continuous Operating Temperature Range	°C	- 40 up to 150	3M

3M™ Thermally Conductive Adhesive Tapes 8940 / 8943

Thermal Resistance Properties	Test	Unit	Value	Test Method
	Thermal Gravimetric Analysis * Mass loss at 200 °C	%	< 0,2	3M
	Mass loss at 150 °C after 4 h	%	< 0,3	

Flame Class:	UL 94 V-0, File E253171, Flame rating applies to adhesive film (3M™ Thermally conductive Tape 8940) bonded to 3.0 mm minimum thickness aluminium on one side and 0.86 mm minimum thickness FR-4 laminate on other side.

Application Guidelines	
	1.) Substrate surfaces should be clean and dry prior to tape application. Isopropyl alcohol (isopropanol) applied with a lint-free wipe or swab should be adequate for removing surface contamination such as dust or finger prints. Do not use "denatured alcohol" or glass cleaners which often contain oily components. Allow the surface to dry for several minutes before applying the tape. More aggressive solvents (such as acetone, methyl ethyl ketone (MEK) or heptane) may be required to remove heavier contamination (grease, machine oils, solder flux, etc.) but should be followed by a final isopropanol wipe as described above. **Note:** Be sure to read and follow the manufacturers' precautions and directions when using primers and solvents. 2) Apply the tape to one substrate at a modest angle with the use of a squeegee, rubber roller pressure to help reduce the possibility of air entrapment under the tape during its application. The liner can be removed after positioning the tape onto the first substrate. 3) Assemble the part by applying compression to the substrates to ensure a good wetting of the substrate surfaces with the tape. Proper application of pressure (amount of pressure, time applied, temperature applied) will depend upon design of the parts. The preferred pressure at room temperature is a minimum of 1 kg/cm^2 for 5 seconds. For fragile parts lower pressure may be needed. Rigid substrates are more difficult to bond without air entrapment as most rigid parts are not flat. Flexible substrates can be bonded to rigid or flexible parts with much less concern about air entrapment because one of the flexible substrates can conform to the other substrate.
Shelf Life	Product shelf life is 2 years from date of manufacture when stored at room temperature conditions 22°C and 50% r.h. in the products original packaging.

Scotch-Weld™ DP760

Product Data Sheet

Updated : February 2009
Supersedes: June 2001

Product Description

DP760 epoxy adhesive is a non-sag, two-part room temperature curing adhesive designed for use when high temperature resistance is required.

Physical Properties
Not for Specification Purposes

	BASE	ACCELERATOR
Base	Toughened Epoxy	Modified Amine
Colour	White	White
Specific Gravity (approx.)	1.26	0.82
Mix Ratio By Volume By Weight	 100 100	 50 32
Viscosity	Non-sagging paste	Non-sagging paste
Worklife at 23°C (min) 5 g 10 g 20 g	 60-80 45-60 35-40	

Typical Performance Characteristics
Not for specification purposes

Overlap Shear Strength (MPa)

Test conditions	Cure cycle 1	Cure cycle 2	Cure cycle 3
- 55 ± 3°C	19.4 (C)	17.4 (C)	21.9 (C)
23 ± 2°C	28.2 (C)	29.1 (C)	30.4 (C)
80 ± 2°C	24.1 (C)	24.2 (C)	25.9 (C)
120 ± 2°C	16.2 (C)	16.1 (C)	15.4 (C)
150 ± 2°C	10.4 (C)	11.9 (C)	10.3 (C)
175 ± 3°C	7.6 (C)	7.3 (C)	7.5 (C)
205 ± 3°C	4.9 (C)	5.2 (C)	5.3 (C)
230 ± 3°C	2.9 (C)	3.0 (C)	3.5 (C)

Test method EN 2243-1

Overlap shear specimens were constructed using 1.6 mm thick 2024 T3 clad aluminum with the surface prepared using the optimized FPL etch.

Typical Performance Characteristics

Not for specification purposes

Roller (Bell) Peel Strength (N/25mm)

Cure cycle 1	Cure cycle 2	Cure cycle 3
184	154	159

Test method EN 2243-2

Roller (Bell) peel specimens were constructed using 1.6 and 0.5 mm thick 2024 T3 clad aluminum with the surface prepared using the optimized FPL etch

Cure cycles :

7 days at 23 ± 2°C under a pressure of 100 kPa the first 24 hours

24 hours at 23 ± 2°C under a pressure of 100 kPa followed by a 60 min post cure at 80 ± 3°C

120 min at 65 ± 3°C under a pressure of 100 kPa.

150 µm diameter glass beads were used to control glue line thickness

Environmental Resistance

Not for specification purposes

Overlap Shear Strength (MPa)

Conditions	Test results
Control (23°C / 50% RH)	28.8 (Cohesive)
D.I. water at 23°C	29.1 (Cohesive)
150°C dry heat	21.4 (Cohesive)
JP4 fuel at 23°C	28.9 (Cohesive)
Engine oil at 23°C	27.8 (Cohesive)
Hydraulic oil at 23°C	27.2 (Cohesive)
50°C ; ≥ 95 % relative humidity	24.9 (Cohesive)
5 % salt spray at 35°C	28.1 (Cohesive)*
* Denotes no corrosion under the glue line	

Test method EN 2243-1

Long term humidity resistance
Not for specification purposes

Overlap Shear Strength (MPa)

Test conditions	Initial Performance		Performance after 750 h at 70°C ≥ 95 % RH	
	Clad AA	Bare AA	Clad AA	Bare AA
- 55 ± 3°C	18.8 (Cohesive)	18.6 (Cohesive)	22.9(Cohesive)	Not tested
23 ± 2°C	28.7 (Cohesive)		24.8 (Cohesive)	19.0 (Adhesive/ Cohesive)
80 ± 2°C	22.9 (Cohesive)	21.9 (Cohesive)	16.5 (Cohesive)	18.0 (Cohesive)
120 ± 2°C	16.5 (Cohesive)	14.6 (Cohesive)	8.3 (Adhesive/Cohesive)	12.8 (Cohesive)
150 ± 2°C	10.4 (Cohesive)	10.0 (Cohesive)	5.6 (Adhesive/Cohesive)	9.0 (Cohesive)
175 ± 3°C	7.9 (Superficial cohesive)	6.9 (Cohesive)	3.7 (Adhesive/Cohesive)	Not tested

Test method EN 2243-1

Table denotes typical results obtained on 1.6 mm thick clad and bare 2024 T3 aluminum alloy with the surface prepared by the optimized FPL etch method after curing for 7 days at 23 C.
150 μm glass beads were used to control the glue line thickness.

Thermal properties

The glass transition temperature (Tg) was determined using Perkin/Elmer DSC7 analyzer with a heating rate of 10°C/min. Second heat values given.
Mid-point : 145-150 °C

Compression strength and Young's modulus

Data generated from a cast block of material (12.5 x 12.5 x 25 mm) and curing for 24 hours at 23+/-3°C followed by a 60 minutes post-cure at 80+/-3°C. Specific gravity of the cured material was measured as 1.11 at 23 °C

Compression strength (MPa)	Young's modulus (MPa)
23 +/- 2°C : 78.8	23 +/- 2°C : 5972
80 +/- 2°C : 48.7	80 +/- 2°C : 4930
120 +/- 2°C : 36.8	120 +/- 2°C : 3633
150 +/- 3°C : 24.2	150 +/- 3°C : 2350

Additional Product Information

Work Life:
After mixing, the mixture remains workable for a time before it becomes too viscous to properly wet the surface to which it is applied.

The work life and rate of cure are both greatly affected by temperature and to some extent humidity, curing faster as temperature and humidity are raised.

Once mixed, the adhesive should be used within 1 hour.

Equipment :
3M Scotch-Weld™ DP760 is supplied in a dual syringe plastic cartridge designed to fit the EPX™ applicator system.

Contact your 3M representative for assistance in selecting application equipment to suit your specific needs.

Clean Up:
Excess adhesive can be cleaned up prior to curing with 3M Solvent No.2.

Note: 3M Solvent No.2 is flammable. When using solvents for clean up it is essential that the correct safety precautions are observed.

A thoroughly cleaned, dry, grease-free surface is essential for maximum performance.

Cleaning methods which will produce a break free water film on metal surfaces are generally satisfactory

Surface Preparation

For high strength structural bonds, paint, oxide films, oils, dust and all other surface contaminants must be completely removed. The level of surface preparation will depend on the required bond strength and environmental resistance required.

Storage Conditions

Rotate stock on a “first in - first out” basis. When stored at room temperature, shelf life is 6 months. 2 years shelf life applies if the material is stored at –18°C.

Shelf Life

6 months from date of dispatch by 3M when stored in the original carton at 4°C and 50% relative humidity.

Precautionary Information

Refer to product label and Material Safety Data Sheet for health and safety information before using the product.

Refer to the Technical Bulletin for information about “Application Guide”

For information please contact your local 3M Office.
www.3M.com

For Additional Information

To request additional product information or to arrange for sales assistance, call 0870 60 800 50 Address correspondence to: 3M 3M United Kingdom PLC 3M House, 28 Great Jackson Street, Manchester, M15 4PA

Technical introduction

1. General points

In order to provide optimum performance of semi-conducting devices it is essential not to exceed the maximum junction temperature indicated by the manufacturer.

Generally this maximum junction temperature can only be maintained without exceeding it by running the device concerned at lower power outputs.

At outputs approaching the maximum ratings semi-conductor devices have to be cooled by so called heatsinks, sometimes called dissipators.

The thermal performance of these heatsinks primarily depends on the thermal conductivity of the material from which they are made, size of surface area and mass.

In addition, surface colour, mounting position,temperature, ambient air velocity and mounting place all have varying influence on the final performance of the heatsink from one application to another..

However, a figure for thermal resistance can be experimentally determined in a reliable manner and used in the equations that follow in part 2.

There are no agreed international standard methods for testing electronic cooling systems or for the determination of the thermal resistance.

Therefore the diagrams and values given in our catalogue have been determined under practical operating conditions and therefore allow the most suitable heatsink from the range to be selected.

We expressly point out that all information and data is given to the best of our knowledge and belief. The user is solely responsible for the proper use of our products and he should check their suitability for the intended application.

Fischer Elektronik do not assume any warranty, whether expressed or implied, for the suitability, function or merchantibility of their products in specific or general applications, and they cannot be held liable for accidental or consequential damage due to non-observance of the above.

Furthermore Fischer Elektronik reserve the right to carry out technical modifications to their products at any time.
All orders are subject to the General Sales Conditions of Fischer Elektronik.

2. The determination of thermal resistance

The thermal resistance is the parameter that is the most important in cooler selection, apart from mechanical considerations.

For determination of the thermal resistance the following equation applies:

Equation 1:

$$R_{thK} = \frac{\vartheta_i - \vartheta_u}{P} - (R_{thG} + R_{thM}) = \frac{\Delta\vartheta}{P} - R_{thGM}$$

In case of an application where the maximum junction temperature is not exceeded the temperature has to be verified.
When the case temperature has been measured the use of the following equation will enable the maximum junction temperature to be calculated:

Equation 2:

$$\vartheta_i = \vartheta_G + P \times R_{thG}$$

The meaning of the determinants:

ϑ_i = maximum junction temperature in °C of the device as indicated by manufacturer.
As a »safety factor« this should be reduced by 20-30 °C.

ϑ_u = ambient temperature in °C.
The rise in temperature caused by radiant heat of the heatsink should be increased by a margin of 10-30 °C.

$\Delta\vartheta$ = difference between maximum junction temperature and ambient temperature.

ϑ_G = measured temperature of device case (equation 2).

P = maximum power rating of device in watts

R_{th} = thermal resistance in K/W

R_{thG} = internal thermal resistance of semiconductor device (as indicated by manufacturer)

Heatsinks profile-overview → **A 13 - 17**
Heatsink special design → **A 135 - 136**
Special profiles → **A138**
Heatsink as visual & decor-parts → **A 10**
Heatsinks for SSR → **A 11 - 12**
Die-cast heatsinks → **A 123 - 136**
Assigment table → **A 18 - 20**
Order example → **A 21**

fischer elektronik

Technical introduction

R_{thM} = thermal resistance of mounting surface. For TO 3 cases the following approximate values apply:

1. dry, without insulatar	0.05 - 0.20 K/W
2. with thermal compound/without insulator	0.005 - 0.10 K/W
3. Aluminium oxide wafer with thermal compound	0.20 - 0.60 K/W
4. Mica wafer (0.05 mm thick) with thermal compound	0.40 - 0.90 K/W

R_{thK} = thermal resistance of heatsink, which can be directly taken from the diagrams

R_{thGM} = sum of R_{thG} and R_{thM}. For parallel connections of several transistors the value R_{thGM} can be determined by the following equation:

Equation 3:
$$\frac{1}{R_{thGM\ ges.}} = \frac{1}{R_{thG1} + R_{thM1}} + \frac{1}{R_{thM2}} R_{thG2} + \cdots + \frac{1}{R_{thGn} + R_{thMn}}$$

The result can be substituted into equation 1.

K = Kelvin, which is now the standard measure of temperature differences, measured in °C, therefore 1°C = 1 K.

K/W = Kelvin per watt, the unit of thermal resistance.

Calculation examples:

1.A TO 3 power transistor with 60 watt rating has a maximum junction temperature of 180 °C and an internal resistance of 0.6 K/W at an ambient of 40 °C with aluminium oxide wafers.
What thermal resistance is required for the heatsink?

given:
P = 60 W
ϑ_j = 180 °C - 20 °C =160 °C (for safety margin)
ϑ_u = 40 °C
R_{thG} = 0,6 K/W
R_{thM} = 0.4 K/W (average value)

find: R_{thK} using equation 1
$$R_{thK} = \frac{\vartheta_j - \vartheta_u}{P} - (R_{thG} + R_{thM}) = \frac{160\ °C - 40\ °C}{60\ W} - (R_{thG} + R_{thM}) = \underline{1{,}0\ K/W}$$

2.Same conditions as above but for three devices with equally distributed power ratings.

solution use equation 1 and equation 3
$$\frac{1}{R_{thGM\ ges.}} = \frac{1}{0{,}6 + 0{,}4\ K/W} + \frac{1}{0{,}6 + 0{,}4\ K/W} + \frac{1}{0{,}6 + 0{,}4\ K/W} = \frac{3}{1}\ W/K$$
$$R_{thGM\ ges} = \frac{1}{3}\ K/W = \underline{0{,}33\ K/W}$$

substitute into Equation 1 gives:
$$R_{thK} = \frac{160\ °C - 40\ °C}{60\ W} - 0{,}33\ K/W = \underline{1{,}67\ K/W}$$

With these values determined, the tabulation on page A 13 - 17 can be used to give a choice of possible heatsink profiles. Then by examination of the drawings and curves the final choice can be made.

3.A transistor with power rating of 50 W and internal thermal resistance of 0.5 K/W has a case temperature of 40 °C.
What is the actual value of junction temperature?

données:
P = 50 W
R_{thG} = 0,5 K/W
ϑ_G = 40 °C

find: ϑ_j using equation 2

$\vartheta_j = \vartheta_G + (P \bullet RthG)$ $\quad \vartheta_j = 40\ °C + (50\ W \bullet 0{,}5\ K/W) = 65\ °C$

fischer elektronik

Technical introduction

Thermal resistances of any profiles with forced convection

$R_{thKf} \approx a \bullet R_{thK}$
R_{thKf} = thermal resistance with forced convection
R_{thK} = thermal resistance with natural convection
a = factor of proportion

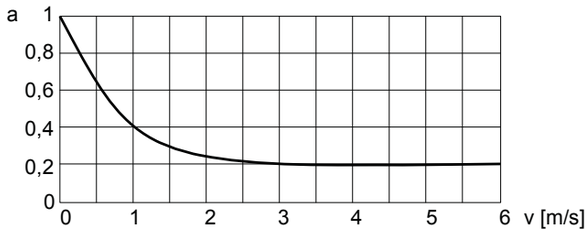

Remarks:

1. The values indicated in the diagrams apply only for heatsinks with black anodised surface, mounted vertically and natural convection.

Correction factors: natural surface: +10 to 15 % for horizontal mounting: + 15 to 20 %

2. Heatsink profiles are extruded to European standard DIN EN 12020 (former DIN 17615).
   For profiles exceeding a circumscribed circle of 300 mm, the tolerances to DIN EN 755 (former DIN 1748) apply.

Important note:
Manufacturers of certain electronic components, especially modules with a large surface area, IGBT etc., specify installation surfaces for heatsinks etc. with an flatness, which is beyond standard tolerances. Such perfect flatness can only be achieved by milling the installation surface. Furthermore, it should be noted that threaded wire inserts may be required in order to reach higher tightening torques in aluminium (e.g. Heli-Coil or similar.). Please observe the semiconductor manufacturers' information.

3. The mentioned heatsink profiles in our catalogue contain so called extrusion marks between the fins for a profile identification.
   To avoid misuse the operator has to check the size and position for the mechanical treatment or placement of the components.

4. Profile extruded threaded channels are no threads conforming to standards, as they have no thread pitch.
   The thread pitch is imitated by staggered webs (ribs). The customer is responsible for appropriate use.

5. Machining of our extruded and non extruded profiles conforms to requirements of DIN ISO 2768 m - unless otherwise stated.
   For all ICK S types DIN ISO 2768c is valid.

6. The lengths of extruded profiles [|↔|] and the pin layouts [✥] indicate only the standard range. We offer every profile cut to customer's exact length and machining requirement made to drawing or sample. We bore, countersink, mill, saw, grind and cut threads into your heat sink to meet your specific requirements. With our modern machine tools including CNC machining centres, multispindled drills (up to 26 drillings/threads at the same time) and digital milling and stamping tools plus our own "in house" tool room we are able to manufacture competetively priced prototypes as well as batch and mass produced parts with short lead times.

7. The standard material of our heatsinks is warm age-hardened aluminium alloy according to EN AW 6060 – T66 (former AlMgSi05 – F22 acc. to DIN 1748). Our standard surface treatments are raw degreased aluminium (Al) and black anodised (SA). On request, we anodise clear natural (ME) or decorative in any colour that is technically possible.

8. If you cannot find a suitable profile within our range of approx. 400 profiles, 13 small heatsinks and 50 finger shaped heatsinks, we can design and produce to your requirements. Please contact us at the start of your next project so that we can work together, either directly or through our representatives. Remember that we have the ability to find the solution for "your" cooling problem.

9. Note on tolerances

All dimensions given in this cataloque for products, items and machined parts are acc. to DIN ISO 2768 m if not otherwise stated. Not included are items like extruded profiles, diecasts, handles, vibration dumpers etc. for which different standards apply.

Update - January 2013

fischer elektronik

Technical introduction

General information

Blind holes are produced after anodising. Through holes are produced before anodising. With completely visual parts, additional painting is recommended. The sections are extruded according to DIN EN 12020. For sections that exceed a circumscribed circle of 300 mm, DIN EN 755 apply. The machining tolerances are specified according to DIN ISO 2768 m.

Visual parts: Please indicate at which place clamp points are allowed! We recommend e.g. supplementary laquering.

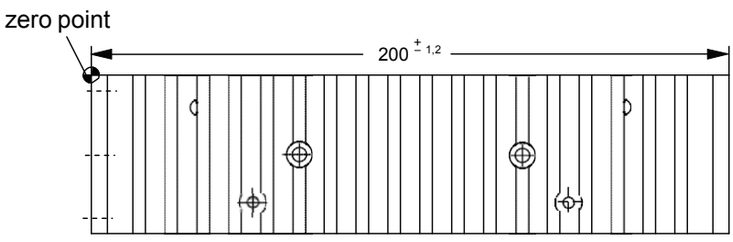

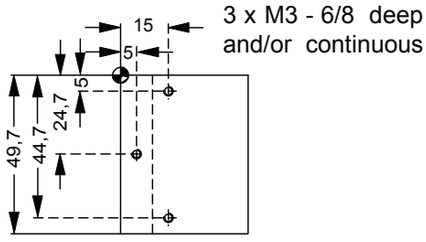

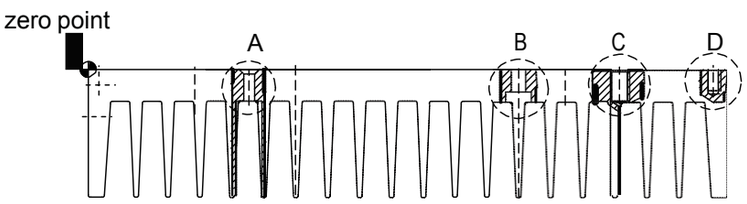

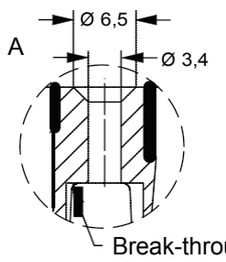

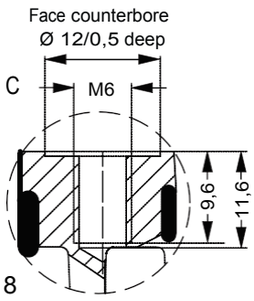

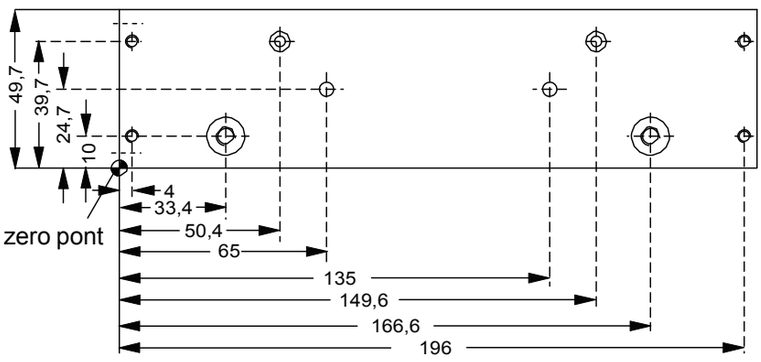

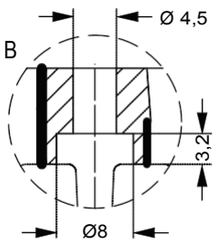

Plunge-through and
counterbore with Ø 8

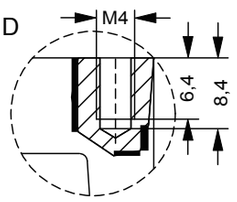

Standard aluminium profiles	→ A 133 - 134	Thermal conductive material	→ E 2 - 22
Extruded heatsinks	→ A 22 - 83	Hole pattern	→ A 21
Lamella heatsinks	→ A 127 - 128	Drilling pattern for SSR	→ A 12
Fluid coolers	→ A 129 - 131	Technical introduction	→ A 2 - 7

Information for dimensioning, shown on SK 47 general:

The deflection can be up to 0.8 mm concave, 0.2 mm convex. If a certain flatness of the bottom surface is required the bottom thickness can be decreased by a maximum of approx. 0.8 mm by means of face-milling. This situation must be taken into consideration with the bore hole depths for blind holes.
Counterbores and bore hole diameters are to be produced according to DIN 74, if not explicitly stated otherwise.
The depth of thread should be calculated as follows.

Example M 5:
thread: <M> 5 x 1.6 mm = 8 mm core bore: 8 mm + 2 mm = 10 mm

Examples:
cutout A: Through-hole according to DIN 74 A m 3, counterbore bottom side, undercut of the fins.
cutout B: Through hole with break-through of the fins according to DIN 74 H m 4, counterbore on fin side.
cutout C: Thread M 6. Depth of thread 1.6 x 6 mm = 9.6 mm, bore depth 9.6 mm + 2 mm = 11.6 mm.
Bore hole on fin base is plunged through. Face counterbore dia. 12 x 0.5 on bottom side.
cutout D: Blind thread M 4. Depth of thread 1.6 mm x 4 = 6.4 mm, bore depth 6.4 mm + 2 mm = 8.4 mm.

Extrusion tolerances – production tolerances

There is often the problem, that the production tolerances cannot be adhered to, due to the extrusion tolerances. The two examples show how the production tolerances can be cut in half by means of suitable dimensioning (here: extension of the zero point from the outer edge to the center of the section).

When taking unfavourable extrusion tolerances into consideration a difference of 1.1 mm arises between the two types of dimensioning with respect to the axis of symmetry.

SK 82

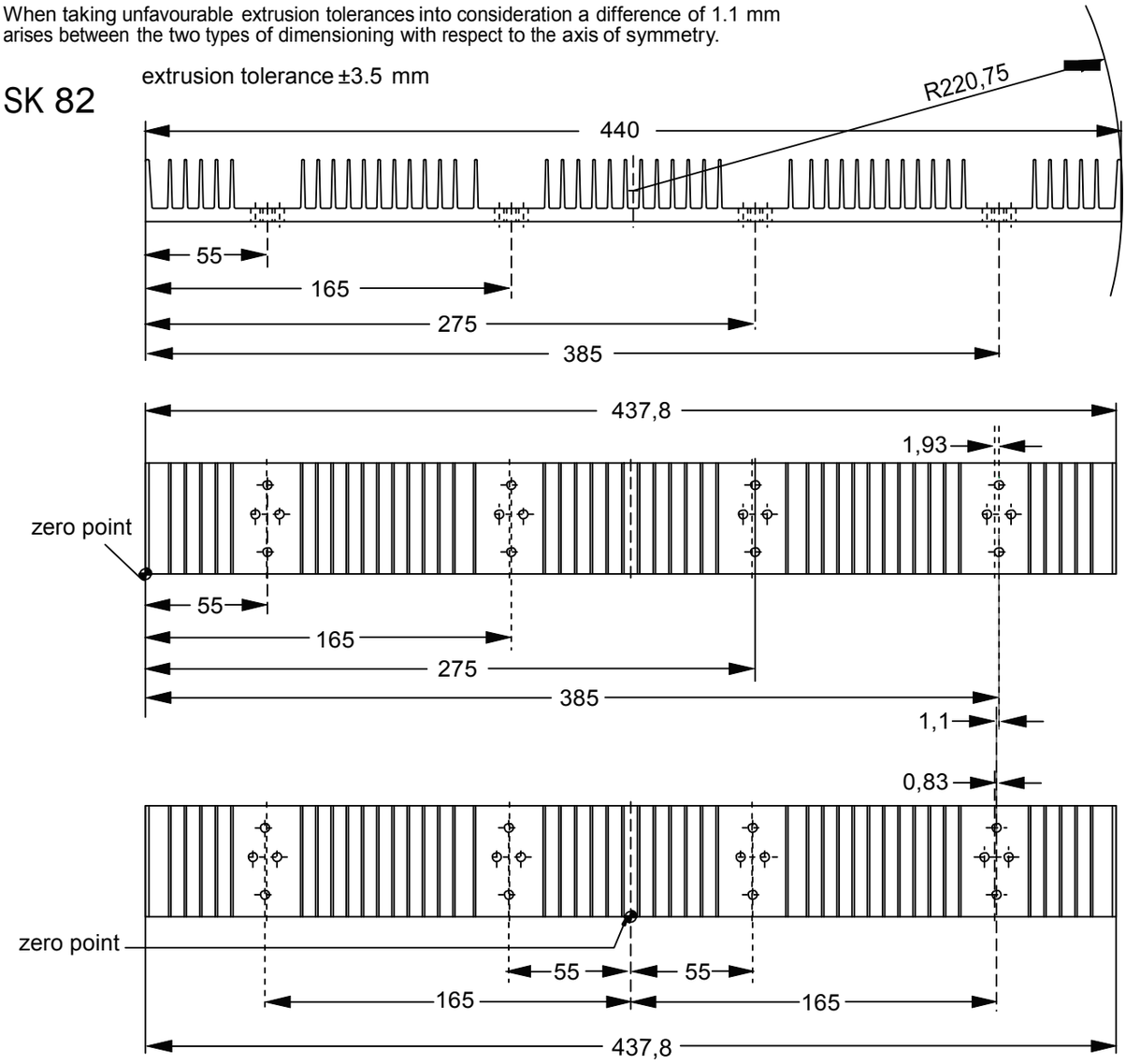

Heatsinks profile-overview	→ A 13 - 17	Heatsinks for SSR	→ A 11 - 12
Heatsink special design	→ A 135 - 136	Die-cast heatsinks	→ A 123 - 136
Special profiles	→ A138	Assigment table	→ A 18 - 20
Heatsink as visual & decor-parts	→ A 10	Order example	→ A 21

SK 34

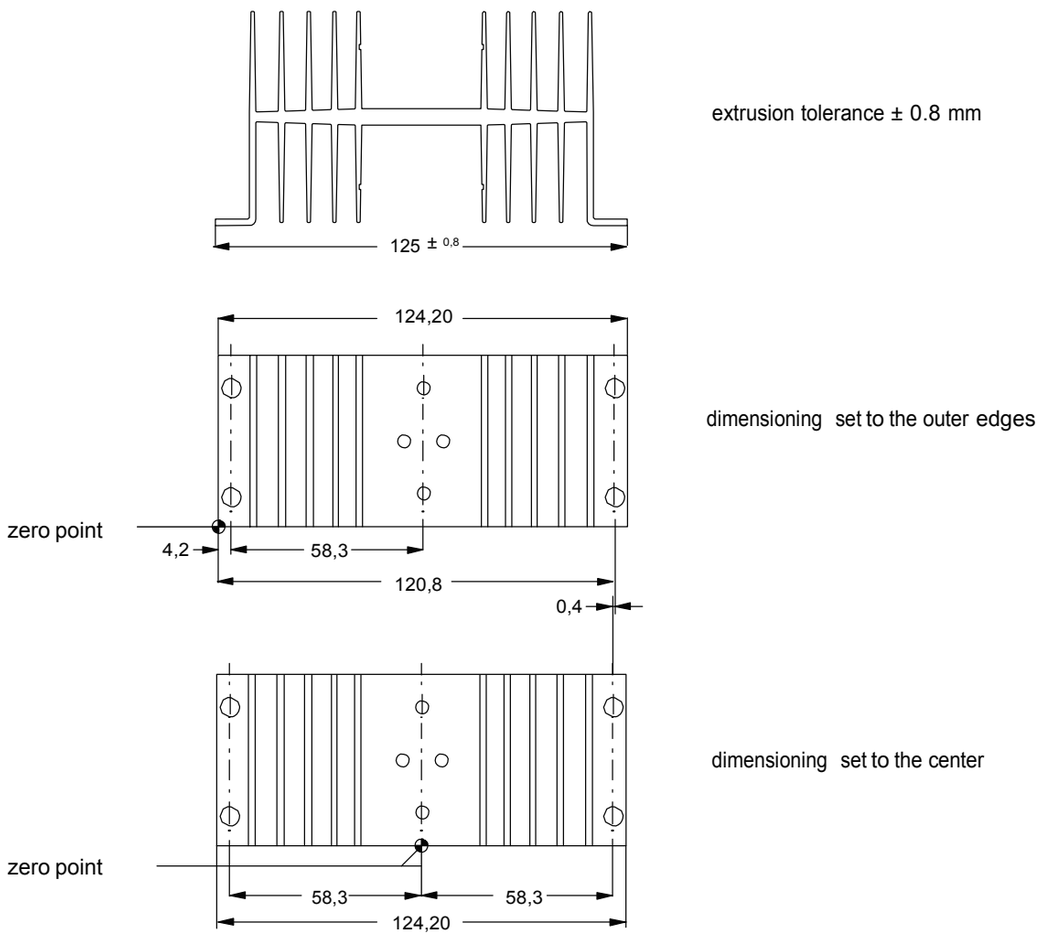

When taking unfavourable extrusion tolerances into consideration, a difference of 0.4 mm arises between the two types of dimensioning with respect to the axis of symmetry.

Milling

If, when milling heatsinks, cooling aggregates, etc., the milling tool diameter is smaller than the area being milled for production reasons, so called „milling grooves“ with steps or edges are produced (see sketch). Even if the roughness depth value for the surface is observed, it is a good idea to specify the area of the component in which no milling edges are allowed.

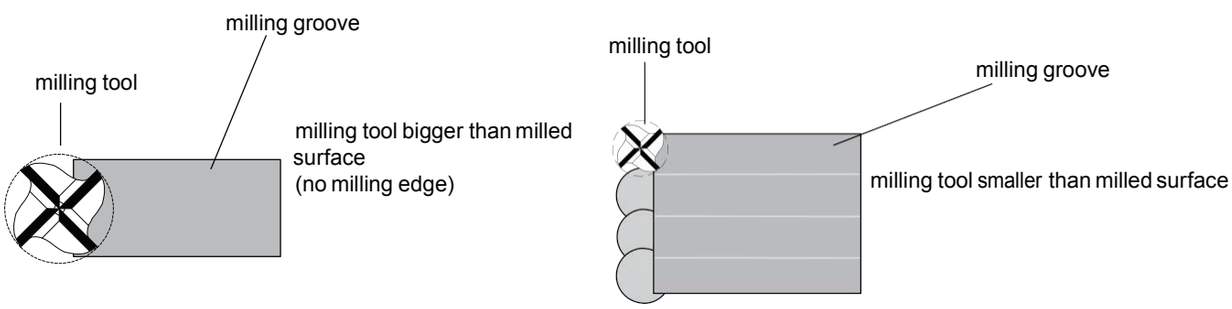

Standard aluminium profiles → A 133 - 134
Extruded heatsinks → A 22 - 83
Lamella heatsinks → A 127 - 128
Fluid coolers → A 129 - 131
Thermal conductive material → E 2 - 22
Hole pattern → A 21
Drilling pattern for SSR → A 12
Technical introduction → A 2 - 7

Silicone Heat Transfer Compound Plus

TECHNICAL DATA SHEET

Product Code: HTSP

PRODUCT DESCRIPTION

HTSP provides the ultimate in thermal conductivity together with the very wide temperature range obtained by using silicone base oils. The exceptional properties obtained from HTSP are due to the novel use of various metal oxide (ceramic) powders. These materials are electrically insulative to ensure that leakage currents can not be formed if the paste should come into contact with other parts of the assembly.

HTSP should be used where a large amount of heat needs to be dissipated quickly and effectively. The heat dissipation from the source (e.g. semiconductor barrier layer) is achieved through many layers of different material before the heat is dissipated through free or forced convection. It should be noted that the use of a thermally conductive paste will only aid the dissipation of heat if the interface where it is used has the lowest thermal conductivity within the system, i.e. is the rate determining step. This is usually the case.

The rate at which heat flows is dependant on the temperature differential, the thickness of the layer, and the thermal conductivity of the material.

A full range of heat transfer products are available from Electrolube. This range includes silicone and non-silicone based pastes (HTS & HTC), an RTV rubber (TCR), an adhesive epoxy (TBS) and an epoxy based potting resin (ER2074).

A non-silicone version of this material is also available, order code HTCP.

FEATURES

* Superior thermal conductivity even at high temperatures.
* Excellent non-creep characteristics.
* Wide operating temperature range with low evaporation weight loss.
* Easy to handle, economic in use and low in toxicity.

ELECTROLUBE, A division of H K Wentworth, Kingsbury Park, Midland Road, Swadlincote, Derbyshire, DE11 0AN
Tel: +44(0) 1283-222111 Fax: +44(0) 1283-550177 www.electrolube.com
ISO 9002 Registered Firm. Certificate No. FM 32082

Silicone Heat Transfer Compound Plus – Page 2

TECHNICAL DATA SHEET

TYPICAL PROPERTIES

Colour:	White
Base:	Silicone Oil
Thermoconductive Components:	Powdered Metal Oxides
Density @ 20°C:	3 g/cm^3
Temperature Range:	-50°C to +200°C
Thermal Conductivity:	3.0 W/m.K
Weight Loss after 96 hours @ 100°C:	= 0.80%
Permitivity @ 10^6 Hz:	4.9
Specific Resistance:	1 x 10^{15} Ohms/cm
Dielectric Strength:	18 kV/mm
Viscosity:	Paste

DIRECTIONS FOR USE

Apply in a thin film, to the base and mounting studs of diodes, transistors, thyristors, heat sinks, silicone rectifiers and semi-conductors, thermostats, power resistors and radiators.

PACKAGING

50 ml Tube (150g)
1 Kg Bulk

ORDER CODE

HTSP50T
HTSP01K

ADDITIONAL INFORMATION

Some useful conversion factors are as follows:

1 cal	=	0.003968 BTU (British Thermal Unit)
1 cal/cm x sec x K	=	0.04964 BTU/in x h x ?F
	=	416.8 W/m x K
1 BTU/h x ft x ?F	=	12 BTU x in/h x sq ft x ?F
	=	0.04134 cal/sec x cm x K
1 BTU x in/h x sq ft x F?	=	0.0003445 cal/sec x cm x K
	=	0.1437 W/m x K
1 BTU/h x ft x ?F	=	1.724 W/m x K
1 W/in x K	=	22.75 BTU/h x ft x ?F
1 cal/sec x cm	=	10.6 W/in x K

ELECTROLUBE, A division of H K Wentworth, Kingsbury Park, Midland Road, Swadlincote, Derbyshire, DE11 0AN
Tel: +44(0) 1283-222111 Fax: +44(0) 1283-550177 www.electrolube.com
ISO 9002 Registered Firm. Certificate No. FM 32082

HTSP
Silicone Heat Transfer Compound Plus

HTSP is a highly thermally conductive non-curing heat transfer paste, designed for use as a thermal interface material. It is recommended where large amounts of heat need to be dissipated efficiently, ensuring the reliable thermal coupling of electronic components. HTSP is based on a silicone oil, offering an exceptionally wide operating temperature range.

- High thermal conductivity; optimum efficiency of heat dissipation
- Very low viscosity for ease of application; designed for use as a thermal interface material
- Based on a silicone oil; offers an exceptionally wide operating temperature range
- Non-curing paste; allows simple and efficient rework of components if required

Approvals	**RoHS-2 Compliant (2011/65/EU):**	**Yes**
Typical Properties	Colour:	Pale Grey
	Base:	Silicone Oil
	Thermo-conductive Component:	Powdered metal oxides
	Density @ 20°C (g/ml):	3.0
	Viscosity @ 1rpm (Pa s):	42-48
	Thermal Conductivity (Guarded Hot Plate):	3.0 W/m.K (calculated)
	Thermal Conductivity (Heat Flow):	2.0 W/m.K
	Temperature Range:	-50°C to +200°C
	Weight Loss after 96 hours @ 100°C:	<0.8%
	Permittivity @ 106Hz:	4.9
	Specific Resistance:	1 x 10^{15} Ohms/cm
	Dielectric Strength:	18 kV/mm

Description	Packing	Order Code	Shelf Life
Silicone Heat Transfer Paste Plus	35ml Syringe	HTSP35SL	48 months
	50 ml Tube	HTSP50T	48 months
	1 Kg Bulk	HTSP01K	72 months
	10 Kg Bulk	HTSP10K	72 months
	25 Kg Bulk	HTSP25K	72 months

Ashby Park, Coalfield Way,
Ashby de la Zouch,
Leicestershire LE65 1JR
T +44 (0)1530 419 600
F +44 (0)1530 416 640
BS EN ISO 9001:2008
Certificate No. FM 32082

Directions for Use

Thermal pastes can be applied to the base and mounting studs of diodes, transistors, thyristors, heat sinks, silicone rectifiers and semi-conductors, thermostats, power resistors and radiators, to name but a few. When the contact surfaces are placed together, a firm metal-to-metal contact will only be achieved on 40 – 60% of the interface, depending on the smoothness of the surfaces. This means that air, which has relatively poor thermal conductivity, will account for the balance of the interface. Only a small amount of compound is required to fill these spaces and thus dramatically increase the effective surface area for heat transfer.

It is important to note that the quality of application of a thermal paste can be as important as the thermal conductivity of the material applied; best results are achieved when a uniform, thin coat is applied between the mating surfaces. Apply a thin layer of compound to one of the contact surfaces using a brush, spatula, roller, automated system or screen printing technique. Ensure that the entire interface is covered to avoid hot-spots from forming. Any excess paste squeezed out during the mounting process should be removed.

Additional Information

There are many methods of measuring thermal conductivity, resulting in large variances in results. Electrolube utilise a heat flow method which takes into account the surface resistance of the test substrate, thus offering highly accurate results of true thermal conductivity. Some alternative methods do not account for such surface resistance and can create the illusion of higher thermal conductivity. Therefore, when comparing thermal conductivity measurements it is important to know what test method has been utilised. For more information please contact the Electrolube Technical Department.

The rate at which heat flows is dependent on the temperature differential, the thickness and uniformity of the layer, and the thermal conductivity of the material. Products with the same comparable thermal conductivity value may have very different efficiencies of heat transfer in the end application depending on how successfully a thin even film can be applied.

A full range of heat transfer products are available from Electrolube: high thermal conductivity pastes (HTCP), silicone based pastes for very high temperature applications (HTS), gap filling materials (HTCPX), Silicone RTVs (TCOR, TCER), epoxy adhesives (TBS) and encapsulation resins (ER2220, UR5633, SC2003).

Bulk Packaging Specifications

Package Size	Diameter	Height
700ml Cartridge	49.6mm	260mm + 15mm for Nozzle
1Kg Bulk Container	92mm	100mm
25Kg Bulk Container	254mm	330mm

Revision 1: Oct 2013

Ashby Park, Coalfield Way,
Ashby de la Zouch,
Leicestershire LE65 1JR
T +44 (0)1530 419 600
F +44 (0)1530 416 640
BS EN ISO 9001:2008
Certificate No. FM 32082

META

ISOLATORI E ACCESSORI DI CABLAGGIO

ISOLATORI E ACCESSORI DI CABLAGGIO

Gli isolatori **META** sono prodotti con materiale poliestere, rinforzato con fibra di vetro, caratterizzato da elevate prestazioni elettriche e meccaniche.
Il materiale poliestere utilizzato è classificato con grado di autoestinguenza V0 in conformità alla **Norma UL94**.

Inoltre le caratteristiche del materiale degli isolatori **META** sono state verificate presso il Laboratorio INTEK S.P.A. per quanto riguarda:
- prove elettriche
- prove meccaniche
- caratteristiche del materiale

Gli isolatori **META** SU RICHIESTA possono essere realizzati in poliestere classificato **CATEGORIA I (classe 1)**
in conformità alla **specifica generale FS304142**, le cui verifiche comprendono:
- reazioni al fuoco secondo le prescrizioni del Decreto del Ministero dell'Interno n° 48 del 26 giugno 1984
- opacità dei fumi emessi
- tossicità e corrosività dei fumi emessi

Gli isolatori **META** SU RICHIESTA possono essere realizzati con poliestere naturale, con reazione al fuoco secondo la **specifica UNIPLAST 228** punteggio 100.

Gli isolatori distanziatori serie GM possono essere forniti anche di colore nero.

Tutti i prodotti META sono realizzati in conformità alle leggi vigenti e, qualora previsto, marcati CE in conformità alla Direttiva Bassa Tensione CEE 73/23 e relativa revisione 93/68.

META** insulators are manufactured using a polyester material, reinforced with glass fibres, having exceptional electrical and mechanical performances. The polyester material, that has been used, is classified with a grade of self-extinguishing V0 in conformity with the **Norm Nema UL94.

*The characteristics of the material of **META** insulators have been tested at the Laboratory Intek S.P.A. for what concerns:*
- *electrical tests*
- *mechanical tests*
- *characteristics of the material*

***META** insulators can be manufactured in polyester classified **CATEGORY I (class 1)** in conformity with the General **Specifications FS 304142**, whose verifications include:*
- *reaction to fire, in conformity with the Home Office Department Order nr. 48 of 26/06/1984*
- *opacity f the fumes*
- *toxicity and corrosivity of the fumes*

***META** insulators can be produced ON REQUEST with a polyester resin in a natural colour, having a reaction to fire that is in accordance with **UNIPLAST 228** score 100.*

The spacing insulators GM can be supplied on request, with black colour.

META insulators are in conformity with the laws in force and, when expected, are marked CE in conformity with the Low Tension Directive CEE 73/23 and the respective revision 93/68.

indice *index*

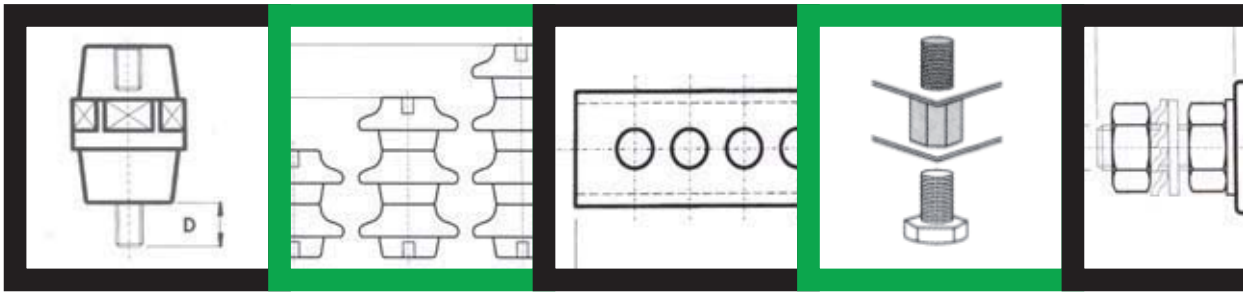

isolatori distanziatori
spacing insulators

MATERIALI PRIVI DI ALOGENI
HALOGEN FREE

Realizzati in resina poliestere caricata con fibre di vetro, garantiscono un'elevata resistenza, sia alle sollecitazioni elettriche che a quelle meccaniche.
Il nuovo profilo progettato per aumentare la linea di fuga rinnova l'immagine del tradizionale isolatore. Una fascia centrale esagonale permette un facile fissaggio. Inserti filettati, di diverso tipo e misure, incorporati alle estremità permettono l'utilizzo dell'isolatore nelle più svariate applicazioni.

They are made of polyester resin stiffened with glass fibres to ensure high endurance to electrical and mechanical stress. The new profile, designed to increase the surface outline, renews the image of the traditional insulator.
The hexagonal central band allows the easy assembling. The insulator ends are fitted with threaded inserts of different types and dimensions to allow the use of the insulator in any possible application.

Temperature di esercizio
Operating temperature
C° - 40 + 130

Resistenza all'arco
Arc resistance
ASTM D-495
> 180 sec.

Assorbimento acqua
Water absorption
ASTM D-570
0,20%

Rigidità dielettrica
Dielectric strength
UNI 4291
> 12 kV/mm

Resistenza alla traccia
Trace resistance
ASTM D-2303
> 300 min.

CARATTERISTICHE TECNICHE/*FEATURES*

Tipo/*Type*	**Carichi di rottura / *Stress on***			**Tensione di scarica *Flashover voltage***		**Tensione di esercizio *Operating voltage***	
da - a	Trazione *Tensile*	Torsione *Twisting*	Flessione *Cantilever*	Interna *Internal*	Superficiale *Surface*	c.a. *a.c.*	c.c. *d.c.*
from - to	daN	daN x mt.	daN	kV a.c.	kV a.c.	V.	V.
GM001 - GM004	-	-	-	-	-	110	150
GM011 - GM014	100	0,2	50	8	3	400	500
GM021 - GM044	150	0,2	60	15	5	600	800
GM051 - GM074	400	3	170	20	7	600	800
GM081 - GM104	600	3	250	25	8	600	800
GM111 - GM137	850	5	450	30	10	1000	1200
GM141 - GM167	850	5	450	40	15	2000	2500
GM171 - GM197	1100	5	550	40	20	3000	3500
GM201 - GM227	1300	10	900	40	20	5000	7500
GM231 - GM257	1500	15	1500	40	25	8000	10000

Valore dei carichi di rottura = +/- 10%
Value of breaking charges = +/- 10%
Il momento flettente non deve essere superiore al 40% della sollecitazione a flessione
The cantilever moment has not be higher than 40% of the cantilever stress

1 daN = 1 Kg.

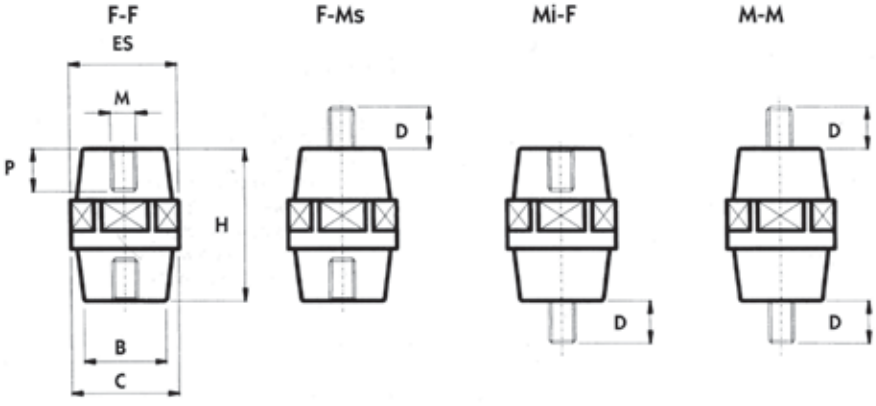

META
ISOLATORI E ACCESSORI DI CABLAGGIO

GM

Esecuzioni/*Executions* Codici/*Codes*				Dimensioni/*Dimensions*							Conf. pezzi (*) *Pack pieces (*)*
F-F	**F-Ms**	**Mi-F**	**M-M**	**H**	**ES**	**B**	**C**	**M**	**P**	**D**	**N°**
GM001	GM002	GM003	GM004	**12**	8	7,8	8	3	3	8	100
GM011	GM012	GM013	GM014	**16**	14	13	15	4	4	12	50
GM021	GM022	GM023	GM024	**20**	17	15	19	4	5	12	50
GM031	GM032	GM033	GM034	**20**	17	15	19	5	5	12	50
GM041 (1)	GM042	GM043	GM044	**20**	17	15	19	6	5	12	50
GM051	GM052	GM053	GM054	**25**	19	16	21	4	7	12	50
GM061	GM062	GM063	GM064	**25**	19	16	21	5	7	14	50
GM071	GM072	GM073	GM074	**25**	19	16	21	6	7	14	50
GM081	GM082	GM083	GM084	**30**	30	27	34	6	8	25	128
GM091 (1)	GM092	GM093	GM094	**30**	30	27	34	8	8	25	128
GM101	GM102	GM103	GM104	**30**	30	27	34	10	8	25	128
GM111	GM112	GM113	GM114	**34**	32	28	36	6	10	25	128
GM121	GM122	GM123	GM124	**34**	32	28	36	8	10	25	128
	GM125	GM126	GM127	**34**	32	28	36	8	10	40	128
GM131	GM132	GM133	GM134	**34**	32	28	36	10	10	25	128
	GM135	GM136	GM137	**34**	32	28	36	10	10	40	128
GM261	GM262	GM263	GM264	**40**	36	29	40	6	29	5	72
GM271	GM272	GM273	GM274	**40**	36	29	40	8	29	6	72
GM281	GM282	GM283	GM284	**40**	36	29	40	10	29	7	72
GM141	GM142	GM143	GM144	**50**	36	29	40	6	15	25	36
	GM145	GM146	GM147	**50**	36	29	40	6	15	40	36
GM151	GM152	GM153	GM154	**50**	36	29	40	8	15	25	36
	GM155	GM156	GM157	**50**	36	29	40	8	15	40	36
GM161	GM162	GM163	GM164	**50**	36	29	40	10	15	25	36
	GM165	GM166	GM167	**50**	36	29	40	10	15	40	36
GM151S				**51**	36	29	40	8	15	25	36
GM161S				**51**	36	29	40	10	15	25	36
GM171	GM172	GM173	GM174	**63**	41	31	45	6	15	25	36
	GM175	GM176	GM177	**63**	41	31	45	6	15	40	36
GM181	GM182	GM183	GM184	**63**	41	31	45	8	15	25	36
	GM185	GM186	GM187	**63**	41	31	45	8	15	40	36
GM191	GM192	GM193	GM194	**63**	41	31	45	10	15	25	36
	GM195	GM196	GM197	**63**	41	31	45	10	15	40	36
GM201	GM202	GM203	GM204	**75**	50	36	55	8	15	25	25
	GM205	GM206	GM207	**75**	50	36	55	8	15	40	25
GM211	GM212	GM213	GM214	**75**	50	36	55	10	25	25	25
	GM215	GM216	GM217	**75**	50	36	55	10	25	40	25
GM221	GM222	GM223	GM224	**75**	50	36	55	12	25	30	25
	GM225	GM226	GM227	**75**	50	36	55	12	25	40	25
GM231	GM232	GM233	GM234	**100**	65	52	72	10	25	25	12
	GM235	GM236	GM237	**100**	65	52	72	10	25	40	12
GM241	GM242	GM243	GM244	**100**	65	52	72	12	25	30	12
	GM245	GM246	GM247	**100**	65	52	72	12	25	40	12
GM251	GM252	GM253	GM254	**100**	65	52	72	16	30	30	12
	GM255	GM256	GM257	**100**	65	52	72	16	30	40	12

GM = Massa poliestere colore rsso
Red polyester resin
(1) Possono essere realizzati, su richiesta, con massa poliestere nera (codici GN041 e GN091)
Can be made, under request, with black polyester resin (codes: GN041 and GN091)

(*) Le confezioni sono riferite alle esecuzioni F-F
The packing refers to F-F execution